



Since January 2020 Elsevier has created a COVID-19 resource centre with free information in English and Mandarin on the novel coronavirus COVID-19. The COVID-19 resource centre is hosted on Elsevier Connect, the company's public news and information website.

Elsevier hereby grants permission to make all its COVID-19-related research that is available on the COVID-19 resource centre - including this research content - immediately available in PubMed Central and other publicly funded repositories, such as the WHO COVID database with rights for unrestricted research re-use and analyses in any form or by any means with acknowledgement of the original source. These permissions are granted for free by Elsevier for as long as the COVID-19 resource centre remains active.

Review

# Applications of heteronuclear NMR spectroscopy in biological and medicinal inorganic chemistry

Luca Ronconi<sup>a</sup>, Peter J. Sadler<sup>b,\*</sup>

<sup>a</sup> School of Chemistry, University of Edinburgh, West Mains Road, Edinburgh EH9 3JJ, UK

<sup>b</sup> Department of Chemistry, University of Warwick, Gibbet Hill Road, Coventry CV4 7AL, UK

Received 12 October 2007; accepted 15 January 2008

Available online 26 January 2008

## Contents

1. Introduction	2240
2. Practical limitations to metal NMR spectroscopy	2242
3. NMR spectroscopy of biologically relevant metals and metalloids	2245
3.1. s-Block: alkali metals (Li, Na, K, Rb, Cs)	2245
3.1.1. Lithium	2245
3.1.2. Sodium	2246
3.1.3. Potassium	2247
3.1.4. Rubidium	2248
3.1.5. Cesium	2249
3.2. s-Block: alkaline earth metals (Mg, Ca)	2249
3.2.1. Magnesium	2249
3.2.2. Calcium	2250
3.3. p-Block: Group 13 (B, Al, Ga, In, Tl)	2251
3.3.1. Boron	2251
3.3.2. Aluminum	2252
3.3.3. Gallium, indium and thallium	2254
3.4. p-Block: Group 14 (Si, Ge, Sn, Pb)	2256
3.4.1. Silicon and germanium	2256
3.4.2. Tin	2256
3.4.3. Lead	2256
3.5. p-Block: Group 15 (As, Sb, Bi) and Group 16 (Te)	2257
3.5.1. Arsenic, antimony and bismuth	2257
3.5.2. Tellurium	2258
3.6. d-Block: Group 3 (Sc, Y) and Group 4 (Ti)	2258
3.6.1. Scandium and yttrium	2258
3.6.2. Titanium	2259
3.7. d-Block: Group 5 (V) and Group 6 (Cr, Mo, W)	2259
3.7.1. Vanadium	2259
3.7.2. Chromium, molybdenum and tungsten	2260

*Abbreviations:* ADP, adenosine diphosphate; AMP, adenosine monophosphate; AES, atomic emission spectroscopy; ATP, adenosine triphosphate; BNCT, boron neutron capture therapy; BPG, 2,3-bisphosphoglycerate; BSA, bovine serum albumin; BSH, sodium borocaptate; DNA, deoxyribonucleic acid; EDTA-N<sub>4</sub>, ethylenediaminetetraacetamide; EFG, electric field gradient; GMP, guanosine monophosphate; HMQC, heteronuclear multiple quantum correlation; Im, imidazole; In, indazole; MQF, multiple quantum filtered; MRI, magnetic resonance imaging; NOE, nuclear Overhauser effect; PET, positron emission tomography; RBC, red blood cell; RNA, ribonucleic acid; rRNA, ribosomal ribonucleic acid; SDS, sodium dodecyl sulfate; tRNA, transfer ribonucleic acid.

\* Corresponding author. Tel.: +44 24 76523818; fax: +44 24 76523819.

E-mail address: [P.J.Sadler@warwick.ac.uk](mailto:P.J.Sadler@warwick.ac.uk) (P.J. Sadler).

3.8.	d-Block: Group 7 (Mn, Tc) .....	2261
3.8.1.	Manganese .....	2261
3.8.2.	Technetium .....	2261
3.9.	d-Block: Group 8 (Fe, Ru, Os) .....	2262
3.9.1.	Iron .....	2262
3.9.2.	Ruthenium and osmium .....	2262
3.10.	d-Block: Group 9 (Co, Rh) .....	2263
3.10.1.	Cobalt and rhodium .....	2263
3.11.	d-Block: Group 10 (Ni, Pd, Pt) .....	2264
3.11.1.	Nickel and palladium .....	2264
3.11.2.	Platinum .....	2264
3.12.	d-Block: Group 11 (Cu, Ag, Au) .....	2265
3.12.1.	Copper .....	2265
3.12.2.	Silver and gold .....	2265
3.13.	d-Block: Group 12 (Zn, Cd, Hg) .....	2266
3.13.1.	Zinc .....	2266
3.13.2.	Cadmium .....	2266
3.13.3.	Mercury .....	2268
3.14.	f-Block: lanthanides .....	2268
4.	NMR spectroscopy of biologically relevant non-metals .....	2269
4.1.	p-Block: Group 16 (O, S, Se) .....	2269
4.1.1.	Oxygen .....	2269
4.1.2.	Sulfur .....	2270
4.1.3.	Selenium .....	2271
4.2.	p-Block: Halogens (F, Cl, Br, I) .....	2271
4.2.1.	Fluorine .....	2271
4.2.2.	Chlorine .....	2271
4.2.3.	Bromine and iodine .....	2272
5.	Conclusions .....	2273
	Acknowledgements .....	2273
	References .....	2273

## Abstract

There is a wide range of potential applications of inorganic compounds, and metal coordination complexes in particular, in medicine but progress is hampered by a lack of methods to study their speciation. The biological activity of metal complexes is determined by the metal itself, its oxidation state, the types and number of coordinated ligands and their strength of binding, the geometry of the complex, redox potential and ligand exchange rates. For organic drugs a variety of readily observed spin  $I = 1/2$  nuclei can be used ( $^1\text{H}$ ,  $^{13}\text{C}$ ,  $^{15}\text{N}$ ,  $^{19}\text{F}$ ,  $^{31}\text{P}$ ), but only a few metals fall into this category. Most are quadrupolar nuclei giving rise to broad lines with low detection sensitivity (for biological systems). However we show that, in some cases, heteronuclear NMR studies can provide new insights into the biological and medicinal chemistry of a range of elements and these data will stimulate further advances in this area.

© 2008 Elsevier B.V. All rights reserved.

**Keywords:** Heteronuclear NMR spectroscopy; Quadrupolar nuclei; Biological systems; Bioinorganic chemistry; Medicinal inorganic chemistry; Metallopharmaceuticals

## 1. Introduction

Bioinorganic chemistry is an interdisciplinary field that draws on disciplines such as biochemistry, inorganic and theoretical chemistry, molecular biology, biophysics and spectroscopy to address the key questions of how metals complement and mediate key biological processes [1]. About 24 elements are currently thought to be essential for mammalian life: H, C, N, O, F, Na, Mg, Si, P, S, Cl, K, Ca, V, Mn, Fe, Co, Ni, Cu, Zn, Se, Mo, Sn, I [2], and 14 of them are metals or metalloids. However, this list may not be complete. For example, boron [3] and chromium may turn out to be essential, and it has been suggested that silicon is essential only to prevent aluminum from being toxic [4]. The biological roles of Cr are surrounded

by controversy [5]. Currently, Cr(VI) compounds are among 88 recognized (class I) human carcinogens. By contrast, many nutritionists regard Cr(III) as an essential micronutrient, acting as an insulin-mimetic, although this opinion has been disputed. No Cr(III)-dependent biomolecules, such as enzymes or cofactors, have yet been unambiguously described.

Inorganic elements play crucial roles in biological processes, and amongst them, metal ions are essential components in all aspects of the chemistry of living organisms. In biological systems, metal ions exist as electron-deficient cations and, hence, are attracted by electron-rich biomolecules, such as proteins and DNA, thus providing innumerable examples of “natural ligands” that bind metal ions to perform important biological functions. Metals play diverse roles in almost all biological

Table 1  
Some metal compounds in clinical use

Compound example (brand name)	Function	Comment
<b>Active complexes</b>		
<i>cis</i> -[Pt <sup>II</sup> Cl <sub>2</sub> (NH <sub>3</sub> ) <sub>2</sub> ] (Cisplatin)	Anticancer	<i>trans</i> -Isomer is inactive
[Gd <sup>III</sup> (DTPA)(H <sub>2</sub> O)] <sup>2-</sup> (Magnevist)	Extracellular contrast agent for MRI	Low toxicity
[ <sup>99m</sup> Tc <sup>I</sup> (CNCH <sub>2</sub> C(CH <sub>3</sub> ) <sub>2</sub> OCH <sub>3</sub> ) <sub>6</sub> ] <sup>+</sup> (Cardiolite)	Myocardial imaging	Positively charged complex taken up by the heart
Co <sup>III</sup> compound-vitamin B <sub>12</sub>	Coenzyme	Deficiency causes pernicious anemia
<b>Active metals</b>		
Li <sub>2</sub> CO <sub>3</sub>	Prophylaxis for bipolar disorders	Li forms weak complexes, labile
[Au <sup>I</sup> (thiomalate)] (Myocrisin)	Antirheumatoid arthritis	Facile thiol exchange on Au <sup>I</sup>
Colloidal Bi <sup>III</sup> subcitrate (De-Nol)	Antibacterial, antilucer	Strong binding of Bi to thiols, facile exchange
Na <sub>2</sub> [Fe <sup>II</sup> (CN) <sub>5</sub> (NO)]·2H <sub>2</sub> O (Nipride)	Hypotensive	Releases NO, relaxes vascular muscles
(Bleomycin)	Anticancer	Requires Fe for DNA attack
<i>p</i> -Xylyl-bicyclam·8HCl (Mozobil)	Stem cell mobilizer	May bind metals <i>in vivo</i>
CaCO <sub>3</sub>	Antacid	Slow release of alkali
La <sub>2</sub> <sup>III</sup> (CO <sub>3</sub> ) <sub>3</sub> (Foznol, Fosrenol)	Chronic renal failure	Reduces phosphate absorption

Adapted from Ref. [160].

processes: as catalytic groups at the active sites of enzymes, stabilizing the tertiary structures of proteins and polynucleotides, and as second messengers interacting with a variety of different small molecules and receptors [6]. Although our understanding of the functions and mechanisms of action of metals has increased in the last decades, the mammalian biochemistry of several essential elements is poorly understood. For example, chromium, nickel and tin seem to be essential for life, but we do not know whether there are human genomic codes for them, or how to use them effectively in medicine, yet. For some elements the genetic code involves proteins which recognize specific metal complexes. For example, only one specific cobalt compound, the coenzyme vitamin B<sub>12</sub>, appears to be essential [7], and in *Escherichia coli* the molybdate-dependent transcriptional regulator ModE acts as a sensor of intracellular molybdate ([MoO<sub>4</sub>]<sup>2-</sup>) concentration and as a regulator for the transcription of several operons that control the uptake and utilization of molybdenum [8]. Zinc is essential for life, and is the second most abundant d-block metal ion in living organisms after iron. It has essentially two possible roles: catalytic or structural. Zinc may also modulate signaling events, as it occurs in processes maintaining zinc homeostasis. An attempt to compile a catalogue of proteins encoded by the human genome, which may require zinc

for their physiological functions has been recently reported [9]. Some 10% of the proteins coded by the human genome (the proteome) potentially have zinc-binding sequences. Selenium provides a good example of the importance of speciation: it is an essential element and, yet, some of its compounds are highly toxic (*e.g.* H<sub>2</sub>Se). Genes which code for selenium incorporation into amino acids have been characterized [10].

Another important aspect concerning metal ions is that both essential and non-essential metals can be used in therapy and diagnosis, and examples of compounds in current clinical use are listed in Table 1. As indicated in Fig. 1, key areas in the design of active compounds are the control of toxicity (side-effects) and targeting of the metal to specific tissues, organs, or cells where activity is needed. Metal ions can be introduced into a biological system either for therapeutic effect or as diagnostic aids. Alternatively, metal ions can be removed from a biological system by judicious use of metal-binding molecules (ligands) [11]. Thus, biomedical inorganic chemistry offers the potential for the design of novel therapeutic and diagnostic agents and for the treatment and understanding of diseases which are currently intractable [12].

The field of bioinorganic chemistry continues to mature, constantly presenting novel and unexpected coordination spheres

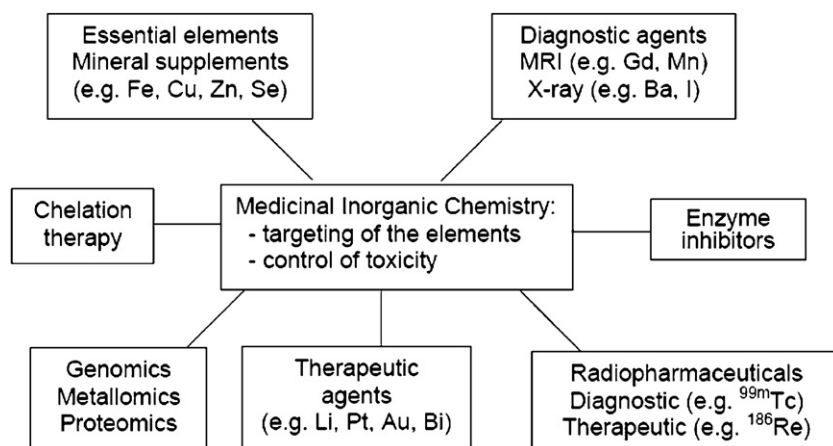


Fig. 1. Some of the areas of medicinal inorganic chemistry (adapted from Ref. [160]).

with metals in unusual oxidation states that often have no precedent in coordination chemistry. Therefore, the growing interest in understanding the coordination chemistry of biometals, and the development of structure-based drug design of inorganic pharmaceuticals, requires suitable and reliable analytical tools to study the speciation of metal ions in biological systems. In this context, NMR spectroscopy is a powerful and versatile technique that can provide site-specific information about chemical bonding, structure and dynamics in molecular systems. Moreover, NMR spectroscopy is one of the two techniques, the other being X-ray crystallography, that can provide atomic level descriptions of the intermolecular receptor–metal ion interactions responsible for molecular recognition [13]. NMR spectroscopy is being applied to the study of an ever-increasing diversity of biological macromolecules. Advances in the field are allowing detailed structural investigations of proteins, nucleic acids and carbohydrates, including investigations of cells and perfused organs under living conditions, which allows quantification of the dynamic properties of metabolites as well as kinetics of enzymatic reactions at steady state or through real time monitoring [14].

To date, most successful applications of NMR to biological systems have been typically carried out in aqueous solutions, and have utilized spin  $I = 1/2$  nuclei, such as  $^1\text{H}$ ,  $^{13}\text{C}$ ,  $^{15}\text{N}$  and  $^{31}\text{P}$ , whereas NMR spectroscopy has proved less powerful when applied to nuclei with spin quantum number  $I$  greater than  $1/2$ , *i.e.* those having a non-spherical charge distribution and an electric quadrupole moment. Unfortunately, for a large number of biologically relevant elements, the only NMR-active isotopes are those with nuclear spins greater than one half. As a result, NMR spectroscopy of quadrupolar nuclei, such as  $^6\text{Li}$ ,  $^{14}\text{N}$  ( $I = 1$ ),  $^7\text{Li}$ ,  $^{11}\text{B}$ ,  $^{23}\text{Na}$ ,  $^{33}\text{S}$ ,  $^{35}\text{Cl}$ ,  $^{39}\text{K}$ ,  $^{71}\text{Ga}$ ,  $^{87}\text{Rb}$  ( $I = 3/2$ ),  $^{17}\text{O}$ ,  $^{25}\text{Mg}$ ,  $^{27}\text{Al}$ ,  $^{67}\text{Zn}$  ( $I = 5/2$ ),  $^{43}\text{Ca}$ ,  $^{45}\text{Sc}$ ,  $^{51}\text{V}$ ,  $^{59}\text{Co}$ ,  $^{133}\text{Cs}$ ,  $^{139}\text{La}$  ( $I = 7/2$ ), and  $^{93}\text{Nb}$  ( $I = 9/2$ ), became viewed as the “poor relation” of spin  $I = 1/2$  nuclei. It must be emphasized, however, that this was solely on grounds of sensitivity and resolution (broad resonances).

The following points are pertinent here: (i) quadrupolar nuclides account for nearly 75% of the stable magnetic nuclides in the periodic table; (ii) for chemists and biologists there is nothing inherently more interesting about spin  $I = 1/2$  nuclei than there is about quadrupolar nuclei (if they were of equal practical difficulty,  $^{17}\text{O}$  NMR would be at least as widely used as  $^1\text{H}$  or  $^{13}\text{C}$  NMR); (iii) although many useful empirical correlations exist between structure and spin  $I = 1/2$  NMR parameters, such correlations are not so widely explored for quadrupolar nuclei; (iv) the inherent sensitivities of spin  $I = 1/2$  and some quadrupolar nuclei are not similar (for example,  $^{45}\text{Sc}$ ,  $^{59}\text{Co}$ ,  $^{51}\text{V}$  and  $^{93}\text{Nb}$  possess magnetic dipole moments that are larger than that of  $^1\text{H}$  and are all >99.5% abundant in their natural elements). If the problem of line-broadening of resonances from quadrupolar nuclei could be solved then there would be enormously increased research activity in this area.

The aim of this review is to survey the use of heteronuclear NMR spectroscopy for investigations of the behavior of metal ions in biological systems. In particular, it will focus on some key results and successful applications of NMR spectroscopy

involving direct detection of metals, and will mainly cover work published during the last two decades. This review will be limited to NMR studies in solution. Solid-state NMR is a branch of NMR spectroscopy that deals with solid or solid-like systems, and is presently undergoing rapid expansion as a result of the significant advances in both NMR methodology and instrumentation that have occurred recently. Although there is growing interest in the applications of this technique to biological systems, this subject lies outside the scope of this work and review articles on this topic have been recently published [15].

This review is organized as follows: the first section provides an overview of metal NMR spectroscopy emphasizing the practical limitations related to quadrupolar nuclei. The second section describes illustrative NMR data for biologically relevant metallic and semi-metallic elements belonging to s-, p-, d-block and lanthanide elements. The last section deals with some significant biological data on non-metallic NMR-active nuclei other than  $^1\text{H}$ ,  $^{13}\text{C}$ ,  $^{15}\text{N}$  and  $^{31}\text{P}$ , whose detection to probe, indirectly, the coordination chemistry of biometals has been extensively reviewed [16].

## 2. Practical limitations to metal NMR spectroscopy

The development of metal (in particular transition metal) NMR spectroscopy has been very uneven because of the very small number of nuclei with favorable nuclear properties for high-resolution NMR. But as the technology evolves, more nuclei and bond types, and also the solid state, are being brought into the spectroscopist's net. The NMR properties of the nuclei with biological and/or medicinal interest are collected in Table 2. Favorable properties for high-resolution NMR spectroscopy are spin quantum number  $I = 1/2$  or, for  $I > 1/2$ , a relatively small value of the nuclear electric quadrupole moment ( $eQ$ ) and a large value of  $I$ , to minimize quadrupolar broadening. Also necessary are a sufficiently large natural abundance ( $A$ ) and magnetogyric ratio ( $\gamma$ , effectively the ratio of the magnetic moment to the spin quantum number), to which the NMR frequency is proportional. The intrinsic NMR receptivity, which is a measure of the intensity of signal, increases as  $|\gamma^3|AI(I+1)$ . Thus, larger values of  $I$  are more favorable, by a factor of 33 from  $I = 1/2$  to  $9/2$ . Transition metal nuclei with natural abundance below 5% that may be usefully studied with enrichment are  $^{57}\text{Fe}$ ,  $^{61}\text{Ni}$ ,  $^{67}\text{Zn}$  and  $^{187}\text{Os}$ .

Spin  $I = 1/2$  nuclei with low  $\gamma$  values have a further problem of too slow relaxation, since the rate depends on  $\gamma$ , and long accumulation times or sensitivity enhancement techniques may be needed for adequate sensitivity; examples are  $^{89}\text{Y}$ ,  $^{183}\text{W}$ ,  $^{57}\text{Fe}$ ,  $^{187}\text{Os}$ ,  $^{103}\text{Rh}$  and  $^{109}\text{Ag}$ .

For the majority of metal nuclei, the spin quantum number  $I$  is greater than  $1/2$  and, therefore, they possess a nuclear electric quadrupole moment  $eQ$  (in addition to their magnetic moment), as the nuclear electric charge distribution is not spherically symmetric. The electric quadrupole is coupled to the spin (magnetic dipole), since transitions in the one change the magnetic environment of the other. Whereas the orientation of the spin dipole is quantized relative to the magnetic field, that of the electric quadrupole is quantized relative to the electric field gradient

Table 2  
NMR properties of some elements of biological and/or medicinal interest

Isotope	Natural abundance (%)	Nuclear spin ( <i>I</i> )	Magnetogyric ratio ( $\gamma$ ) ( $\times 10^7$ rad T <sup>-1</sup> s <sup>-1</sup> )	Quadrupole moment ( <i>eQ</i> ) ( $\times 10^{28}$ C m <sup>-2</sup> )	Relative receptivity (to <sup>13</sup> C) <sup>a</sup>
<b>Non-metals</b>					
<sup>1</sup> H	99.98	1/2	26.7519	–	5666
<sup>13</sup> C	1.108	1/2	6.7283	–	1
<sup>14</sup> N	99.635	1	1.9338	$1.99 \times 10^{-2}$	5.69
<sup>15</sup> N	0.365	1/2	–2.712	–	0.022
<sup>17</sup> O	$3.7 \times 10^{-2}$	5/2	–3.6279	$-2.6 \times 10^{-2}$	0.06
<sup>19</sup> F	100	1/2	25.181	–	4761.5
<sup>31</sup> P	100	1/2	10.841	–	377
<sup>33</sup> S	0.76	3/2	2.055	$-5.5 \times 10^{-2}$	0.097
<sup>35</sup> Cl	75.53	3/2	2.624	–0.1	20.2
<sup>37</sup> Cl	24.47	3/2	2.1842	$-7.9 \times 10^{-2}$	3.8
<sup>77</sup> Se	7.58	1/2	5.12	–	2.98
<sup>79</sup> Br	50.54	3/2	6.7228	0.37	226
<sup>81</sup> Br	49.46	3/2	7.2468	0.31	277
<sup>127</sup> I	100	5/2	5.3817	–0.79	530
<b>Metalloids</b>					
<sup>10</sup> B	19.58	3	2.875	$8.5 \times 10^{-2}$	22.1
<sup>11</sup> B	80.42	3/2	8.584	$4.1 \times 10^{-2}$	754
<sup>29</sup> Si	4.7	1/2	–5.3188	–	2.09
<sup>73</sup> Ge	7.76	9/2	–0.9357	–0.18	0.617
<sup>75</sup> As	100	3/2	4.595	0.29	143
<sup>121</sup> Sb	57.25	5/2	6.4355	–0.28	520
<sup>123</sup> Sb	42.75	7/2	3.4848	–0.36	111
<sup>123</sup> Te	0.87	1/2	–7.049	–	0.89
<sup>125</sup> Te	6.99	1/2	–8.498	–	12.5
<b>Metals</b>					
<sup>6</sup> Li	7.42	1	3.9371	$-8 \times 10^{-4}$	3.58
<sup>7</sup> Li	92.58	3/2	10.3976	$-4 \times 10^{-2}$	1540
<sup>23</sup> Na	100	3/2	7.0801	0.1	525
<sup>25</sup> Mg	10.13	5/2	–1.639	0.22	1.54
<sup>27</sup> Al	100	5/2	6.976	0.15	1170
<sup>39</sup> K	93.12	3/2	1.2498	$4.9 \times 10^{-2}$	2.69
<sup>41</sup> K	6.88	3/2	0.686	$6 \times 10^{-2}$	0.033
<sup>43</sup> Ca	0.145	7/2	–1.8025	0.2	0.053
<sup>45</sup> Sc	100	7/2	6.5081	–0.22	1710
<sup>47</sup> Ti	7.28	5/2	–1.5105	0.29	0.864
<sup>49</sup> Ti	5.51	7/2	–1.5109	0.24	1.118
<sup>50</sup> V <sup>b</sup>	0.24	6	2.6717	$6 \times 10^{-2}$	0.755
<sup>51</sup> V	99.76	7/2	7.0453	$-5 \times 10^{-2}$	2150
<sup>53</sup> Cr	9.55	3/2	–1.512	$3 \times 10^{-2}$	0.49
<sup>55</sup> Mn	100	5/2	6.608	0.4	994
<sup>57</sup> Fe	2.19	1/2	0.8661	–	0.004
<sup>59</sup> Co	100	7/2	6.317	0.38	1570
<sup>61</sup> Ni	1.19	3/2	–2.394	0.16	0.24
<sup>63</sup> Cu	69.09	3/2	7.0974	–0.211	365
<sup>65</sup> Cu	30.91	3/2	7.6031	–0.195	201
<sup>67</sup> Zn	4.11	5/2	1.6768	0.16	0.67
<sup>69</sup> Ga	60.4	3/2	6.4323	0.19	237
<sup>71</sup> Ga	39.6	3/2	8.1731	0.12	319
<sup>85</sup> Rb	72.15	5/2	2.5909	0.26	43
<sup>87</sup> Rb	27.85	3/2	8.7807	0.13	277
<sup>89</sup> Y	100	1/2	–1.3155	–	0.668
<sup>95</sup> Mo	15.72	5/2	1.75	0.12	2.88
<sup>97</sup> Mo	9.46	5/2	–1.787	1.1	1.84
<sup>99</sup> Tc	100	9/2	6.0211	0.3	2134
<sup>99</sup> Ru	12.72	3/2	–1.234	$7.6 \times 10^{-2}$	0.83
<sup>101</sup> Ru	17.07	5/2	–1.383	0.44	1.56
<sup>103</sup> Rh	100	1/2	–0.846	–	0.177
<sup>105</sup> Pd	22.23	5/2	–0.756	0.8	1.41
<sup>107</sup> Ag	51.82	1/2	–1.087	–	0.195
<sup>109</sup> Ag	48.18	1/2	–1.25	–	0.276
<sup>111</sup> Cd	12.75	1/2	–5.6926	–	6.93



Table 2 (Continued)

Isotope	Natural abundance (%)	Nuclear spin ( <i>I</i> )	Magnetogyric ratio ( $\gamma$ ) ( $\times 10^7$ rad T <sup>-1</sup> s <sup>-1</sup> )	Quadrupole moment ( <i>eQ</i> ) ( $\times 10^{28}$ C m <sup>-2</sup> )	Relative receptivity (to <sup>13</sup> C) <sup>a</sup>
<sup>113</sup> Cd	12.26	1/2	-5.955	-	7.6
<sup>113</sup> In	4.28	9/2	5.8782	0.83	83.8
<sup>115</sup> In	95.72	9/2	5.8908	0.83	1890
<sup>115</sup> Sn	0.35	1/2	-8.801	-	0.70
<sup>117</sup> Sn	7.61	1/2	-9.589	-	19.54
<sup>119</sup> Sn	8.58	1/2	-10.0138	-	25.2
<sup>133</sup> Cs	100	7/2	3.5277	$-3 \times 10^{-3}$	269
<sup>183</sup> W	14.4	1/2	1.12	-	0.059
<sup>187</sup> Os	1.64	1/2	0.616	-	0.001
<sup>189</sup> Os	16.1	3/2	0.8475	0.8	2.13
<sup>195</sup> Pt	33.7	1/2	5.768	-	19.1
<sup>197</sup> Au	100	3/2	0.4625	0.59	0.06
<sup>199</sup> Hg	16.84	1/2	4.8154	-	5.42
<sup>201</sup> Hg	13.22	3/2	-1.7776	0.44	1.08
<sup>203</sup> Tl	29.5	1/2	15.436	-	289
<sup>205</sup> Tl	70.5	1/2	15.589	-	769
<sup>207</sup> Pb	22.6	1/2	5.54	-	11.8
<sup>209</sup> Bi	100	9/2	4.342	-0.38	777
<sup>138</sup> La	0.089	5	3.5295	-0.47	0.43
<sup>139</sup> La	99.91	7/2	3.801	0.22	336
<sup>155</sup> Gd	14.73	3/2	-1.0152	n.a.	0.23
<sup>157</sup> Gd	15.68	3/2	-1.2566	n.a.	0.46

Source: <http://www.bruker-nmr.de/guide/eNMR/chem/NMRnuclei.html>.

<sup>a</sup> The absolute receptivity of a nucleus (*R*) depends on its sensitivity (*S*) and natural abundance (*A*) according to the equation  $R = A S$ . The receptivity of a nucleus X relative to <sup>13</sup>C is defined as the ratio  $R(X)/R(^{13}\text{C})$ , where  $R(^{13}\text{C})$  is the absolute receptivity of <sup>13</sup>C at natural abundance.

<sup>b</sup> Radioactive.

(EFG) *eQ* at the nucleus due to the electrons and the other nuclei.

As the nuclear quadrupole moment interacts with the EFG at the nuclear site, it is convenient to define a nuclear electric quadrupolar coupling constant  $\chi = e^2 Q q / h$  (in Hz), which describes the strength of this interaction. Therefore, the nuclear energy levels depend on both the EFG and the magnetic field. In the liquid phase, rapid and isotropic molecular tumbling averages the quadrupolar (as well as the dipolar) interactions; but the relaxation of the electric quadrupole with fluctuations of the EFG (e.g. in molecular collisions) relaxes the nuclear spin as well, and fast relaxation leads to uncertainty over the line position, *i.e.* quadrupolar broadening. The quadrupolar relaxation rate and the line-width are proportional to  $\chi^2 (1 + \eta^2/3)(2I + 3)/I^2(2I - 1)$  (where  $\eta$  is the asymmetry parameter of the EFG, maximally equal to 1, and 0 for axial symmetry) and also to the rotational correlation time for isotropic tumbling ( $\tau_c = 4\pi\eta_0 r^3 / 3k_B T$ , where  $\eta_0$  is the viscosity of the medium and *r* is the molecular radius). Thus, the quadrupolar broadening increases sharply with increase in *Q* and in the EFG *q*. Again, higher values of *I* are advantageous because of the line-width dependence on  $(2I + 3)/I^2(2I - 1)$ , which decreases by a factor of 67.5 from *I* = 1 to 9/2 [17].

The interaction of the nuclear quadrupole moment with the electric field gradients arising from the local electronic environment provides a strong relaxation mechanism for the spin states, often resulting in short-lived states with broad resonance lines. This is particularly true in environments where ionic motion is restricted, such as in biological systems. In general, quadrupolar nuclei display broad resonances in NMR spectra, unless

they are in highly symmetric electrical environments, which reduce the magnitude of the electric field gradients at the nuclei (extreme narrowing conditions). Biological macromolecules which introduce high electric field gradients, in conjunction with non-averaging motional characteristics, can make quadrupolar interaction effective. However, the binding of quadrupolar metal ions can be studied by NMR spectroscopy, potentially even in cells. This is possible because the binding of metal ions to a biomolecule can cause a substantial increase in the effective correlation time ( $\tau_c$ ), thus leading to a measurable change in relaxation behavior of the ions.

For a given nucleus, line-widths are minimized for small molecules in low-viscosity samples ( $\tau_c$  small), with highly symmetrical environments of the metal nucleus (*q* small). Examples are tetraoxo [MO<sub>4</sub>] or fully fluorinated [MF<sub>6</sub>] species, or perhaps [M(CO)<sub>6</sub>], and for some quadrupolar metal nuclei, these are the only types of compounds for which an NMR signal has been reported.

Another severe hindrance to the development of transition metal NMR spectroscopy is caused by the fact that some nuclei in specific oxidation states, such as high spin Fe(II), Fe(III), Co(II), Ni(II), Cu(II) and Ru(III), are paramagnetic. Paramagnetic compounds contain unpaired electrons, and the unpaired electron density has a drastic effect on both the chemical shift and the line-widths of signals in the NMR spectra of metalloproteins containing one or more paramagnetic transition metals.

Line-broadening of NMR signals corresponding to the paramagnetic metal itself and to the nuclei in the neighborhood of the paramagnetic center is a severe limitation for high-resolution NMR spectroscopy. Relaxation of the unpaired electron(s) gives

rise to the major source of line-broadening of resonances for paramagnetic compounds in solution spectra, as the relative electron relaxation is sensed by the resonating nucleus through dipolar coupling. In addition, the delocalization of the unpaired electron(s) throughout the molecule is another factor that causes extreme line-broadening [18]. In some cases, extreme line-broadening prevents the detection of any NMR signal.

The hyperfine shift is another factor to take into account when NMR studies are carried out on paramagnetic systems. The hyperfine shift is defined as the difference in chemical shift between that of a paramagnetic molecule and that of an analogous diamagnetic system. Both contact (through-bond) and pseudo-contact (through-space) shifts are important contributors to the hyperfine shift. In particular, the hyperfine shifts of nuclei in paramagnetic molecules can be well outside (even hundreds of ppm) the window of signals for diamagnetic analogues. The wide range of chemical shift values observed for paramagnetic compounds (large high frequency and low frequency shifts) is often attributed to the different resulting spin delocalization mechanisms [18,19].

On the other hand, in some circumstances the effects produced by a paramagnetic metal ion can be used to probe the active sites of metalloproteins and analyzed to give additional constraints for structural calculations on paramagnetic proteins, leading to NMR structures with greater precision. In fact, many NMR structures of a variety of paramagnetic metalloproteins have been reported to date. For example, the quantification of the shortening of both  $T_1$  and  $T_2$  (line-broadening), and paramagnetic shifts can be exploited to obtain information on the distance from a paramagnetic center to an NMR-active nucleus [20].

In conclusion, the development of NMR techniques for the direct detection of metal ions in biological systems has been hampered by the quadrupolar and paramagnetic properties of some of the biometals of interest. Nevertheless, several successful studies have been carried out in the field, and are summarized in the following sections.

### 3. NMR spectroscopy of biologically relevant metals and metalloids

#### 3.1. *s*-Block: alkali metals (Li, Na, K, Rb, Cs)

##### 3.1.1. Lithium

Lithium is normally present only at trace levels within the human body, and no natural biological or nutritional roles have been established [21]. In the ionic form, Li(I) is absorbed readily into blood following subcutaneous, intraperitoneal or oral administration, and binds very weakly to plasma proteins [22]. There are several medical uses for Li(I) compounds, but the major application is in psychiatry. Li, usually administered orally as  $\text{Li}_2\text{CO}_3$ , is the treatment of choice for acute mania and for prophylaxis in bipolar disorders [23].

Interest in Li NMR spectroscopy and imaging in biology and experimental medicine arises primarily from the clinical use of Li salts to treat mania and manic-depressive illness. Naturally occurring Li consists of the  ${}^6\text{Li}$  ( $I = 1$ ) and  ${}^7\text{Li}$  ( $I = 3/2$ ) iso-

topes with 7.42% and 92.58% abundances, respectively. Both Li isotopes are weakly quadrupolar relative to other alkali metals, which derives from their small quadrupole moments and the small Sternheimer antishielding factor of  $\text{Li}^+$  [24], reflecting its small size and simple electronic structure. Both isotopes yield narrow spectral lines and long spin–lattice relaxation times ( $T_1$ ), typically 2–8 s.  ${}^7\text{Li}$  is the isotope of choice for most studies because of its higher natural isotopic abundance and magnetic moment, and more favorable relaxation properties than  ${}^6\text{Li}$ .

Because of the simple electronic structure and aqueous chemistry of the  $\text{Li}^+$  ion, the chemical shift range is small, and spectra usually have a single (averaged) resonance from all environments. This complicates interpretation of  ${}^7\text{Li}$  NMR signals from biological systems, which are usually heterogeneous. It is often advantageous to resolve signals from the different compartments, either based on differences in relaxation properties, or by adding a shift reagent to separate the intra- and extracellular resonances [25]. Each local Li environment and compartment may potentially have a characteristic concentration and spin relaxation behavior.

One area of investigation is ionic transport across the cellular membrane and compartmentation to elucidate the mechanism(s) of therapeutic action and toxicity in clinical practice. Another is the development of non-invasive, *in vivo* analytical tools to measure brain lithium concentration and speciation in humans, as both an adjunct to treatment and a mechanistic probe. The available literature related to the use of  ${}^7\text{Li}$  NMR spectroscopy *in vitro* and *in vivo* has been recently reviewed [26]. In particular,  ${}^7\text{Li}$  NMR investigations of the human brain have been carried out at a high magnetic field (3 T), and the relationship between brain and serum lithium measurements in lithium-treated bipolar patients has been determined, demonstrating the feasibility of  ${}^7\text{Li}$  NMR human studies [27].

The beneficial effect of Li in mania and depression results from its action on the brain, and, hence, the amount of Li present in the brain may be important with regard to patient response. As brain Li cannot be monitored readily at present, it is a common practice to measure the concentration of the ions in the serum where repeated measurements can be made inexpensively. Moreover, because of the sedative and possible neurotoxic side-effects of lithium, it is important to monitor and maintain the lithium concentration within the safe therapeutic range by measuring  $\text{Li}^+$  concentrations in serum or plasma. Although plasma lithium values are used to monitor the therapy, the lithium in red blood cells may be a better predictor of  $\text{Li}^+$  concentrations in the brain than serum levels [28].  ${}^7\text{Li}$  NMR spectroscopy is a valuable analytical tool to quantify Li in whole blood, plasma, or RBCs. In a recent study [29], male Sprague–Dawley rats were treated with different amounts of  $\text{Li}_2\text{CO}_3$ ; 24 h after drug administration, blood was drawn from the rats *via* cardiac puncture, and aliquots, mixed with a known amount of anticoagulant (citrate phosphate dextrose) and 20 mg of a shift reagent ( $[\text{Tm}(\text{DOTP})]^{5-}$ , thulium(III)-1,4,7,10-tetraazacyclododecane-1,4,7,10-tetrakis(methylenephosphonate)),  ${}^7\text{Li}$  NMR provided a clear discrimination between plasma and RBC lithium signals. The  ${}^7\text{Li}$  spectrum (obtained in 30 min) in Fig. 2 shows two peaks  $\sim 13$  ppm apart corresponding to plasma (extracellular) and RBC



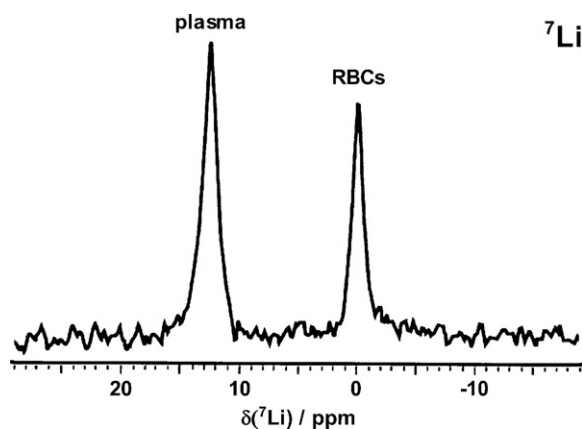


Fig. 2.  $^7\text{Li}$  NMR spectrum of a blood sample treated with  $\text{Li}_2\text{CO}_3$  recorded in 30 min using a home-built solenoid coil at 7 T field strength. The chemical shift of lithium accumulated in RBCs has been set to 0 ppm. The RBC and plasma  $^7\text{Li}$  resonances are separated by 13 ppm by the addition of 20 mg of  $[\text{Tm}(\text{DOTP})]^{5-}$  as shift reagent (adapted from Ref. [29]).

(intracellular) lithium. Quantification of lithium was achieved by comparing peak intensities with standards prepared using blood from untreated rats, and the results showed excellent agreement (less than 0.1% average difference) with other commonly employed techniques, confirming that  $^7\text{Li}$  NMR spectroscopy has the potential to become routine for lithium analysis. Moreover, this technique has the advantage of reduced pre-analytical preparation time and small blood samples with lithium concentration in the neighborhood of  $0.08 \text{ mequiv. L}^{-1}$  can be measured with high accuracy and reproducibility needed for clinical purposes.

### 3.1.2. Sodium

The major functions of sodium ions relate to concentration gradients across membranes, the cotransport of solutes, and the preservation of pH ( $\text{Na}^+/\text{H}^+$  transport).  $\text{Na}^+$  is also involved in several pathological processes. Cell death, edema formation, tumor growth, electrophysiologic processes and ion transport all involve alteration in intracellular and extracellular sodium levels [6b]. The detected role of  $\text{Na}^+$  in the regulation of metabolism in cells is poorly understood, largely as a result of the paucity of methods for studying its interactions with cellular constituents. NMR spectroscopy provides a non-destructive method to observe sodium, offering new potential for specific measurements on intact living tissues.

Among the observable nuclei in biological tissues,  $^{23}\text{Na}$  is favored because of its high natural abundance (100%), relatively high sensitivity to NMR detection, and high concentrations in tissues (5–150 mM). All these advantages are shadowed by the quadrupolar properties of  $^{23}\text{Na}$  ( $I=3/2$ ). Nevertheless, line-shape analysis of  $^{23}\text{Na}$  NMR resonances can provide information on  $\text{Na}^+$  binding [30]. In a standard NaCl solution at 25 °C, both the  $T_1$  and  $T_2$  relaxation times of  $^{23}\text{Na}$  are about 60 ms, when extreme narrowing conditions are met. Outside extreme narrowing conditions, *i.e.* the bound state, relaxation times are shortened indicating different mobility conditions than in a free solution [31]. The study of relaxation processes can describe in

this way, the dynamics of sodium ions in a living system, and correlate the dynamics with the pathological or normal state of the system itself.

In most living cells, the transmembrane gradients of sodium ions are essential for proper cell function; thus, changes in ion concentrations on each side of the membrane result in profound functional disorders of the cell. In several diseases or pathological states (hypertension, cystic fibrosis, oncogenesis, infected cells) a change in this equilibrium occurs due to abnormalities in ion-binding sites or in transport processes across the membrane. Sodium relaxation studies can provide qualitative information on the interaction of  $\text{Na}^+$  ions with molecules [32]. NMR relaxation techniques are able to discriminate between different adjacent sodium ion compartments, whether or not they are physically separated, as long as they display different molecular motions and, thus, induce different relaxation characteristics. The use of multiple echoes to provide relaxation information has greatly increased the usefulness of  $^{23}\text{Na}$  NMR spectroscopy, and the use of paramagnetic shift reagents or contrast reagents allows the differentiation of intra- and extracellular sodium pools, but toxicity of the currently available shift reagents may be problematic. In instances where toxicity is not a severe problem, shift reagents have been used to monitor fluid dynamics as well as to distinguish different sodium pools, and this method has been mostly applied to cell suspensions, kidney tubules, glands and small organs [33]. For example, the shift reagent dysprosium(III)-tripolyphosphate ( $[\text{Dy}(\text{PPP})_2]^{7-}$ ) was used in experiments with sequential frequency-selective radiofrequency pulses to excite selectively the well-resolved resonances of shifted and unshifted sodium and produce separate images of the different sodium pools. This technique depends on the complete resolution of the sodium resonances and requires separate experiments for each sodium species. The less toxic shift reagents dysprosium(III)-triethylenetetraminehexaacetate ( $[\text{Dy}(\text{TTHA})]^{3-}$ ) and  $[\text{Tm}(\text{DOTP})]^{5-}$  have also been employed, but they do not produce fully resolved intracellular and extracellular sodium resonances. Nonetheless, these experiments allowed the simultaneous generation of separate images of the intracellular and extracellular sodium pools, and, therefore, the direct monitoring of the movement of sodium on a regional basis.

Multiple-quantum and multiple-quantum filtered pulse sequences have proved to be useful to define the interactions of quadrupolar nuclei with biomolecules. The relaxation profile of a specific magnetization or coherence of a quadrupolar ion can be readily monitored against a background of NMR signal from unbound ions. These methods yield estimates of the relaxation rate constants, the fraction of bound ions, the binding constants, the rotational correlation time ( $\tau_c$ ), and the quadrupolar coupling constant of the nucleus in its bound state. For example, Torres et al. have determined the apparent binding constants ( $K_f$ ) for  $\text{Na}^+$  and a protein, bovine serum albumin (BSA), a nucleic acid yeast RNA, and a self-associating macroassembly, the detergent sodium dodecyl sulfate (SDS) using the relaxation behavior of selected  $^{23}\text{Na}^+$  magnetization coherences [34]. These three macromolecular systems were chosen as representatives of different classes of biomolecules that are likely to have diverse  $\text{Na}^+$ -binding environments. The relaxation analysis provided

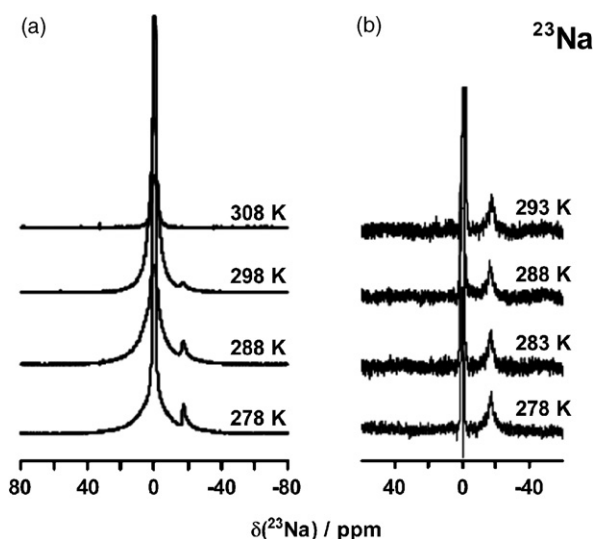


Fig. 3. (a) Variable-temperature  $^{23}\text{Na}$  NMR spectra of 0.80 M  $\text{Na}_2(5'\text{-GMP})$  obtained on a Bruker Avance-500 spectrometer ( $B_0 = 11.75\text{ T}$ ) operating at 132.26 MHz for  $^{23}\text{Na}$ . (b)  $^{23}\text{Na}$  NMR spectra of  $\text{d}(\text{TG}_4\text{T})$  obtained on a Bruker Avance-600 spectrometer ( $B_0 = 14.1\text{ T}$ ). An inversion-recovery sequence was used to partially suppress the large signal from the free  $\text{Na}^+$  ions. A recovery delay of 13 ms (close to the null point) was used. Typically, 250k scans were accumulated with a recycle time of 50 ms. The  $\text{d}(\text{TG}_4\text{T})$  DNA sample was prepared at 8 mM strand concentration in 10 mM sodium phosphate buffer (pH 7.1) and 100 mM NaCl. All  $^{23}\text{Na}$  chemical shifts are referenced to  $\text{Na}^+(\text{aq})$  at 0.0 ppm (adapted from Ref. [36]).

single estimates of the apparent binding constants for  $^{23}\text{Na}^+$  to RNA ( $K_f = \sim 40\text{ M}^{-1}$ , strong binding) and BSA ( $K_f = \sim 0.3\text{ M}^{-1}$ , weak binding), whereas two binding sites were identified in the presence of SDS, with  $K_f$  values of  $\sim 26\text{ M}^{-1}$  (strong binding) and  $\sim 8\text{ M}^{-1}$  (weak binding), respectively.

Detection of alkali metal cations in DNA G-quadruplexes has usually relied on either direct solid-state techniques, such as X-ray crystallography and solid-state NMR, or indirect methods using surrogate spin  $I = 1/2$  probes, such as  $^{15}\text{NH}_4^+$  and  $^{205}\text{Tl}^+$ , in solution NMR experiments [35]. On the basis of these studies, two types of alkali metal-binding sites are generally found in G-quadruplex structures, one type being loosely coordinated to phosphate groups, and the other residing inside the G-quadruplex channel. The latter type of alkali metal cations is tightly bound to the G-quadruplex structure and has long been considered to be “invisible” to NMR spectroscopy in solution. In this context, Won et al. [36] have reported the first direct solution NMR detection of the  $\text{Na}^+$  residing inside G-quadruplex channel structures formed by  $5'\text{-GMP}$  and the DNA oligomer,  $\text{d}(\text{TG}_4\text{T})$ . Fig. 3a shows  $^{23}\text{Na}$  NMR spectra for 0.80 M  $\text{Na}_2(5'\text{-GMP})$  in an aqueous solution at pH 8. The signal centered at 0 ppm exhibits a bi-Lorentzian line-shape, which is due to a slow exchange of  $\text{Na}^+$  cations between phosphate-bound and free states. The small peak at  $-17\text{ ppm}$  is due to the  $\text{Na}^+$  cations residing inside the  $5'\text{-GMP}$  channel. The signal intensity for the channel  $\text{Na}^+$  cations decreases as the sample temperature is increased from 278 to 308 K, an indication of “melting” of the  $5'\text{-GMP}$  aggregates. Analogously (b),  $^{23}\text{Na}$  NMR spectra of  $\text{d}(\text{TG}_4\text{T})$  show the channel  $\text{Na}^+$  signal at  $-17\text{ ppm}$  but, in this case, the total integrated area for this signal remains approximately unchanged between

278 and 293 K, indicating that the G-quadruplex structure of  $\text{d}(\text{TG}_4\text{T})$  does not melt at 293 K. These findings open up many new possibilities in the study of cation binding and transport dynamics in G-quadruplex DNA. For example, it might now be possible not only to monitor cation transport through a G-quadruplex channel, but also to measure cation-binding affinity for the channel site in a direct and site-specific manner.

### 3.1.3. Potassium

Potassium salts are essential for both animals and plants. The potassium cation ( $\text{K}^+$ ) is the major ion in intracellular fluids (typically 140 mM), whereas  $\text{Na}^+$  is found in higher concentrations than  $\text{K}^+$  outside of the cell (145 mM vs. 5 mM).  $\text{K}^+$  is involved in the control of transmembrane potentials and regulates the equilibrium of cellular electrolytes and osmotic pressure. In contrast to divalent ions, it interacts weakly with most biological ligands, so it is unlikely to be involved in the triggering of biological activity by direct bonding. Although serving principally as a counter-ion for negatively charged solutes and nucleic acids, potassium is also required for the activation of a large number of enzymes [37].

Conventional methods of analysis for intracellular ions, such as flame photometry and radioisotope tracer techniques, have the disadvantage of requiring time-consuming destructive methods to achieve physical separation of intra- and extracellular compartments. Furthermore, there are uncertainties associated with the possibility of non-specific binding of ions to the cell membrane and of ion fluxes occurring during the separation procedure. Clearly, a non-destructive and non-invasive method would be welcome. NMR spectroscopy might offer such an approach. Naturally occurring K consists of the  $^{39}\text{K}$  and  $^{41}\text{K}$  isotopes with 93.12% and 6.82% abundances, respectively. Like the other alkali metals, both K isotopes are quadrupolar.  $^{39}\text{K}$  is the isotope of choice for most NMR studies because of its higher natural isotopic abundance, but the low sensitivity (compared to  $^7\text{Li}$  and  $^{23}\text{Na}$  NMR experiments) has proved to be a major drawback, as confirmed by the few data reported in the literature.

Most intracellular  $\text{K}^+$  is bound to ribosomes. It stabilizes the negatively charged ribose-phosphate backbone and specific structural motifs. Examples include RNA tertiary structure, DNA backbone conformation, and telomeric DNA in chromosomes. The first direct solution NMR detection of  $\text{K}^+$  residing inside G-quadruplex channel structures formed by  $5'\text{-GMP}$  and a DNA oligomer,  $\text{d}(\text{TG}_4\text{T})$  has been achieved [36]. As shown in Fig. 4, two  $^{39}\text{K}$  NMR signals are clearly observed at 278 K. The peak at 0 ppm is due to surface/free  $\text{K}^+$  cations, whereas the signal at  $\sim 18\text{ ppm}$  can be assigned to the channel  $\text{K}^+$  cations. The signal intensity for the channel  $\text{K}^+$  cations decreases as the sample temperature is increased from 278 to 298 K, an indication of “melting” of the  $5'\text{-GMP}$  aggregates. It was also found that  $\text{K}^+$  ions move through the G-quadruplex channel at a much slower rate than that for  $\text{Na}^+$ .  $^{39}\text{K}$  NMR studies have also been carried out to investigate the interaction of  $\text{K}^+$  with ribosomes [38] and quadruplex DNA [39], and attempts have been made to quantify intracellular  $\text{K}^+$  *in vitro* [40,41].

More satisfactory results have been achieved for investigations of  $\text{K}^+$  transport in human erythrocytes by  $^{39}\text{K}$

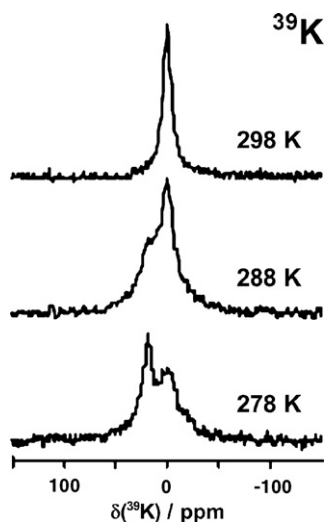


Fig. 4. Variable-temperature  $^{39}\text{K}$  NMR spectra of 0.53 M  $\text{Na}_2(5'\text{-GMP})$  in presence of 0.10 M  $\text{K}^+$  obtained on a Bruker Avance-500 spectrometer ( $B_0 = 11.75$  T) operating at 23.33 MHz for  $^{39}\text{K}$  nucleus. Typically, 500k scans were accumulated with a recycle time of 10 ms. All  $^{39}\text{K}$  chemical shifts are referenced to  $\text{K}^+(\text{aq})$  at 0.0 ppm (adapted from Ref. [36]).

NMR spectroscopy with an anionic paramagnetic shift reagent,  $[\text{Dy}(\text{PPP})_2]^{7-}$  [42]. The intra- and extracellular  $^{39}\text{K}$  NMR signals are well separated (over 10 ppm, Fig. 5) at 5 mM concentration of the shift reagent. The NMR visibility of intracellular  $\text{K}^+$  was determined to be 100% in human erythrocytes. The measured intracellular concentration of  $\text{K}^+$  was  $110 \pm 12$  mM, thus establishing, at least in principle, the suitability of NMR spectroscopy for measuring  $\text{K}^+$  fluxes as well as ion concentrations in human RBCs.

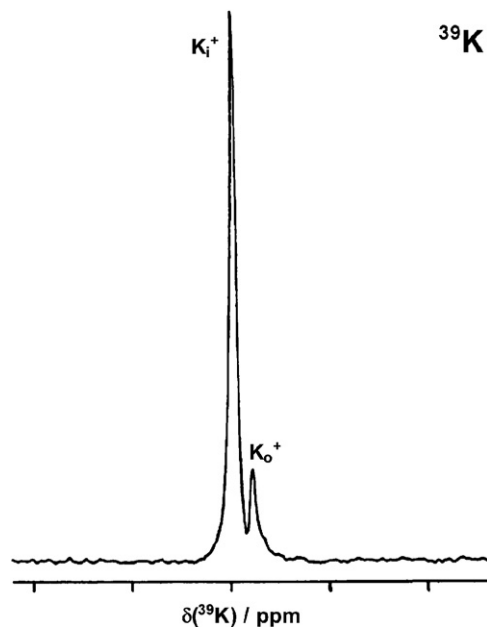


Fig. 5.  $^{39}\text{K}$  NMR spectrum of human RBCs resuspended in the NMR buffer at  $37^\circ\text{C}$ .  $K_i^+$  and  $K_o^+$  represent the intra- and extracellular  $^{39}\text{K}$  peaks, respectively. Hematocrit was 61.2%. One division in the spectrum is equal to 50 ppm (adapted from Ref. [42]).

### 3.1.4. Rubidium

Rubidium appears to have no natural biological role. It has two NMR-active isotopes, and despite the higher natural abundance of  $^{85}\text{Rb}$  (72.15%),  $^{87}\text{Rb}$  (27.85%) is the isotope of choice for NMR studies because of its more favorable spectroscopic properties.  $^{87}\text{Rb}$  is a spin  $I = 3/2$  quadrupolar nucleus and, as such, relaxes very rapidly, giving rise to broad resonance lines. The  $T_1$  and  $T_2$  relaxation times of  $^{87}\text{Rb}$  in free solution at  $25^\circ\text{C}$  are 2.5 ms, corresponding to a resonance of a natural line-width of 128 Hz.

$\text{Rb}^+$  is an established biological probe for  $\text{K}^+$  [43]. The rates of influx and efflux of  $\text{Rb}^+$  in living tissues and isolated cells have been measured by  $^{87}\text{Rb}$  NMR spectroscopy [44]. The relatively high natural abundance, low biological abundance, and high NMR sensitivity of  $^{87}\text{Rb}$  (about an order of magnitude greater than that of  $^{39}\text{K}$ ) make it a good tracer for  $\text{K}^+$  influx and efflux studies by NMR in cells and perfused organs [45]. Moreover, imaging the distribution of  $^{87}\text{Rb}$ , which mimics  $\text{K}^+$  as a substrate for the  $\text{Na}^+/\text{K}^+ \text{-ATPase}$  pump in myocardial cells, by MRI has potential for distinguishing necrotic and reversibly damaged tissue [46].

$\text{Rb}^+$  uptake data can be used to approximate  $\text{K}^+$  influx if there are no significant differences in ion selectivity of the different  $\text{K}^+$ -transporting systems. In addition to the  $\text{Na}^+$  pump,  $\text{K}^+$  and  $\text{Rb}^+$  are transported through the  $\text{Na}^+/\text{K}^+/\text{2Cl}^-$  cotransporter [47]. It is known that the kinetic properties of  $\text{K}^+$  and  $\text{Rb}^+$  with respect to  $\text{Na}^+/\text{K}^+ \text{-ATPase}$  are similar for cardiac and skeletal muscles, nerves, RBCs, human erythrocytes, cardiomyocytes and other tissues, and the equilibrium transmembrane  $\text{Rb}^+$  gradient is similar to that of  $\text{K}^+$  [45]. This implies similar ion selectivity of the systems transferring these ions inside and outside cells, thus supporting the role of  $\text{Rb}^+$  as a mimic for  $\text{K}^+$ .  $\text{Rb}^+$  uptake rates determined by  $^{87}\text{Rb}$  NMR spectroscopy (Fig. 6) are similar to those measured with atomic emission spectroscopy

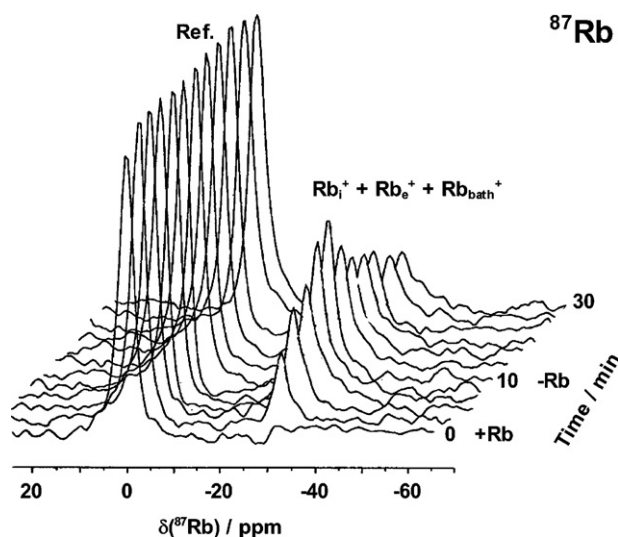


Fig. 6.  $^{87}\text{Rb}$  NMR spectra (referenced to internal  $\text{Rb}^+(\text{aq})$  at 0.0 ppm) of perfused rat heart during  $\text{Rb}^+$  load and washout. The hearts were perfused with phosphate-free Krebs–Henseleit buffer. The perfusate was equilibrated with 95%  $\text{O}_2/5\%$   $\text{CO}_2$ , with the pH maintained at 7.4. The buffer used for  $\text{Rb}^+$  loading contained 0.94 mM  $\text{Rb}^+$  and 3.76 mM  $\text{K}^+$  (adapted from Ref. [45]).

(AES), allowing estimates of  $K^+$  influx rates, which are comparable to those obtained with radioisotope tracers. The method does not require shift reagents because of the 8.5 times faster kinetics of  $Rb^+$  equilibration in the extracellular space compared with the intracellular space and the much higher concentration of  $Rb^+$  in the latter. Under normal physiological conditions,  $Rb^+$  influx occurs mainly through  $Na^+/K^+$ -ATPase, whereas the contribution of the  $Na^+/K^+/2Cl^-$  cotransporter and  $K^+$  channels to  $Rb^+$  influx is small. In addition, the rate of  $Rb^+$  accumulation measured non-invasively by  $^{87}Rb$  NMR spectroscopy can be used as an index of the  $Na^+$  influx rate.

Cardiac sarcolemmal  $K_{ATP}$  channels are crucial in adaptation to stress caused by metabolic inhibition and moderate exercise, which requires not only down-regulation of energy spending, but also up-regulation of mitochondrial ATP synthesis. To investigate sarcolemmal and mitochondrial effects of a Kir6.2 ( $K^+$  ion-selective subunit of the channel) knockout,  $^{87}Rb$  NMR has been used, showing that Kir6.2 knockout results in a lack of stimulation of the unidirectional potassium efflux from the heart which creates a primary defect leading to the development of non-insulin-dependent (type 2) diabetes [48].

### 3.1.5. Cesium

Interest in the biochemistry and physiology of cesium ions derives primarily from three areas: (i) applications related to alkali metal ion transport and enzyme activation; (ii) toxicological problems related to the uptake and passage through food chains of radioactive  $Cs^+$  produced in fission reactions; and (iii) applications of  $Cs^+$  as a pharmacologic agent in the treatment of behavioral depression [49]. The development of  $^{133}Cs$  NMR spectroscopy as a tool for  $Cs^+$  analysis has triggered the recent interest in the biochemistry and physiology of  $Cs^+$  in biological systems. As a congener of  $K^+$ , it accumulates in the intracellular space, primarily through the action of  $Na^+/K^+$ -ATPase. A unique observation on the NMR behavior of  $Cs^+$  is the resolution of intra- and extracellular  $^{133}Cs$  NMR resonances in  $Cs^+$ -loaded cell suspensions in the absence of shift reagents. The NMR chemical shift range of  $^{133}Cs$  is much larger than that of other alkali metal nuclei, and it is extremely sensitive to changes in chemical environment, solvents, temperature, and counter-ions present [50].  $^{133}Cs$  has a nuclear spin  $I = 7/2$ , a small quadrupole moment (giving rise to narrow NMR lines), and a relaxation rate approximately 200 times smaller than those of the other NMR detectable alkali metal nuclei.  $Cs^+$  is 100% visible by  $^{133}Cs$  NMR spectroscopy and its biomedical applications have been recently reviewed [51].

Intra- and extracellular resonances are readily resolved for suspended human erythrocytes and for perfused rat hearts treated with CsCl without the addition of paramagnetic shift reagents, required to resolve resonances of the other alkali metal ions, and the resulting spectra exhibit two resonances separated in chemical shift by 1.0–1.4 ppm (Fig. 7) [49]. In addition, it is possible to resolve the NMR signals of  $^{133}Cs$  in different tissue compartments on the basis of chemical shift or relaxation properties. This compartmental resolution applies not only to the intra- and extracellular spaces, but to subcellular compartments as well. For example, the interaction of the  $Cs^+$  with the anionic intracellular

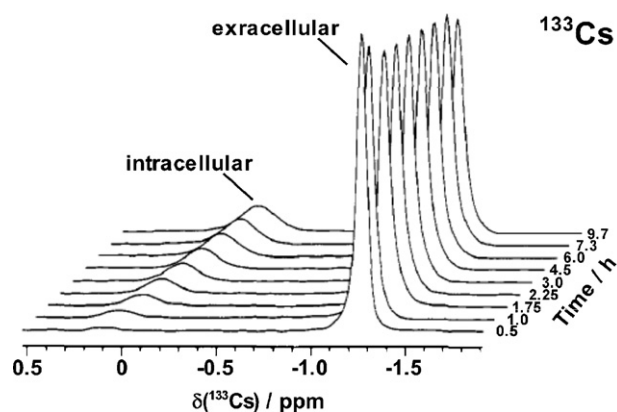


Fig. 7.  $^{133}Cs$  NMR spectra of human erythrocytes suspended in a buffer containing 140 mM NaCl and 10 mM CsCl. The origin of the chemical shift scale is arbitrary (adapted from Ref. [49]).

components of human RBCs has been investigated [52]. Investigations of  $Cs^+$  binding for RBCs using spin–lattice ( $T_1$ ) and spin–spin ( $T_2$ )  $^{133}Cs$  NMR relaxation measurements have shown that  $Cs^+$  binds more strongly to 2,3-bisphosphoglycerate (BPG) and RBC membranes than to any other intracellular component in RBCs at physiological concentrations.

$^{133}Cs$  NMR spectroscopy has also been used to evaluate the ion transport across membranes and the kinetic/chemical environment of the intracellular space in systems ranging from RBCs to rat brain [51,53]. It was demonstrated that, as a congener of  $K^+$ ,  $Cs^+$  accumulates in the intracellular space, primarily through the action of  $Na^+/K^+$ -ATPase and, thus, cesium is a valuable tool for non-invasively probing biological systems.

## 3.2. s-Block: alkaline earth metals (Mg, Ca)

### 3.2.1. Magnesium

Together with  $K^+$ ,  $Mg^{2+}$  is one of the major intracellular ions (typically 30 mM), and is 90% bound to ribosomes (complexes of RNA and proteins that mediate protein synthesis). Magnesium is vital to the regulation of the structures of tRNA and rRNA [54] and is an essential cofactor for many RNA and DNA processing enzymes [55] and for those enzymes using ATP, ADP, or AMP as substrates [56]. As metallotherapeutic drugs, magnesium salts are frequently prescribed to treat diseases such as gestational hypertension, preeclampsia and eclampsia, asthma, strokes, acute myocardial infarction, and arrhythmias [57]. Magnesium readily forms complexes with biological substrates and may serve to either define a particular conformation or catalytically activate chemical functionality toward reaction. The role of the metal ion is critically dependent on the coordination environment that it adopts, and so it is useful to understand the binding chemistry of  $Mg^{2+}$  in a biological context.

$^{25}Mg$  is a spin  $I = 5/2$  nucleus, and the interaction of its quadrupole moment with electric field gradients provides a very effective relaxation mechanism [58]. The observed line-shapes are sensitive to the motional and exchange dynamics of the  $Mg^{2+}$  ions, and thus provide insights into the interaction between  $Mg^{2+}$  and the various biomolecules. Given its low natural abundance (10.13%) and low receptivity (relative to  $^{13}C$ ), the use of iso-



Table 3

Determination of kinetic and thermodynamic parameters for  $\text{Mg}^{2+}$  binding to phosphate-containing ligands by  $^{25}\text{Mg}$  NMR spectroscopy

Ligand	$K_a$ ( $\text{M}^{-1}$ )	$\Delta G^*$ (kcal mol $^{-1}$ )	$k_{\text{off}}$ ( $\times 10^{-3}$ s $^{-1}$ )	$k_{\text{on}}$ ( $\times 10^{-3}$ s $^{-1}$ )	$K_{\text{os}}$ ( $\text{M}^{-1}$ )
tRNA (native)	220	12.8	2.5	$5.5 \times 10^5$	220
tRNA (non-native)	250	13.1	1.6	$4.0 \times 10^5$	250
[Glucose-1-P] $^{2-}$	15	12.7	2.9	$4.3 \times 10^4$	0.43
[Glucose-6-P] $^{2-}$	8	12.7	3.1	$2.5 \times 10^4$	0.25
$\text{CH}_3\text{CO}_2\text{PO}_3^{2-}$	9	13.1	1.5	$1.4 \times 10^4$	0.14
$\text{AMP}^{2-}$	18	12.7	3.4	$6.2 \times 10^4$	0.62
$\text{ADP}^{3-}$	$2.2 \times 10^3$	12.8	2.5	$5.5 \times 10^6$	55
$\text{ADPH}^{2-}$	13	12.1	7.7	$8.5 \times 10^4$	0.85
$\text{ATP}^{4-}$	$3.0 \times 10^3$	12.4	5.0	$1.5 \times 10^7$	150
$\text{ATPH}^{3-}$	6	12.5	4.2	$5.1 \times 10^4$	0.51

Adapted from Ref. [59].

topically enriched  $^{25}\text{Mg}^{2+}$  allowed a total line-shape analysis of  $^{25}\text{Mg}$  NMR spectra to determine the association constant ( $K_a$ ), the free energy of activation ( $\Delta G^*$ ), outer-sphere association constants ( $K_{\text{os}}$ ), and off-rate ( $k_{\text{off}}$ ) and on-rate ( $k_{\text{on}}$ ) for magnesium binding to several biologically relevant macromolecules, as summarized in Table 3 [59]. This work has provided a detailed knowledge of the coordination chemistry of  $\text{Mg}^{2+}$  with polyphosphate anions, supporting the outer-sphere coordination of  $[\text{Mg}(\text{H}_2\text{O})_6]^{2+}$  to RNA, and suggesting that magnesium binding to a terminal phosphate leads to facile protonation of an inner phosphate that results in a reactive pyrophosphate-type center.

$^{25}\text{Mg}$  NMR has also been used to investigate the interaction between  $\text{Mg}^{2+}$  and calmodulin (a calcium-binding protein that can bind to and regulate a multitude of different protein targets, thereby affecting many different cellular functions) [60]. Tsai et al. demonstrated that  $\text{Mg}^{2+}$  shows opposite site preference relative to  $\text{Ca}^{2+}$  and binds to sites I and II of calmodulin with a binding constant of  $\sim 2000 \text{ M}^{-1}$ , whereas it binds weakly to sites III and IV. Since the intracellular concentration of  $\text{Mg}^{2+}$  is higher than that of  $\text{Ca}^{2+}$ , they hypothesized that sites I and II are constantly occupied by  $\text{Mg}^{2+}$  at the resting state. Analogously, the interactions between  $\text{Mg}^{2+}$  and other biomolecules, such as adenylate kinase (a phosphotransferase enzyme requiring  $\text{Mg}^{2+}$  to catalyze the production of ATP from ADP) [61] and several biological polyelectrolytes [62], have been studied by  $^{25}\text{Mg}$  NMR spectroscopy. In both cases, it was demonstrated that magnesium ions bind loosely to the investigated actin filaments, and thus show a behavior typical of counter-ions.

### 3.2.2. Calcium

Calcium is an important element in the human body and is located principally in the bones and teeth as apatite, a calcium phosphate mineral. Blood is also a huge reservoir of calcium in animals. Calcium is distributed throughout all tissues where it has special roles in controlling blood pressure, nerve impulse transmission, muscle action, blood clotting and cell permeability [6b]. Calcium supplements (usually carbonate, citrate, gluconate or lactate salts) are taken to protect against osteopenia, osteoporosis, and hypertension, and calcium-based drugs play a role in preventing high blood cholesterol, diabetes, and major pregnancy complications.  $\text{CaCO}_3$  is also marketed as an antacid

relieving the pain and discomfort of indigestion, heartburn and other symptoms related to excess stomach acid [63].

Together with  $\text{Na}^+$ ,  $\text{Ca}^{2+}$  is one of the major extracellular ions (typically 4 mM). A combination of rapid exchange kinetics and strong ligand binding allows  $\text{Ca}^{2+}$  to be an effective trigger ion for the activation of biological reactions. Many processes of signal transduction involve the release of calcium ions as one part of an interconnected set of pathways. Increases in intracellular  $\text{Ca}^{2+}$  are sensed by a family of calcium-binding proteins. A prototypical member of this family is calmodulin, which couples changes in the intracellular calcium concentration to the state of activation of a variety of enzymes, such as protein kinases, NAD kinase, and phosphodiesterases, as well as some  $\text{Ca}^{2+}$ -ATPases [64].

$^{43}\text{Ca}$  is a spin  $I = 7/2$  nucleus and is the only spectroscopically observable isotope of this biologically important element. The NMR properties of  $^{43}\text{Ca}$  are unfavorable due to its low resonance frequency, low natural abundance (0.145%), and the fact that magnetic relaxation is dominated by the quadrupole relaxation, thus explaining the paucity of data available. Nevertheless,  $^{43}\text{Ca}$  NMR has provided a few insights into the structural and motional characteristics of calcium-binding sites in a number of calcium-binding proteins [65]. In general it is extremely difficult to observe directly NMR signals from quadrupolar ions bound to proteins. If there is a reasonably fast chemical exchange of ions between the bulk solution and the protein-binding sites valuable information about the ion binding can be obtained. For example, the  $^{43}\text{Ca}$  NMR signals from  $\text{Ca}^{2+}$  ions bound to the Ca-binding proteins parvalbumin, troponin-c and calmodulin have been observed [66]. The observation was made possible through the use of isotopically enriched  $^{43}\text{Ca}^{2+}$ . The chemical shift of  $^{43}\text{Ca}^{2+}$  ion bound to the three proteins is ca. +60 ppm (relative to free  $\text{Ca}^{2+}$  ions in aqueous solution), and all have a similar magnitude of the quadrupole coupling constant. This observation supports the argument that the  $\text{Ca}^{2+}$ -binding sites in these proteins have the same arrangements of oxygen ligands coordinated to the  $\text{Ca}^{2+}$  ion. A similar study has been carried out to evaluate the exchange rates and the binding constants of  $\text{Ca}^{2+}$  ions to the high-affinity and low-affinity binding sites on calmodulin [67]. The temperature dependence of the  $^{43}\text{Ca}$  NMR signals showed that the two classes of sites have exchange rates differing by a

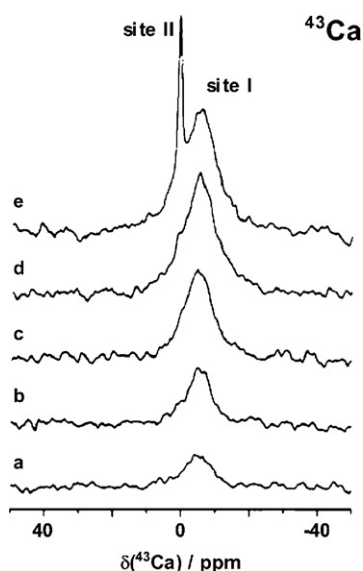


Fig. 8.  $^{43}\text{Ca}$  NMR spectra of the titration of 0.33 mM equine apolyszyme with  $^{43}\text{Ca}^{2+}$  at pH 6.0. 200k scans were collected in each experiment: (a) 0.23 equiv. of  $^{43}\text{Ca}^{2+}$ ; (b) 0.46 equiv. of  $^{43}\text{Ca}^{2+}$ ; (c) 0.69 equiv. of  $^{43}\text{Ca}^{2+}$ ; (d) 0.92 equiv. of  $^{43}\text{Ca}^{2+}$ ; (e) 1.15 equiv. of  $^{43}\text{Ca}^{2+}$  (adapted from Ref. [68]).

factor of about 40 at room temperature. At temperatures  $\leq 30^\circ\text{C}$ , only the two sites with fast exchange (*i.e.* the low-affinity sites) were probed by  $^{43}\text{Ca}$  NMR.

The calcium-binding properties of equine and pigeon lysozyme as well as those of bovine and human  $\alpha$ -lactalbumin have been investigated by  $^{43}\text{Ca}$  NMR spectroscopy [68]. An example is given in Fig. 8. Upon addition of the isotopically enriched  $^{43}\text{Ca}$  to equine lysozyme, a broad peak ( $\Delta\nu_{1/2} = 253$  Hz) appears at  $-5.3$  ppm, and the signal increases linearly in intensity up to 1 equiv. of metal ion. This resonance corresponds to calcium bound to the single high-affinity calcium site in this protein. In the presence of excess metal ion, a sharp signal ( $\Delta\nu_{1/2} = 10$  Hz) is also observed at 1 ppm, in the vicinity of free calcium. All proteins were found to contain one high-affinity calcium-binding site. The chemical shifts, line-widths, relaxation times, and quadrupolar coupling constants for the respective  $^{43}\text{Ca}$  NMR signals were quite similar; this is indicative of a high degree of homology between the strong calcium-binding sites of these four proteins. The measured chemical shifts ( $\delta = -3$  to  $-7$  ppm) and quadrupolar coupling constants ( $\chi = 0.7$ – $0.8$  MHz) are quite distinct from those observed for typical EF-hand calcium-binding proteins, suggesting a different geometry for the calcium-binding loops. The correlation times for bound calcium ions in these proteins are in the range of 4–8 ns, indicating that the flexibilities of these binding sites are limited. Evidence for the existence of a second weak calcium-binding site was obtained for bovine  $\alpha$ -lactalbumin, but not for the other investigated proteins.

### 3.3. *p*-Block: Group 13 (B, Al, Ga, In, Tl)

#### 3.3.1. Boron

Boron is regarded as a non-essential element for mammalian life, even if it may turn out to be a necessary “ultratracer”

element [3]. The main medicinal application of boron is the tumor-targeted delivery of boron derivatives for boron neutron capture therapy (BNCT) [69]. This therapy is based on the nuclear reaction that occurs when  $^{10}\text{B}$ , a stable isotope, is irradiated with neutrons of the appropriate energy to produce  $^{11}\text{B}$  in an unstable form, which then undergoes instantaneous nuclear fission to produce high-energy alpha particles and recoiling  $^7\text{Li}$  nuclei ( $^{10}\text{B} + n_{\text{th}} \rightarrow [^{11}\text{B}] \rightarrow \alpha + ^7\text{Li}$ ). These heavy charged particles have pathlengths of approximately one cell diameter (10–14  $\mu\text{m}$ ) and deposit most of their energy within the boron-containing cells. If enough low-energy thermal neutrons ( $n_{\text{th}}$ ) reach the treatment volume, and  $^{10}\text{B}$  is selectively delivered to tumor cells in amounts higher than in the surrounding normal tissues, then they can be destroyed as a result of the  $^{10}\text{B}(n,\alpha)^7\text{Li}$  capture reaction that causes local tumor cell necrosis. In theory, BNCT provides a means for the specific molecular and cellular targeting of high linear energy transfer radiation to tumor cells with the concomitant sparing of normal cells. BNCT has been used clinically to treat patients with brain cancers, such as glioblastoma multiforme, with high-grade gliomas, and a much smaller number with primary and metastatic melanoma. Delivery vehicles synthesized for this application include sodium borocaptate (BSH,  $\text{Na}_2\text{B}_{12}\text{H}_{11}\text{SH}$ ), boranophosphonates and boranobis(phosphonates), and boranophosphate-oligodeoxynucleotides, in which  $\text{BH}_3$  is linked to the phosphate backbone of antisense oligodeoxynucleotides [70].

Boron NMR is typically suitable to study the binding of boron agents. Both  $^{10}\text{B}$  and  $^{11}\text{B}$  have NMR activity, but  $^{11}\text{B}$  has higher sensitivity (16.5% vs. 2% relative to  $^1\text{H}$ ) and higher natural abundance (80.42% vs. 19.58%). Even though  $^{10}\text{B}$  is the active nucleus for neutron capture in BNCT, the more sensitive  $^{11}\text{B}$  is more appropriate in NMR studies, and the isotopic difference does not alter either the structure and binding or the pharmacokinetic effects of the agent. Both  $^{10}\text{B}$  ( $I=3$ ) and  $^{11}\text{B}$  ( $I=3/2$ ) are quadrupolar nuclei and their relaxation times in common BNCT agents in biological environments are rather short. NMR research efforts have primarily been applied in two directions: first, to investigate the metabolism and pharmacokinetics of BNCT agents *in vivo*, and, second, to use localized NMR spectroscopy and/or MRI for non-invasive mapping of the administered molecules in treated animals or patients. While the first goal can be pursued using  $^{11}\text{B}$  NMR for natural abundance samples, molecules used in BNCT are  $>95\%$  enriched in  $^{10}\text{B}$ , and must be therefore detected by  $^{10}\text{B}$  NMR. In particular, the *in vivo* distribution of these agents can be imaged using  $^{10}\text{B}$  MRI [71].

The first attempts to investigate the interaction between boron derivatives and biomolecules by  $^{11}\text{B}$  NMR spectroscopy were conducted over a decade ago. Peptide boronic acids are exceptionally potent inhibitors of serine proteases. Owing to the large number of serine proteases that have been demonstrated to play crucial roles in biological systems, the high affinity and specificity achievable with boronic acid-based inhibitors make them of considerable interest both as research tools and as potential therapeutic agents. A number of boronic acid inhibitors form boron–histidine adducts with  $\alpha$ -lytic protease. An  $^{11}\text{B}$  NMR study on this MeOSuc-Ala-Ala-Pro-boroPhe-histidine adduct



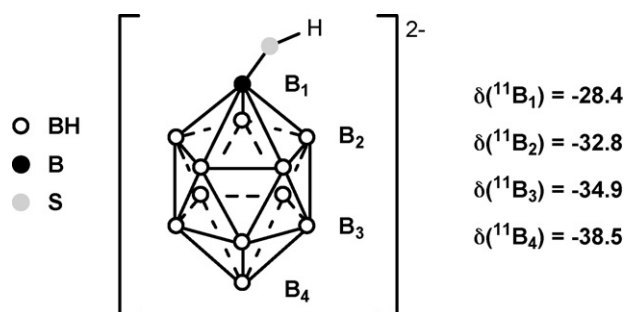


Fig. 9. Schematic illustration of the BSH anion. There is a net negative charge of 2 in the boron-hydride cage.  $\delta(^{11}\text{B})$  of free BSH are referenced to saturated  $\text{H}_3\text{BO}_3$  at 0.0 ppm (adapted from Ref. [73]).

complex and on two other complexes known to be serine adducts (namely  $\alpha$ -lytic protease with MeOSuc-Ala-Ala-Pro-boroVal and chymotrypsin with MeOSucAla-Ala-Pro-boroPh) showed, in all cases, resonances at *ca.*  $-16.6$  ppm, demonstrating that the boron atom is tetrahedral in both the histidine and serine adduct (trigonal boron species are reported to resonate at around 0 ppm) [72].

The interaction between the BNCT agent sodium borocaptate (BSH) and serum albumin is of interest since it is related to the pharmacokinetics of BSH.  $^{11}\text{B}$  NMR was used to achieve quantitative analysis of this interaction *via* both chemical shifts and relaxation rates of  $^{11}\text{B}$  nuclei in BSH [73]. The 12 boron nuclei of BSH can be classified into four groups, each showing a well-defined chemical shift (Fig. 9). Covalent binding of BSH to a large protein changes the chemical environment around the  $^{11}\text{B}$  nuclei causing changes in both the chemical shifts (the formation of a disulfide bridge between BSH and serum albumin moves the  $^{11}\text{B}$  chemical shift of the S-attached boron atom, labeled as  $\text{B}_1$  in Fig. 9, *ca.* 3 ppm downfield) and the relaxation rates of the quadrupolar nuclei. However, the observation of no chemical shift change under the employed experimental conditions, the measured values of relaxation rates, and the calculated binding parameters indicated a non-covalent binding between BSH and serum albumin (bovine, human or dog). The nature of this interaction may, in part, be electrostatic. Bound and free BSH are in fast exchange at temperatures between 295 and 310 K, and the number of BSH-binding sites on these proteins is about 3–5.

Cytochrome-*c* is a globular, 12 kDa, heme protein with a positively charged surface that serves as an electron carrier in cell mitochondria. Ionic interactions with the surface of the cytochrome are believed to play a significant role in the direction of the interaction between the cytochrome and the enzymatic aggregates, cytochrome reductase and oxidase, thus influencing the efficiency of electron transfer [74]. Cytochrome-*c* is known to bind small anions, including metabolites such as phosphate ions and ATP. This interaction affects the mobility of the electron carrier protein and has been interpreted as an extra role for the protein as an ion carrier. The binding of borate ion to cytochrome's surface has been studied by  $^{11}\text{B}$  NMR [75]. Fig. 10a shows the  $^{11}\text{B}$  spectrum at 11.4 T of a 100 mM borate solution with 4 mM ferricytochrome-*c* at pH 9.7 and 5 °C. The large peak at 7.1 ppm (peak z) has the same shift as that of the weighted average of 70%  $\text{B}(\text{OH})_4^-$  exchanging with 30% of

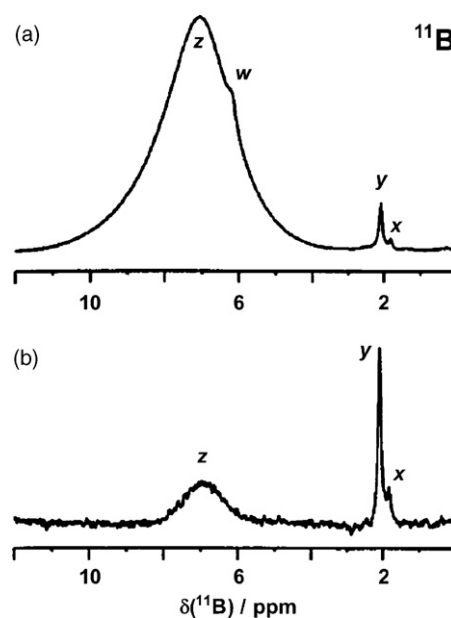


Fig. 10. The  $^{11}\text{B}$  (a) single quantum and (b) MQF ( $\tau = 1.4$  ms) NMR spectra of 100 mM borate solution with 4 mM ferricytochrome-*c* at 5 °C, 11.4 T, and pH 9.7 (adapted from Ref. [75]).

$\text{B}(\text{OH})_3$ . The peaks at 2.1 (peak y) and 1.8 (peak x) ppm are assigned to  $\text{B}(\text{OH})_4^-$  specifically bound to two conformations of ferricytochrome-*c* that are present at pH 9.7 [76]. The assignment is based on the chemical shift which is similar to that of free  $\text{B}(\text{OH})_4^-$  (2.0 ppm), and the narrow line-width of 14 Hz which is consistent with the tetrahedral symmetry of this species [76]. The peak at around 6 ppm (peak w) in Fig. 10a is presently unassigned. A multiple quantum filtered (MQF) NMR experiment yields a spectrum with three peaks (b), two at the specific binding site at around 2 ppm and one at the chemical shift of the borate/boric acid bulk peak at 7.1 ppm, suggesting two different types of binding sites designated as I (for slowly exchanging borate ion) and II (for fast exchanging borate ion and boric acid), respectively. Thus, detection of binding by MQF NMR experiments proved to be sensitive to fast exchanging ligands as well as to very weak binding that could not be detected using conventional single-quantum methods.

### 3.3.2. Aluminum

Aluminum is the third most abundant metal in the Earth's crust, which comprises approximately 8 wt.% Al, and the natural element consists entirely of the  $^{27}\text{Al}$  isotope. It is a non-essential element that during the last three decades has been recognized as a potentially toxic element linked to neurological problems, especially dialysis encephalopathy, and possibly Alzheimer's disease, and also to some bone disorders and problems in the hematopoietic system, muscles and joints [77]. The normal blood plasma aluminum concentration is about  $0.005 \text{ mg L}^{-1}$ . Blood contains less than 1% of the aluminum body burden, of which about 80% is bound to proteins. It accumulates mainly in the liver, bones and spleen of humans and animals. Because of its low solubility in solution under neutral conditions, Al was regarded as a non-toxic element and its environmental and

biological effects were not investigated until recently. But due to the increasing acidity of the environment and concomitant dissolution of aluminum minerals, the concentration of this element in fresh waters can increase considerably. On the other hand, aluminum-based drugs are sold as antacids ( $[\text{Al}(\text{OH})_3]$ ,  $[\text{Al}_2(\text{CO}_3)_3]$ ) and in the treatment of malaria ( $[\text{Al}(\text{OH})_3]$ ). Three aluminum salts (alum,  $[\text{Al}(\text{OH})_3]$ ,  $[\text{Al}(\text{PO}_4)]$ ) have been also added to many vaccines, including widely used formulations for diphtheria, hepatitis B and tetanus, as adjuvant (“vaccine boosters”) [78]. Moreover, the magnetic resonance characteristics of this nuclide also make it suitable for medical applications ( $^{27}\text{Al}$ -based MRI is feasible) [79].

$^{27}\text{Al}$  is more amenable to NMR studies than its congeners due to a higher receptivity and the existence of only one isotope. Another attractive feature of this nucleus is the relatively small quadrupole moment associated with its high nuclear spin ( $I=5/2$ ). These two favorable factors result in a much higher relative peak height (by one order of magnitude or more compared to the other elements of Group 13). This means that sufficient signal-to-noise ratios can be obtained even with dilute ( $\sim 0.01$  M) solutions of aluminum compounds.  $^{27}\text{Al}$  line-widths may vary from 3 Hz to several kHz, and the signal may even completely vanish into the baseline noise in some instances. This negative aspect of quadrupolar relaxation is counterbalanced by the additional information obtained concerning molecular symmetries from the magnitude of quadrupolar line-broadenings. The range of  $^{27}\text{Al}$  NMR chemical shifts is about 450 ppm.

The major metal transport protein in blood plasma is the bilobal glycoprotein transferrin. Transferrin is too big for complete structural determination in solution by current multi-dimensional NMR techniques ( $^1\text{H}$  NMR signals are intrinsically broad due to slow molecular tumbling), but  $^{27}\text{Al}$  NMR can be used to investigate directly the metals in their specific binding sites and to reveal subtle inter-site differences [80]. Human serum transferrin (Fig. 11) is the protein that transports  $\text{Fe}^{3+}$  ions and it is a member of a small group of monomeric non-heme proteins (MW  $\sim 76$ – $81$  kDa), which includes lactoferrin, ovotransferrin and melanotransferrin. It has two binding sites for ferric ions (these are found in a six-coordinate, distorted

octahedral coordination geometry) which are identified as C-terminal and N-terminal sites. Two tyrosines, one histidine and one aspartate constitute four protein ligands for the metal ion, which requires a synergistic anion for the formation of stable transferrin complexes. *In vivo* bidentate  $\text{CO}_3^{2-}$  serves this purpose by coordinating directly to the metal in the fifth and sixth coordination positions. Since serum transferrin is normally only about 30% saturated with iron, it retains a relatively high capacity for binding to other metal ions. Vogel and Aramini demonstrated the feasibility of using  $^{27}\text{Al}$  NMR to probe the binding of  $\text{Al}^{3+}$  to ovotransferrin and its half-molecules in the presence of carbonate or oxalate as synergistic anions [81]. The ovotransferrin-bound  $^{27}\text{Al}$  NMR signals have some rather unusual properties characteristic of quadrupolar nuclei bound in slow exchange to large macromolecules far from extreme narrowing conditions. First, the maximum intensity of the protein-bound  $^{27}\text{Al}$  signal is substantially lower than that observed for equimolar solutions of the free metal ion. Second, the signals exhibit a unique pulse angle dependence where a maximum in peak intensity is attained at pulse lengths that are less than half the  $90^\circ$  pulse for an aqueous  $\text{Al}^{3+}$  solution. Third,  $^{27}\text{Al}$  signals for  $\text{Al}^{3+}$  bound to the half-molecules of ovotransferrin are much broader than those for the intact protein, reflecting the importance of molecular motion on the detectability of quadrupolar nuclei. Fourth, an increase in the external magnetic field strength causes line narrowing and a 2–4 ppm downfield dynamic frequency shift (Fig. 12) [82]. These data are all consistent with the idea that only the central ( $1/2 \rightarrow -1/2$ ) transition of the  $^{27}\text{Al}$  nucleus is observed. The chemical shifts of the  $^{27}\text{Al}$  signals from  $\text{Al}_2$ -ovotransferrin were found to be within the range +40 to  $-46$  ppm, which is in accordance with a six-coordinate (octahedral) Al complex. From these assignments and titration experiments it was found that in the presence of carbonate the N-terminal site of ovotransferrin binds  $\text{Al}^{3+}$  with a higher affinity than does the C-site. However, changing the synergistic anion to oxalate alters the specificity (Fig. 13) [81].

The interaction of  $\text{Al}^{3+}$  with biologically relevant phosphates is important [6b]. In membrane systems,  $\text{Al}^{3+}$  ion binds strongly to the phosphate head groups of the membrane lipids. The neuro-

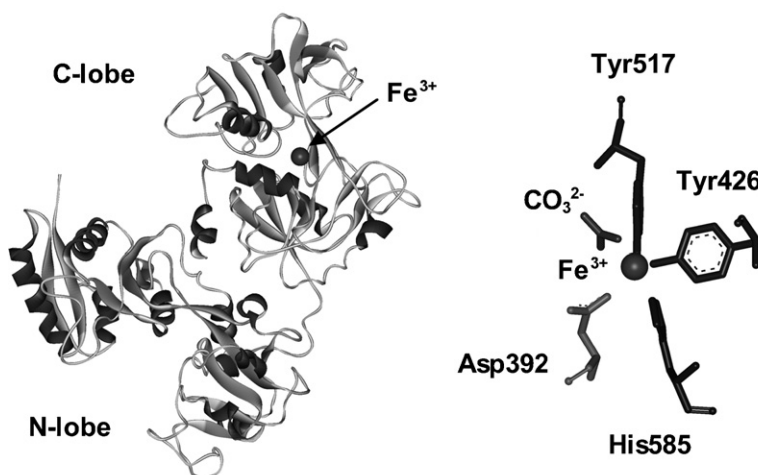


Fig. 11. Backbone structure of human serum transferrin (coordinates supplied by Zuccola [245]); only the C-lobe site is occupied by iron in this structure.

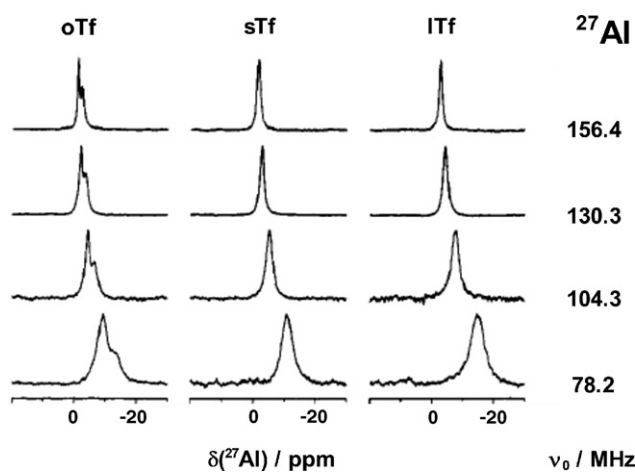


Fig. 12.  $^{27}\text{Al}$  NMR spectra (referenced to external 1.0 M  $[\text{Al}(\text{NO}_3)_3]$  in  $\text{D}_2\text{O}$  at 0.0 ppm) of ovotransferrin (oTf, 1.13 mM, pH 7.5), serotransferrin (sTr, 1.09 mM, pH 7.3), and lactoferrin (lTf, 0.73 mM, pH 7.5) in the presence of 20 mM  $\text{Na}_2^{13}\text{CO}_3$  and 2.0 equiv. of  $\text{Al}^{3+}$  (75%  $\text{H}_2\text{O}/25\%$   $\text{D}_2\text{O}$ , 150 mM KCl, 25 °C) at four magnetic fields: 7.0 T ( $\nu_0 = 78.2$  MHz), 9.4 T ( $\nu_0 = 104.3$  MHz), 11.7 T ( $\nu_0 = 130.3$  MHz), and 14.1 T ( $\nu_0 = 156.4$  MHz) (adapted from Ref. [82]).

toxicity of  $\text{Al}^{3+}$  is also manifested by inhibiting certain enzymes, such as ATPase. It is possible that the  $\text{Al}^{3+}$  ion, once bound to ATP, interferes with  $\text{Mg}^{2+}$  so that any consequent reactions requiring  $\text{Mg}^{2+}$ –ATP complex participation are inhibited. This has prompted the study of the binding of  $\text{Al}^{3+}$  to ATP by  $^{27}\text{Al}$  NMR. The line-widths of these complexes typically fall within the range 150–500 Hz. Detellier and co-workers [83] studied these interactions at pH 7.4 using multinuclear NMR spectroscopy. The  $^{27}\text{Al}$  NMR study allowed them to identify two complexes coexisting in equilibrium: 2:1  $[\text{Al}(\text{ATP})_2]$  and 1:1  $[\text{Al}(\text{ATP})]$  complexes.

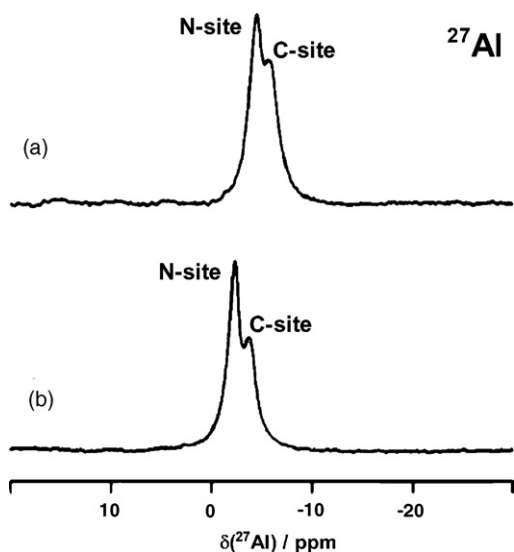


Fig. 13.  $^{27}\text{Al}$  NMR spectra (referenced to external 1.0 M  $[\text{Al}(\text{NO}_3)_3]$  in  $\text{D}_2\text{O}$  at 0.0 ppm) of (a) 1.20 mM ovotransferrin in the presence of 5 mM  $\text{Na}_2^{13}\text{C}_2\text{O}_4$  and 2.0 equiv. of  $\text{Al}^{3+}$  (75%  $\text{H}_2\text{O}/25\%$   $\text{D}_2\text{O}$ , 150 mM KCl, pH 7.4, 25 °C), and (b) 1.13 mM ovotransferrin in the presence of 20 mM  $\text{Na}_2^{13}\text{CO}_3$  and 2.0 equiv. of  $\text{Al}^{3+}$  (75%  $\text{H}_2\text{O}/25\%$   $\text{D}_2\text{O}$ , 150 mM KCl, pH 7.6, 25 °C) at a magnetic field strength of 11.7 T (130.3 MHz) (adapted from Ref. [81a]).

$^{27}\text{Al}$  NMR spectroscopy has also been employed to study aluminum-containing complexes present in natural waters [77]. For example, Casey and co-workers studied the rates of solvent exchange in aqueous  $\text{Al}^{3+}$ –maltolate complexes [84]. Maltolate is a natural product that can be isolated from larch trees but is now widely used as a food additive. It is soluble in water, and tris complexes of  $\text{Al}^{3+}$  with this ligand are toxic and cause brain disease. With the help of a multi-temperature  $^{27}\text{Al}$  NMR study, it was shown that the maltolate labilizes the inner-sphere water molecules of  $\text{Al}^{3+}$  complexes to an extent similar to other bidentate ligands, such as methylmalonate, dicarboxylate and carboxylate plus phenolic ligands. Coordination of a single maltolate ligand into the inner-coordination sphere of  $[\text{Al}(\text{H}_2\text{O})_6]^{3+}$  increases the exchange rate of the remaining bound water molecules with bulk solution by a factor of  $\sim 10^2$ . Addition of a second ligand, to form the bis-bidentate complex,  $[\text{Al}(\text{maltolate})_2(\text{H}_2\text{O})_2]^+$ , increases the rate by an additional factor of 6–7.

### 3.3.3. Gallium, indium and thallium

Although none of the Group 13 elements is considered essential to life, their trivalent ions are, nonetheless, of much biological interest. Gallium is present in human tissues at a level of only  $10^{-4}$  to  $10^{-3}$  ppm [85]. It has two naturally occurring isotopes ( $^{69}\text{Ga}$ , 60.4%;  $^{71}\text{Ga}$ , 39.6%) and 13 radioactive nuclides.  $^{67}\text{Ga}$  ( $\gamma$ ,  $t_{1/2} = 3.25$  days) and  $^{68}\text{Ga}$  ( $\beta^+$ ,  $t_{1/2} = 68$  min) are two radioisotopes with appropriate energies and half-lives for  $\gamma$ -scintigraphy and positron emission tomography (PET), respectively. As well as imaging applications, the Auger electrons emitted by  $^{67}\text{Ga}$  possess potent cytotoxicity pointing towards potential therapeutic applications of the radionuclide, while the positrons emitted by  $^{68}\text{Ga}$  may also have therapeutic applications in the prevention of restenosis by intracoronary radiation therapy [86]. Although most reports of gallium pharmaceutical chemistry concern applications of its radioisotopes, the tumor-seeking and antineoplastic properties of  $\text{Ga}^{3+}$  were recognized 30 years ago. The safety and activity of simple gallium salts, mainly intravenous gallium nitrate, have been extensively studied in clinical trials since 1975 [87]. Development of anticancer gallium complexes has been pursued as a strategy to circumvent the limitations faced with simple gallium salts. In particular, efforts to improve the bioavailability of gallium *via* the oral route have recently led to the selection of the complexes tris(8-quinolinolato)gallium(III) (KP46) [88] and tris(3-hydroxy-2-methyl-4H-pyran-4-onato)gallium(III) (gallium maltolate) [89] for clinical studies.

Despite the non-ideal imaging characteristics of its gamma emissions,  $^{111}\text{In}$  ( $\gamma$ ,  $t_{1/2} = 2.82$  days) is also a popular radiolabel for targeting biomolecules which is widely employed in nuclear medicine for  $\gamma$ -imaging, probably because of the simplicity of its bioconjugate chemistry. Its radioisotopes are administered to the patients in the form of stable chelates [86].

$^{69/71}\text{Ga}$  ( $I = 3/2$ ) and  $^{113/115}\text{In}$  ( $I = 9/2$ ) are NMR-active isotopes. They are characterized by a high sensitivity to detection by NMR and large chemical shift ranges, two factors that make their study relatively easy.  $^{71}\text{Ga}$  has higher receptivity and narrower

Table 4

$^{71}\text{Ga}$  and  $^{115}\text{In}$  NMR chemical shifts and line-widths ( $W_{1/2}$ ) of some complexes of Group 13 metal ions with potential applications in imaging and radioimmunotherapy

Ligand	$^{71}\text{Ga}$		$^{115}\text{In}$	
	$\delta$ (ppm)	$W_{1/2}$ (Hz)	$\delta$ (ppm)	$W_{1/2}$ (Hz)
H <sub>2</sub> O	0	53	0	375–18,000
NOTA	+171	210	–	–
NODASA	+165	1000	–	–
NOTP	+110	434	–	–
H <sub>3</sub> ppma	–62.3	50	–14.7	1,630
TAMS	+34	3400	–	26,000
TAPS	+57	1230	–	22,00

Adapted from Ref. [77]. Ligands: NOTA, 1,4,7-triazacyclononane-1,4,7-triacetate; NODASA, 1,4,7-triazacyclononane-1-succinic acid-4,7-diacetate; NOTP, 1,4,7-triazacyclononane-1,4,7-tris-(methylenephosphonate); H<sub>3</sub>ppma, tris(4-(phenylphosphinato)-3-methyl-3-azabutyl)amine; TAMS, 1,1,1-tris((2-hydroxy-5-sulfobenzyl)-amino)methyl)ethane; TAPS, 1,2,3-tris((2-hydroxy-5-sulfobenzyl)-amino)propane.

line-widths than  $^{69}\text{Ga}$ , which means that  $^{71}\text{Ga}$  is usually the more favorable isotope for direct NMR observations despite its lower natural abundance. The chemical shift range of the gallium nucleus is approximately 1400 ppm [90].  $^{113}\text{In}$  and  $^{115}\text{In}$  have large quadrupole moments which make their line-widths very sensitive to the environmental symmetry of the indium nucleus. The low receptivity of  $^{113}\text{In}$  accounts for the lack of NMR studies based on this nuclide. The chemical shift range of the indium nucleus is approximately 1100 ppm [91].

Gallium- and indium-based radiopharmaceuticals are generally chelated with suitable ligands that form kinetically and thermodynamically stable complexes *in vivo*. Triazamacrocyclic ligands with different types of pendant arms often prove to be suitable. The thermodynamic stability of gallium and indium complexes with potential applications in imaging and radioimmunotherapy has been widely investigated *in vitro* and *in vivo* by NMR. Examples are summarized in Table 4 [77].

The redox chemistry of thallium is considerably different from that of the other elements of the group; under standard conditions the most stable oxidation state is  $\text{Tl}^+$ , although  $\text{Tl}^{3+}$  may also exist under biological conditions [77]. Thallium salts are poisonous due to the ability of the thallos ion to mimic alkali metal ions, especially  $\text{K}^+$  [92].

$^{203}\text{Tl}$  and  $^{205}\text{Tl}$  are the only non-quadrupolar NMR-active nuclei in the Group 13 family, and have high receptivities,  $^{203}\text{Tl}$  being only slightly less receptive than  $^{31}\text{P}$ , while  $^{205}\text{Tl}$ , the third most receptive spin  $I = 1/2$  nuclide, is twice as receptive as  $^{31}\text{P}$ . Because of its similarity to the alkali metal ions,  $\text{Tl}^+$  has potential as a probe for  $\text{Na}^+$  and  $\text{K}^+$  in biological systems. Like  $^{27}\text{Al}$ ,  $^{205}\text{Tl}$  NMR can be used to investigate directly the specific binding sites of transferrins. Due to its high receptivity,  $^{205}\text{Tl}$  NMR signals of protein-bound Tl ions can be observed even at mM concentrations. The first  $^{205}\text{Tl}$  NMR study of human serum transferrin was reported over 20 years ago by Bertini et al. [93]. These authors showed that  $^{205}\text{Tl}$  NMR is a convenient probe to monitor the occupancy of the two available transferrins and characterized the dithallium(III)-transferrin and

the monothallium derivatives with bicarbonate as synergistic ion. The high affinity of the protein for trivalent metal ions was thought to be responsible for the stabilization of the 3+ oxidation state of the metal. Two distinct  $^{205}\text{Tl}$  NMR signals (at +2075 and +2055 ppm downfield from an aqueous solution of  $\text{Tl}^+$  at infinite dilution) of similar shape were found for the  $(\text{Tl(III)})_2$ -transferrin derivative at physiological pH. The two signals are relatively broad ( $\Delta\nu_{1/2} \approx 100$  Hz) and show a different pH dependence (the signal at +2055 ppm was shown to be more resistant to acidification). At physiological pH the  $\text{Tl}^{3+}$  ion was shown to bind sequentially to the two sites; the signal at +2055 ppm appeared first and was assigned to  $\text{Tl}^{3+}$  bound to the acid-resistant C-terminal site. The signal at +2075 ppm was assigned to  $\text{Tl}^{3+}$  bound to the N-terminal site. Using  $^{13}\text{C}$  NMR spectroscopy to study the  $^{205}\text{Tl}$ -transferrin- $^{13}\text{CO}_3$  derivative, the same group showed that the  $^{13}\text{C}$  nucleus of the synergistic anion is strongly magnetically coupled to the  $^{205}\text{Tl}$  nucleus so that its  $^{13}\text{C}$  signal is split into a doublet. So, the  $^{13}\text{C}$  NMR spectrum of  $^{205}\text{Tl}_2$ -transferrin- $(^{13}\text{CO}_3)_2$  would originate from the superposition of two doublets, the extent of the coupling constants (290 and 265 Hz) being typical of a  $^2J(^{205}\text{Tl}-^{13}\text{C})$  coupling. This result constituted evidence of carbonate coordination to the metal [94]. Similar experiments were carried out by Aramini and Vogel to investigate the binding of  $^{205}\text{Tl}$  to chicken ovotransferrin in the presence of carbonate as the synergistic anion [95]. Two  $^{205}\text{Tl}$  NMR signals due to the bound metal ion in the two high-affinity iron-binding sites of the protein were detected, and, from titration studies, it was demonstrated that  $\text{Tl}^{3+}$  shows no site preference in ovotransferrin. Again, when  $^{13}\text{C}$ -labelled carbonate was used, two closely spaced doublets in the carbonyl region of the  $^{13}\text{C}$  NMR spectrum of ovotransferrin were recorded due to spin-spin coupling between the bound metal ion and carbonate (ranging from  $^2J(^{205}\text{Tl}-^{13}\text{C}) = 270$  to 290 Hz).

The interaction of monovalent thallium with yeast pyruvate kinase has been investigated by  $^{205}\text{Tl}^+$  NMR [96]. Pyruvate kinase from almost all sources requires monovalent and divalent metal ions. Potassium is the physiologically important cation, but numerous 1+ cations, including  $\text{Tl}^+$ , can activate this enzyme.  $\text{TlNO}_3$  activates pyruvate kinase to 80–90% activity compared to  $\text{KCl}$  in the presence of  $\text{Mn}(\text{NO}_3)_2$  as the activating 2+ cation. At higher concentrations of  $\text{Tl}^+$ , enzyme inhibition is observed, and the extent of this inhibition is dependent on the nature and concentration of the divalent cation. The effect of  $\text{Mn}^{2+}$  on the  $1/T_1$  and  $1/T_2$  values of  $^{205}\text{Tl}^+$  in the presence of yeast pyruvate kinase was determined by  $^{205}\text{Tl}$  NMR spectroscopy. The temperature dependence of the relaxation rates indicates that fast exchange conditions prevail for  $^{205}\text{Tl}^+$  longitudinal relaxation rates. The distance between  $\text{Tl}^+$  and  $\text{Mn}^{2+}$  at the active site of yeast pyruvate kinase was calculated from the paramagnetic contribution of  $\text{Mn}^{2+}$  to the longitudinal relaxation rates of  $\text{Tl}^+$  bound to yeast pyruvate kinase.  $^{205}\text{Tl}^+$  NMR spectroscopy has been also used to monitor possible structural alterations introduced at the active site of yeast pyruvate kinase by mutation of Thr298 [97]. The  $\text{Tl}^+$ - $\text{Mn}^{2+}$  distances at the active site of yeast pyruvate kinase have been calculated from the paramagnetic contribution of  $\text{Mn}^{2+}$  to the longitudinal relax-



ation rates of  $^{205}\text{Tl}^+$  bound to several complexes of the Thr298 mutants and to wild type yeast pyruvate kinase. The primary results of these studies demonstrated that mutations of Thr298 in yeast pyruvate kinase result in changes in the interactions between the monovalent cation and the divalent cation. These cations interact with the phosphoryl group of the substrate at the active site of the enzyme.

### 3.4. *p*-Block: Group 14 (Si, Ge, Sn, Pb)

#### 3.4.1. Silicon and germanium

Silicon is a highly abundant element in minerals and soils, but its role in living systems, if any, is poorly understood. It is currently debatable whether silicon is essential for human life. Silicon is not particularly toxic but finely divided silicates or silica can cause major damage to lungs.

$^{29}\text{Si}$  is a spin  $I = 1/2$  nucleus (4.7% natural abundance) and the only spectroscopically observable isotope of silicon.  $^{29}\text{Si}$  MRI has potential for imaging silicone prostheses in humans [98].  $^{29}\text{Si}$  relaxation times of silicone gels average  $T_1 = 21.2 \pm 1.5$  s and  $T_2 = 207 \pm 40$  ms, with no significant difference between virgin and explanted gels. Three volunteers with silicone gel-filled breast implants and one subject with an intraocular silicone oil injection were thus examined with a total acquisition time of 10–15 min per image. In all  $^{29}\text{Si}$  images, the shape of the silicone object is well depicted. Although at present conventional proton images are superior in resolution and signal-to-noise ratio,  $^{29}\text{Si}$  imaging has the advantage of optimal specificity, since only the silicone itself is visible.

$^{29}\text{Si}$  NMR can be employed to study the biological and medicinal chemistry of silicon, but low natural abundance and low receptivity have hindered the development of this technique so far.

Germanium has no biological role but it is said to stimulate the metabolism. Nevertheless, organogermanium compounds may exert some biological activity [99]. For example, spirogermanium, a germanium-containing azaspirane derivative, is reported to have *in vitro* and *in vivo* cytotoxicity in a number of pre-clinical tumor models, and to exhibit antiarthritic and immunoregulatory activities [100]. It underwent phases I–II clinical trials, but turned out to be too inactive for further clinical use.

Though the natural abundance of  $^{73}\text{Ge}$  is higher than  $^{29}\text{Si}$ , recording of  $^{73}\text{Ge}$  resonances is very difficult because of the low value of  $\gamma$ , along with its nuclear spin of  $9/2$  and large quadrupole moment. Electric field gradients around  $^{73}\text{Ge}$  lead to excessive broadening of the signals. In solution  $^{73}\text{Ge}$  NMR, symmetrical germanium complexes give sharp signals, whereas the signal broadens as the symmetry is lowered. For instance, the half-width of the  $^{73}\text{Ge}$  peak for tetramethylgermane, a compound with high geometrical symmetry, is only 1.4 Hz while corresponding values of germacyclohexane, 1-methylgermacyclohexane and 1,1-dimethylgermacyclohexane are 15.4, 22.3 and 15.6 Hz, respectively. When either halogen or oxygen atoms are asymmetrically substituted, as in 1-bromo-1-methylgermacyclohexane, excessive broadening takes place

to such an extent that observation of signals is impossible [101]. As far as we know, no  $^{73}\text{Ge}$  NMR studies on biologically relevant systems have been reported to date.

#### 3.4.2. Tin

Tin may be an essential element for man. The chemistry of organotins has attracted much attention during the last fifty years, owing to potential biological and industrial applications. Tin has been evaluated as the third most important pollutant in the ecosystem, which has raised the concern that tin may enter into the human food chain, be accumulated in the environment, and finally in other biological systems [102]. Organotin(IV) derivatives are potential metallopharmaceuticals, exhibiting *in vitro* antitumor activity against a number of human tumor cell lines [103]. Organotin(IV) derivatives also have potential interest as antimicrobial, antiinflammatory, cardiovascular, trypanocidal, antiherpes and antituberculosis agents [104].

The merits of tin NMR in assessing structural characteristics of organotin compounds (*e.g.* substitution pattern on tin, coordination number, influence of solvent) were recognized in the early 1970s. This is because of the reasonably favorable magnetic properties of tin nuclei. Tin has no less than 10 natural isotopes, among which three have non-zero spin, all  $I = 1/2$ . Among these,  $^{115}\text{Sn}$  is the least NMR favorable isotope, because of its extremely low natural abundance (0.35%). As a result, it has only rarely been studied, *e.g.* to overcome difficulties in unraveling strongly coupled homonuclear  $^nJ(^{119}\text{Sn}-^{119}\text{Sn})$  scalar coupling satellites in ditin compounds [105]. The “twins”  $^{117}\text{Sn}$  and  $^{119}\text{Sn}$  nuclei have rather similar properties, but  $^{119}\text{Sn}$  NMR spectroscopy is, nevertheless, by far the most widely used in tin chemistry because of both its slightly higher magnetic moment and natural abundance. Thus, not surprisingly, the use of NMR in tin chemistry has been abundantly reviewed (*e.g.* [106]). The use of  $^{117/119}\text{Sn}$  NMR spectroscopy to investigate the interaction between organotin complexes and biomolecules such as amino acids, peptides, carbohydrates, nucleic acids, and DNA, has been recently and extensively reviewed, including equilibrium, structural and biological studies [107], and will not be further discussed in this paper.

#### 3.4.3. Lead

Although lead is probably not essential for man, its toxicology is of great interest. Lead is a ubiquitous environmental contaminant. Although the use of lead (as  $[\text{PbEt}_4]$ ) in gasoline and paint has now been banned in most developed countries, lead is still one of the ten most common contaminants [108].

On the other hand, lead has been investigated for its potential applications in medicine. The potentially therapeutic radioisotope  $^{212}\text{Pb}$  has a number of theoretical attractions including  $\alpha$ -emission by short-lived daughter radionuclides, and its application is encouraged by the development of a new generator system [109] and the observation that when  $^{212}\text{Pb}$ -conjugated antibodies are internalized, radioactivity is retained inside cells [110].

Although the thermodynamics of lead complexation in aqueous solution has been studied extensively [111], relatively few spectroscopic studies on the aqueous coordination chemistry

of Pb(II) have been reported. There is one lead isotope with a nuclear spin that can be exploited for NMR spectroscopy,  $^{207}\text{Pb}$ ,  $I = 1/2$ . This isotope has an excellent receptivity (11.8 times greater than that of  $^{13}\text{C}$ ), high natural abundance (22.6%), and large chemical shift range (over 16000 ppm). Although  $^{207}\text{Pb}$  NMR spectroscopy has been used extensively to characterize Pb(IV)-alkyl derivatives, relatively few studies have been conducted on soluble Pb(II) coordination compounds ([112] and references therein).

The toxicological properties of lead have spurred a number of investigations into the interactions of this metal ion with various proteins [113]. For example,  $\text{Pb}^{2+}$  can bind very tightly to, and even displace  $\text{Ca}^{2+}$  from, calmodulin, calbindin and troponin-c. Moreover,  $\text{Pb}^{2+}$  can substitute  $\text{Ca}^{2+}$  in the activation of several enzymes, including protein kinase-c, phosphodiesterase, and myosin light chain kinase, the latter two in a calmodulin-dependent manner. Therefore, model systems are needed for lead bound to Ca-binding sites in proteins, as these interactions are thought to account for lead's toxicity. For example, the high-affinity  $\text{Ca}^{2+}$ -binding sites of carp ( $pI$  4.25) and pike ( $pI$  5.0) parvalbumins, as well as those of mammalian calmodulin and its C-terminal tryptic half-molecule ( $\text{TR}_2\text{C}$ ), have been investigated by  $^{207}\text{Pb}$  NMR spectroscopy [114]. For the parvalbumins, two  $^{207}\text{Pb}$  signals are observed ranging in chemical shift from +750 to +1260 ppm downfield of aqueous  $[\text{Pb}(\text{NO}_3)_2]$ , corresponding to  $^{207}\text{Pb}^{2+}$  bound to the two high-affinity helix-loop-helix  $\text{Ca}^{2+}$ -binding sites in each of these proteins. Four  $^{207}\text{Pb}$  signals, which fall in the same chemical shift window, can be discerned for calmodulin (Fig. 14). Experiments on  $\text{TR}_2\text{C}$  allowed the assignment of each signal as due to  $^{207}\text{Pb}^{2+}$  occupying a helix-loop-helix site in either the N- or the C-lobe of the intact protein (Fig. 14).  $^{207}\text{Pb}$  and  $^1\text{H}$  NMR titration studies on calmodulin have provided evidence that  $\text{Pb}^{2+}$  binding to all four sites

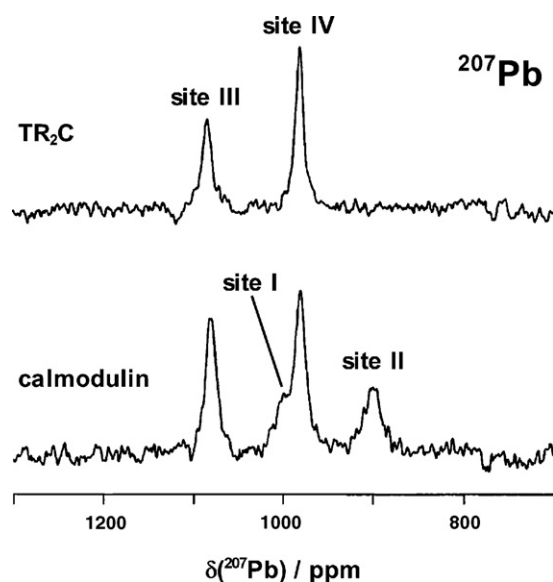


Fig. 14.  $^{207}\text{Pb}$  (104.435 MHz) NMR spectra of the  $^{207}\text{Pb}^{2+}$  forms of bacterially expressed mammalian calmodulin (1.47 mM, 4.0 equiv.  $^{207}\text{Pb}^{2+}$ , 100 mM KCl, pH 7.1, 85k scans) and its C-terminal domain fragment  $\text{TR}_2\text{C}$  (1.11 mM, 2.0 equiv.  $^{207}\text{Pb}^{2+}$ , 100 mM KCl, pH 7.0, 80k scans) (adapted from Ref. [114]).

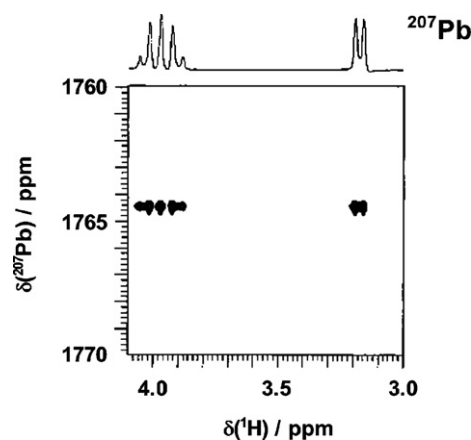


Fig. 15. 2D [ $^1\text{H}$ ,  $^{207}\text{Pb}$ ] HMQC NMR spectrum of  $[\text{Pb}(\text{EDTA-N}_4)]^{2+}$  (Pb-ethylenediaminetetraacetamide), 99.9%  $\text{D}_2\text{O}$ , pH 6.1, 25 °C). Coupling is observed from  $^{207}\text{Pb}$  to  $^1\text{H}$  through three bonds. The lead chemical shift was referenced to external 1 M  $[\text{Pb}(\text{NO}_3)_2]$  in 99.9%  $\text{D}_2\text{O}$  at pH 3.3 (adapted from Ref. [112]).

occurs simultaneously, in contrast to the behavior of this protein in the presence of  $\text{Ca}^{2+}$ . The large chemical shift dispersion observed for the  $^{207}\text{Pb}$  signals of the three investigated proteins illustrates the remarkable sensitivity of this parameter to subtle differences in the chemical environment of the protein-bound  $^{207}\text{Pb}$  nucleus.

Recently, Claudio et al. [112] have reported the first 2D [ $^1\text{H}$ ,  $^{207}\text{Pb}$ ] HMQC spectrum (Fig. 15), and demonstrated that this experiment can provide useful information about the lead coordination environment in aqueous Pb(II) complexes. This technique allows  $^{207}\text{Pb}$ - $^1\text{H}$  couplings through up to three bonds to be identified and should prove useful for the investigation of Pb(II) in more complex systems (e.g. biological and environmental samples).

A new  $\text{N}_2\text{S}$ (alkylthiolate)-coordinated Pb(II) compound (2-methyl-1-[methyl(2-pyridin-2-ylethyl)amino]propane-2-thiolatolead perchlorate,  $[\text{PATH-Pb}]\text{ClO}_4$ ) has been synthesized and characterized by X-ray diffraction and  $^{207}\text{Pb}$  NMR [115].  $[\text{PATH-Pb}]^+$  is the first reported three-coordinate Pb complex with an alkanethiolate ligand and, hence, is a model for Pb-cysteine interactions in proteins. The Pb center displays distorted trigonal-planar geometry.  $^{207}\text{Pb}$  NMR spectroscopy revealed a resonance at +5318 ppm, much further downfield than Pb complexes with N- or O-donor ligands. Given recent evidence of three-coordinate Pb binding in proteins with cysteine-rich metal-binding sites,  $[\text{PATH-Pb}]^+$  is a useful model for Pb sites in biological systems.

### 3.5. *p*-Block: Group 15 (As, Sb, Bi) and Group 16 (Te)

#### 3.5.1. Arsenic, antimony and bismuth

Despite arsenic's reputation as a highly toxic substance, this element may actually be necessary for good health. Studies on animals such as chickens, rats, goats and pigs show that it is necessary for proper growth, development and reproduction. In these studies, the main symptoms of arsenic deficiency were retarded growth and development. Arsenic compounds occur



naturally in marine organisms (such as arsenobetaines in flat fish) and are used as growth promoters for farm animals. It is suspected, but not yet proven, that arsenic may be an essential element necessary for the functioning of the nervous system and for growth. Arsenic trioxide ( $\text{As}_2\text{O}_3$ , Trisenox) has been approved by the Food and Drug Administration to treat a rare and deadly form of leukemia called acute promyelocytic leukemia [116].

Antimony appears to have no known role in the body. Sb(III) compounds cause damage to the liver and are used in some cases to induce vomiting and sweating. Some Sb(V) derivatives are used to treat the parasitic disease leishmaniasis [117].

Bismuth has no known natural biological role, and is relatively non-toxic. However it has been used for some time as a medicine (*e.g.* as tripotassium dicitratobismuthate) for treatment of gastrointestinal disorders. It is now used for treatment of some stomach ulcers since it is effective against the bacterium *Helicobacter pylori*. It is also to be found in antihemorrhoid creams such as Anusol cream and Hemocaneas as bismuth oxide and in Anusol ointment as bismuth subgallate [118]. It has been recently found that bismuth complexes may inhibit the severe acute respiratory syndrome (SARS) coronavirus [119].

$^{75}\text{As}$ ,  $^{121/123}\text{Sb}$ , and  $^{209}\text{Bi}$  are magnetically active isotopes. They are characterized by a high sensitivity to detection by NMR and large quadrupole moments which make their line-widths very sensitive to the environmental symmetry of the nuclei.  $^{75}\text{As}$  is the only NMR-active isotope of arsenic, 100% natural abundance, nuclear spin  $I=3/2$  and a chemical shift range of approximately 800 ppm. Despite the different spin quantum numbers,  $^{121}\text{Sb}$  ( $I=5/2$ ) and  $^{123}\text{Sb}$  ( $I=7/2$ ) nuclei have rather similar properties, but  $^{121}\text{Sb}$  NMR is, nevertheless, by far the most widely used in antimony chemistry because of both its higher natural abundance and higher receptivity. The chemical shift range of the antimony nuclei is approximately 5000 ppm.  $^{209}\text{Bi}$  is the only NMR-active isotope of bismuth, 100% natural abundance, nuclear spin  $I=9/2$ , and a chemical shift range of approximately 5000 ppm. Although both the natural abundances and their receptivities are favorable, recording of NMR spectra of these nuclei is known to be very difficult as they give rise to rather broad signals (in particular for  $^{209}\text{Bi}$ ). As far as we know, no NMR studies concerning the involvement of As, Sb or Bi in biologically relevant systems have been reported to date.

### 3.5.2. Tellurium

Tellurium is a noble metalloid which may act as a Lewis acid as well as a Lewis base. It has no known biological role and most tellurium compounds are highly toxic. Organotellurium compounds are potent immunomodulators (both *in vitro* and *in vivo*) with a variety of potential therapeutic applications. For example, ammonium trichloro(dioxoethylene-*O,O'*)tellurate (AS101) is said to be effective in treatment of AIDS and cancer. It confers protection against side-effects of both radiotherapy and chemotherapy, such as protection of the bone marrow and prevention of alopecia. It also exhibits synergistic effects with a variety of other drugs such as Taxol, a well-recognized advantage in chemotherapy. AS101 is also effective against systemic lupus erythematosus and psoriasis [120].

Tellurium has two naturally occurring NMR-active isotopes,  $^{123}\text{Te}$  (0.87%) and  $^{125}\text{Te}$  (6.99%), with nuclear spin  $I=1/2$ .  $^{125}\text{Te}$  has higher receptivity and natural abundance than the former isotope, which makes it the more favorable isotope for direct NMR observations. The use of  $^{125}\text{Te}$  NMR spectroscopy to probe the ligand chemistry of tellurium has been widely reviewed [121].

Tellurium coordination chemistry is dominated by sulfur ligands. In light of the unique Te(IV)-thiol chemistry, it has been investigated as a selective cysteine protease inhibitor. Although no inhibitory activity of serine, metallo-, or aspartic proteases was observed, AS101 exhibited time- and concentration-dependent inactivation of cysteine proteases.  $^{125}\text{Te}$  NMR has been used to follow the interaction between the thiol cysteine and Te(IV) or Te(VI) compounds [122]. Although  $^{125}\text{Te}$  NMR resonances are highly sensitive to the environment (*e.g.* solvent, concentration, temperature, etc.), they can be divided into frequency ranges corresponding to the tellurium oxidation state. Most  $[\text{TeX}_4]$  compounds ( $X$ =different heteroatoms or strong electron-withdrawing groups such as  $\text{CF}_3$ ) resonate at 1100–2000 ppm, whereas the corresponding Te(II) compounds resonate at  $\delta < 1000$  ppm. The data reported in this study demonstrated a clear distinction in reactivity toward thiol nucleophiles of Te(IV) and Te(VI) compounds. While the latter do not interact with the thiols, as it is evident from the lack of any shift in their  $^{125}\text{Te}$  NMR spectra, all the investigated Te(IV) compounds exhibited a significant shifts upon interaction with cysteine. For example, AS101 exhibited a downfield shift from +1700 to +1807 ppm, respectively, attributable to the formation of  $[\text{Te}(\text{cys})_4]$ , showing that Te(IV) compounds are selective cysteine protease inhibitors, while exhibiting no inhibitory activity toward other families of proteases.

## 3.6. *d*-Block: Group 3 (Sc, Y) and Group 4 (Ti)

### 3.6.1. Scandium and yttrium

Scandium has no known biological role. It is relatively non-toxic, although there have been suggestions that some of its compounds might be carcinogenic and can cause lung embolisms, especially during long-term exposure [6b].

Yttrium is not normally found in human tissues, and plays no known biological role. Targeted radionuclide therapy of cancer using the high-energy  $\beta$ -emitting isotope  $^{90}\text{Y}$  is now in advanced clinical trials (using the conjugates of somatostatin receptor-binding peptides), with promising results, at least at a palliative level [123].

The monoisotopic species  $^{45}\text{Sc}$  ( $I=7/2$ ) has high resonance frequency, high receptivity, and a relatively small quadrupole moment [124]. Despite these desirable qualities,  $^{45}\text{Sc}$  NMR spectroscopy has scarcely been employed in biological studies of scandium complexes to date. As already shown for  $^{27}\text{Al}$  (see Section 3.3.2),  $^{45}\text{Sc}$  NMR can be used to probe the metal-binding sites in large proteins. The solution chemistry of scandium is based entirely on  $\text{Sc}^{3+}$ , which almost exclusively forms six-coordinate complexes. This makes  $\text{Sc}^{3+}$ , whose ionic radius is slightly larger than that of  $\text{Fe}^{3+}$  (0.75 Å vs. 0.65 Å), a suitable probe for the  $\text{Fe}^{3+}$ -binding sites of transferrins in which the metal ion is coordinated by six donor atoms, four from the side-chains

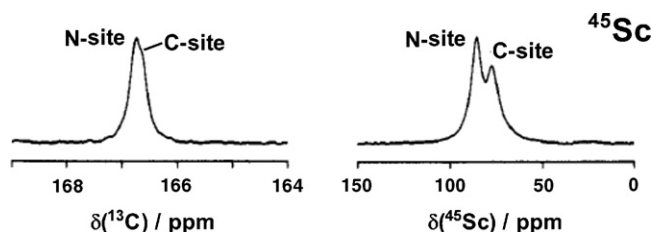


Fig. 16.  $^{13}\text{C}$  and  $^{45}\text{Sc}$  NMR spectra (referenced to external neat TMS and 1.0 M  $\text{ScCl}_3$  in  $\text{D}_2\text{O}$ , respectively, at 0.0 ppm) of 1.05 mM ovotransferrin in the presence of 10 mM  $\text{Na}_2^{13}\text{CO}_3$  and 1.9 equiv. of  $\text{Sc}^{3+}$  (75%  $\text{H}_2\text{O}/25\%$   $\text{D}_2\text{O}$ , 150 mM KCl, pH 7.6,  $25^\circ\text{C}$ ) (adapted from Ref. [82c]).

of four protein residues and two from the synergistic anion (*i.e.* carbonate), in a distorted octahedral geometry. For example, the binding of  $\text{Sc}^{3+}$  to chicken ovotransferrin has been investigated by  $^{45}\text{Sc}$  and  $^{13}\text{C}$  NMR spectroscopy [82c]. In the presence of carbonate, two  $^{45}\text{Sc}$  and  $^{13}\text{C}$  signals were detected which were assigned using the proteolytic half-molecules of ovotransferrin to bound  $\text{Sc}^{3+}$  and  $^{13}\text{CO}_3^{2-}$  in both metal ion-binding sites of the protein (Fig. 16). Several properties of the transferrin-bound  $^{45}\text{Sc}$  signals, such as their dependence on pulse length, magnetic field, protein size, and temperature, are consistent with the detection of only the central ( $m = 1/2 \rightarrow -1/2$ ) transition of the quadrupolar nucleus under far from extreme narrowing conditions. From  $^{45}\text{Sc}$  chemical shift and line-width data for the  $\text{Sc}^{3+}$ /carbonate form of ovotransferrin at four magnetic fields, the values of the quadrupolar coupling constant ( $\chi$ ) and rotational correlation time ( $\tau_c$ ) have been calculated for the bound metal ion in each site of the protein. This work represented the first  $^{45}\text{Sc}$  NMR study of a metalloprotein and is another example of the feasibility of quadrupolar metal ion NMR spectroscopy to investigate metal ion-binding sites in large proteins.

As a monoisotopic species with  $I = 1/2$  and a wide chemical shift range ( $\sim 1300$  ppm) [125], the  $^{89}\text{Y}$  nucleus should be attractive for NMR study. That it has not been routinely used in the characterization of yttrium complexes is a consequence of several factors, including its low receptivity and resonance frequency. In addition, its relaxation time is long, leading to problems with detection and to the necessity for lengthy experiments. So far, no  $^{89}\text{Y}$  NMR experiments of any biological interest have been carried out, whereas its use in the characterization of organometallic and coordination compounds containing yttrium has been recently reported ([126] and references therein).

### 3.6.2. Titanium

Titanium is believed to be a non-essential element, although recent observations indicate that  $\text{Ti}^{4+}$  might have a variety of biological roles [127]. In medicine titanium is used to make hip and knee replacements, pace-makers, bone-plates and screws and cranial plates for skull fractures. It has also been used to attach false teeth. Two  $\text{Ti}(\text{IV})$  derivatives (budotitane and titanocene dichloride) have been investigated as potential metallotherapeutic drugs [128]. In particular, titanocene dichloride,  $[\text{TiCl}_2\text{Cp}_2]$ , entered phase I clinical trials in 1993. In contrast to the pre-clinical studies, where hepatic or liver toxicity was

the dose-limiting side-effect, nephrotoxicity was identified as the dose-limiting side-effect along with hypoglycemia, nausea, reversible metallic taste immediately after administration and pain during infusion. However, the absence of any effect on proliferative activity of the bone marrow, which is the usual dose-limiting side-effect of organic drugs, was a very promising result that suggested titanocene dichloride may have significant potential for possible use in combination therapy. Two phase II clinical trials involving patients with advanced renal cell carcinoma and breast metastatic carcinoma have been reported. However, the results using titanocene dichloride as a single agent in chemotherapy were not sufficiently promising against other treatment regimes to warrant further studies, and titanocene dichloride has been discontinued from further clinical trials [129].

Titanium has two naturally occurring NMR-active isotopes,  $^{47}\text{Ti}$  ( $I = 5/2$ ) and  $^{49}\text{Ti}$  ( $I = 1/2$ ).  $^{49}\text{Ti}$  has slightly higher receptivity and narrower line-width than the former isotope, which means that  $^{49}\text{Ti}$  is usually the more favorable isotope for direct NMR observations in spite of the lower natural abundance. These properties restrict detection of NMR signals to neat liquids or very soluble compounds [130]. The  $^{47/49}\text{Ti}$  chemical shifts of titanocene dichloride were determined over 20 years ago ( $\delta(^{47/49}\text{Ti}) \approx -772$  ppm referenced to external neat liquid  $[\text{TiCl}_4]$ ) [131], but no further biological investigations have been performed by means of Ti NMR spectroscopy.

## 3.7. d-Block: Group 5 (V) and Group 6 (Cr, Mo, W)

### 3.7.1. Vanadium

Vanadium exists in a variety of oxidation states, from  $-3$  to  $+5$ . *In vivo*, given the constraints of standard physiological conditions (pH 3–7, aerobic aqueous solution, room temperature) oxidation states  $4+$  and  $5+$  prevail, with thermodynamically plausible species including vanadate, a mixture of  $[\text{HV}^{\text{V}}\text{O}_4]^{2-}$  and  $[\text{H}_2\text{V}^{\text{V}}\text{O}_4]^-$ , and vanadyl,  $\text{V}^{\text{IV}}\text{O}^{2+}$ . Vanadium is normally present at very low concentrations ( $<10^{-8}$  M) in virtually all cells in plants and animals. Vanadium in oxidation states  $3+$ ,  $4+$  and  $5+$  readily forms V–O bonds and binds N and S as well, forming chemically robust, coordination compounds. From a coordination chemistry point of view, vanadium is remarkably flexible. V(V) has particularly non-rigid stereochemical requirements and can form coordination complexes in geometries ranging from tetrahedral and octahedral to trigonal- and pentagonal-bipyramidal. V(IV) is much less flexible, with square-pyramidal or, if a sixth position is occupied, distorted octahedral geometries. Vanadium complexes readily undergo redox reactions under physiological conditions, and forms both cationic and anionic complexes in the pH range likely to be encountered physiologically (pH 2–8). *In vivo*, the key redox interplay is between V(V) and V(IV), with the two oxidation states coexisting in equilibrium both intra- and extracellularly [132].

Vanadium is widely recognized as a biologically important element, as confirmed by the discovery of the two naturally occurring vanadium proteins, a V-bromoperoxidase and a V-nitrogenase [133]. In addition, it has received much attention in

recent years due to the discovery of many therapeutic properties. Several vanadium salts and their complexes have shown insulin-mimetic pharmacological properties, including stimulation of glucose transport into cells and its oxidation *via* glycolysis, glycogen synthesis and lipogenesis, as well as inhibition of gluconeogenesis and glycogenolysis. These antidiabetic properties of vanadium compounds, which have been demonstrated by *in vitro*, *in vivo* and clinical studies, have attracted much interest as potential therapeutic agents for diabetes mellitus. They can be administered orally and promote glucose uptake in animal models of type 1 and type 2 diabetes. However, toxicity, although lower in vanadium complexes than for their salts, is still a major drawback, in particular for V(IV) compounds [134]. Moreover, the anticancer potential of, for example, vanadocene derivatives and a vanadium(IV) aspirin complex are being investigated [86]. Coordination complexes of vanadium which may have pharmacological relevance, include not only vanadate  $[\text{V}^{\text{V}}\text{O}_x\text{L}_y]$  and vanadyl  $[\text{V}^{\text{IV}}\text{OL}_z]$  complexes, but also the peroxovanadates  $[\text{V}^{\text{V}}\text{O}(\text{O}_2)(\text{H}_2\text{O})(\text{L}-\text{L}')^n]^{n-}$  ( $n=0, 1$ ) and  $[\text{V}^{\text{V}}\text{O}(\text{O}_2)_2(\text{L}-\text{L}')^n]^{n-}$  ( $n=1, 2, 3$ ) [134a].

$^{51}\text{V}$  NMR is a powerful and selective probe of vanadium in biological systems. Unlike many other biologically relevant isotopes, the NMR receptivity of the  $^{51}\text{V}$  nucleus ( $I=7/2$ ) is exceptionally high due to a large magnetic moment, an unusually small quadrupole moment, relatively large gyromagnetic ratio, high natural abundance (99.76%), and rapid quadrupolar relaxation in solution. The  $^{51}\text{V}$  NMR chemical shifts are very sensitive to changes in the nature of the ligands, thereby providing an excellent diagnostic tool for detailed investigations of vanadium bound to macromolecules [133].

Inorganic vanadium salts were the first compounds for which insulin-enhancing behavior was detected *in vivo*. Several vanadium complexes with organic ligands were found to be more potent and less toxic than vanadium salts, likely owing to an increase in selectivity. Peroxovanadium compounds were found to increase effectiveness, possibly because these compounds can inhibit PTPases irreversibly by oxidation. Additionally, the oxidative ability of peroxovanadate complexes strongly depends on the ligand. Most peroxovanadates are hydrolytically unstable; thus, an appropriate ligand should minimize hydrogen peroxide decomposition in aqueous solution while improving selectivity, such that potency is high and toxicity is low. Speciation studies of vanadium with hydrogen peroxide and a variety of ligands are required to gain information about the insulin-enhancing character of vanadium and to find the most suitable ligand for the treatment of diabetes [135]. Recent results *in vitro* indicate that the insulin-enhancing vanadate–citrate agents may hydrolyze completely under physiological conditions. Thus, the speciation of both the ternary  $\text{H}^+/\text{H}_2\text{V}^{\text{V}}\text{O}_4^-/\text{citrate}^{3-}$  and quaternary  $\text{H}^+/\text{H}_2\text{V}^{\text{V}}\text{O}_4^-/\text{H}_2\text{O}_2/\text{citrate}^{3-}$  systems have been investigated by  $^{51}\text{V}$  NMR under physiological conditions [135].

$^{51}\text{V}$  NMR spectroscopy has been successfully employed to probe the solution chemistry and stability under physiologically relevant conditions of several vanadium-based insulin-mimetic agents, such as the leading compound bis(maltolato)oxovanadium(IV) (which entered phase II clinical trials late in 2007) [136], its kojato analogue [137],

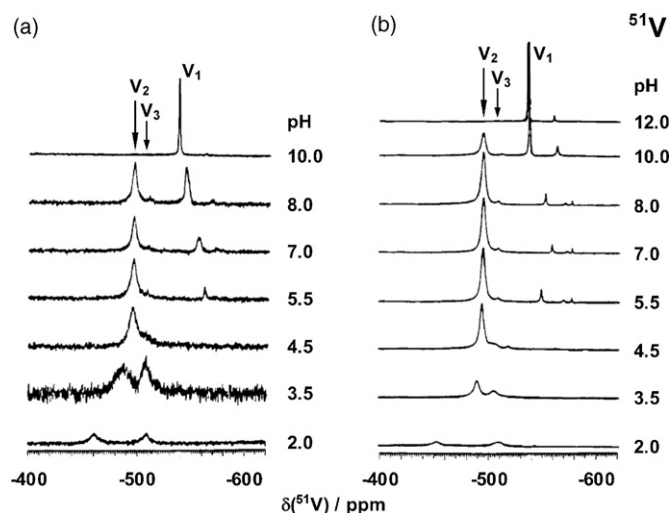


Fig. 17. Variable pH  $^{51}\text{V}$  NMR spectra (referenced to external neat  $[\text{VOCl}_3]$  at 0.0 ppm) of a 0.15 M NaCl aqueous solution of (a)  $[\text{V}^{\text{IV}}\text{O}(\text{maltolato})_2]$  (10 mM) and (b)  $\text{NH}_4[\text{V}^{\text{V}}\text{O}_2(\text{maltolato})_2]$  (10 mM) at 25 °C (adapted from Ref. [136]).

and a pro-drug of peroxovanadate insulin-mimetic hexakis(benzylammonium)decavanadate(V)dehydrate [138]. An example of the suitability of this technique is illustrated in Fig. 17, in which the variable pH  $^{51}\text{V}$  NMR spectra of a solution of  $[\text{V}^{\text{IV}}\text{O}(\text{maltolato})_2]$  and of genuine  $[\text{V}^{\text{V}}\text{O}_2(\text{maltolato})_2]^-$  are reported. As shown in Fig. 17a, in basic solution only one peak ( $\text{V}_1$ ,  $-537$  ppm) assigned to mixed protonation states of vanadate was recorded. As the pH was lowered, peaks  $\text{V}_2$  ( $[\text{V}^{\text{V}}\text{O}_2(\text{maltolato})_2]^-$ ) and  $\text{V}_3$  ( $[\text{V}^{\text{V}}\text{O}_2(\text{maltolato})(\text{OH})(\text{H}_2\text{O})]^-$ ) appeared at  $-496$  and  $-510$  ppm, respectively. As the acidity of the solution was increased, peak  $\text{V}_1$  shifted to  $-560$  ppm and disappeared below pH 5.5. No spectra could be observed below pH 2. By comparison with the variable pH  $^{51}\text{V}$  NMR spectra of  $\text{NH}_4[\text{V}^{\text{V}}\text{O}_2(\text{maltolato})_2]$  (Fig. 17b), these results proved that some V(V) complexes form in a solution of  $[\text{V}^{\text{IV}}\text{O}(\text{maltolato})_2]$ , even under relatively acidic conditions. The mechanism for the formation of these vanadate complexes is by oxidation of  $[\text{V}^{\text{IV}}\text{O}(\text{maltolato})_2]$  with  $\text{O}_2$  to form  $[\text{V}^{\text{V}}\text{O}_2(\text{maltolato})_2]^-$  and subsequently vanadate oligomers [136].

Other applications of the favorable NMR properties of  $^{51}\text{V}$  include the use of  $^{51}\text{V}$  NMR to probe vanadium(V)-protein interactions (in particular transferrins) [82a, 133, 139], and, more recently, the study of the uptake, intracellular reduction and binding of the aerobic oxidation products of oxovanadium(IV) compounds in human erythrocytes [140], and the interactions of vanadium(V)-citrate complexes with the sarcoplasmic reticulum calcium pump [141].

### 3.7.2. Chromium, molybdenum and tungsten

Chromium may be an essential trace element for mammals and may be involved in the maintenance of proper carbohydrate and lipid metabolism, although this is uncertain. Even mild dietary deficiency of chromium is sometimes associated with a medical condition known as Syndrome X, a constellation of symptoms, including hyperinsulinemia, high blood pressure,



high triglyceride levels, high blood sugar levels, and low HDL cholesterol levels, that increase the risk of heart disease. Recent research has revealed that the chromium-binding oligopeptide chromodulin may play a role in the autoamplification of insulin signaling. Attempts to develop chromium-containing nutritional supplements and therapeutics have been made [142]. In anything other than trace amounts, chromium compounds should be regarded as highly toxic. The health effects of chromium are at least partially related to the oxidation state of the metal at the time of exposure. Cr(III) and Cr(VI) compounds are thought to be the most biologically significant. Cr(VI) is generally considered much more toxic than Cr(III), and prolonged exposure to Cr(VI) has been associated with increased incidence of lung cancer.

Molybdenum is an essential trace element for virtually all life forms. In humans, molybdenum is known to function as a cofactor for three enzymes (molybdoenzymes): sulfite oxidase, xanthine oxidase, and aldehyde oxidase. Among these three enzymes, only sulfite oxidase is known to be crucial for human health [143]. As a metallopharmaceutical, molybdocene dichloride, an analogue of titanocene dichloride (see Section 3.6.2), and its derivatives are still under investigation as anticancer agents, and tetrathiomolybdate ( $[\text{MoS}_4]^-$ ) has been developed as an effective anti-copper therapy for the initial treatment of Wilson's disease, an autosomal recessive disorder that leads to abnormal copper accumulation [129].

Opinions are mixed about the need for tungsten in plant and animal life processes. It is not known if humans need tungsten for good health although it has been shown to be necessary for certain bacteria [144]. The known insulin-mimetic effects of tungstate led to polyoxotungstate clusters being evaluated as insulin-mimetics in animal models [145].

There are several technical problems involved in the routine measurement of  $^{53}\text{Cr}$  resonances.  $^{53}\text{Cr}$ , the only NMR-active isotope of chromium, has a small magnetic moment which results in a low Larmor frequency and low sensitivity. It has a spin  $I=3/2$  and a relatively large quadrupole moment which leads to short nuclear relaxation times  $T_1$  and  $T_2$  (particularly if the local symmetry of the complex is low), the latter resulting in large experimental line-widths. The low natural isotope abundance (9.55%) combined with the small overall receptivity results in extremely low sensitivity to detection by NMR spectroscopy. To date, only a few  $^{53}\text{Cr}$  solution NMR measurements have been achieved, and none of them has any biological interest [146].

Molybdenum has two naturally occurring NMR-active isotopes,  $^{95}\text{Mo}$  and  $^{97}\text{Mo}$ , with nuclear spin  $I=5/2$ . These quadrupolar nuclei are characterized by a low sensitivity to detection by NMR and low natural abundance (15.72% and 9.46%, respectively), two factors that make their study rather complicated.  $^{183}\text{W}$  is the only non-quadrupolar NMR-active nucleus in the Group 6 family, but it is also characterized by low natural abundance (14.4%) and extremely low receptivity. Thus, despite the interesting biological properties of molybdenum and tungsten, both  $^{95/97}\text{Mo}$  and  $^{183}\text{W}$  NMR spectroscopy have not often been used to investigate the biological chemistry of these two metals.  $^{183}\text{W}$  NMR has been used

to characterize some heteropolytungstates tested as anti-HIV agents [147].

### 3.8. *d*-Block: Group 7 (Mn, Tc)

#### 3.8.1. Manganese

Manganese has many roles in biological systems. Manganese can exist in 11 oxidation states (from +7 to  $-3$ ), more than any other element, but the aqueous chemistry of manganese is dominated by Mn(II) complexes. Both Mn(II) and Mn(III) are found in enzymes. The ionic radius of  $0.9 \text{ \AA}$  places  $\text{Mn}^{2+}$  in between that of  $\text{Mg}^{2+}$  and  $\text{Ca}^{2+}$ , so it is not surprising that there is overlap in function with these two ions in providing structural charge stabilization of enzymes and, in some cases, substrates such as Mn-ATP. In this regard, manganese has been useful in substitutions of  $\text{Mg}^{2+}$  and  $\text{Ca}^{2+}$  as a handle for NMR and EPR spectroscopic probes of active site architecture and catalysis [148]. Manganese also acts as a superacid catalyst in several hydrolytic enzyme-catalyzed reactions [149]. The classes of enzymes that have manganese cofactors are very broad and include oxidoreductases, transferases, hydrolases, lyases, isomerases, ligases, lectins, and integrins. The Mn-superoxide dismutase enzyme is probably one of the most ancient, as nearly all organisms living in the presence of oxygen use it to deal with the toxic effects of superoxide, formed by the one-electron reduction of dioxygen [150]. In addition to its important biological role, manganese may have several therapeutic uses, including the treatment of arthritis, cancer, cardiovascular diseases, and HIV [151].

Given the biological relevance of manganese, NMR spectroscopy is a potential analytical tool to investigate its behavior.  $^{55}\text{Mn}$  has spin  $I=5/2$ , a natural abundance of 100%, a Larmor frequency close to that of  $^{13}\text{C}$ , and a chemical shift range of approximately 3500 ppm.  $^{55}\text{Mn}$  NMR spectroscopy has found limited applications due to the relatively large quadrupole moment of  $^{55}\text{Mn}$  which can result in large  $^{55}\text{Mn}$  quadrupolar couplings [125]. Unfortunately, both Mn(II) and Mn(III) centers are paramagnetic, thus preventing the direct detection of these nuclei in solution. On the other hand, the presence of a paramagnetic center can be used to probe the active sites of metallobiomolecules *via* the analysis of paramagnetic shifts and line-broadenings [152].

#### 3.8.2. Technetium

Technetium does not occur naturally on Earth and it was the first element to be produced artificially.  $^{99}\text{Tc}$  is a  $\beta$ -emitting radionuclide with a long half-life ( $2.13 \times 10^5$  years) and is generated as a by-product of nuclear power plants and atomic weapons tests. Interest in technetium chemistry is due to its extensive use in nuclear medicine. Radiopharmaceuticals containing  $^{99\text{m}}\text{Tc}$  linked to a variety of carrier biomolecules are in clinical use [153]. Such extensive use of this radionuclide in medicine requires more detailed structural information about these radiopharmaceuticals to facilitate the prediction of the *in vivo* stability and target-organ distribution.

Measurement of the main parameters of  $^{99}\text{Tc}$  NMR spectra, chemical shifts and line-widths, allows monitoring of the oxida-

tion state of the element and establishment of the composition and structure of various complexes, and observation of the variation of these parameters with time allows study of the kinetics of chemical processes involving technetium compounds. The  $^{99}\text{Tc}$  nuclide is extremely convenient for NMR spectroscopy due to its high receptivity and natural abundance. Although  $^{99}\text{Tc}$  has a significant quadrupole moment, the effect of line-broadening in solution is attenuated by a large spin  $I = 9/2$ ; in fact, for  $^{99}\text{Tc}$  the resonances are amongst the narrowest for quadrupolar nuclei. However, due to the presence of unpaired electrons, Tc(II), Tc(IV) and Tc(VI) compounds cannot be studied by  $^{99}\text{Tc}$  NMR spectroscopy. A review on  $^{99}\text{Tc}$  NMR spectroscopy has been published recently [154], and even if this technique has not been used yet to investigate specifically the behavior of technetium in biological systems, the reported examples show that  $^{99}\text{Tc}$  NMR can be successfully used in studying not only complex formation in solutions but also kinetics of reactions.

### 3.9. d-Block: Group 8 (Fe, Ru, Os)

#### 3.9.1. Iron

Iron is the fourth most abundant element in the Earth's crust, but only a trace element in biological systems, making up only 0.004% of the body's mass. Yet, it is an essential component or cofactor of numerous metabolic reactions. Every living cell in both plants and animals contains iron. Approximately two thirds of this iron (70%) in man is contained in hemoglobin; the other third is stored in the bone marrow, spleen, liver and muscles. Myoglobin and enzymes contain about 15% of the iron, and ferritin almost as much (14%). Only about 1% is in transit in serum. In animals, plants and fungi, iron is often incorporated into heme. Heme is an essential component of cytochrome proteins, which mediate redox reactions, and of oxygen carrier proteins such as hemoglobin (carries oxygen in the blood from the lungs to tissues throughout the body) and myoglobin (stores oxygen for the muscles to use when they contract). Iron also contributes to redox reactions in the iron–sulfur clusters of many enzymes, such as nitrogenase (involved in the synthesis of ammonia from nitrogen) and hydrogenase. Non-heme iron proteins include the enzymes methane monooxygenase (oxidizes methane to methanol), ribonucleotide reductase (reduces ribose to deoxyribose), hemerythrins (oxygen transport and fixation in marine invertebrates) and purple acid phosphatase (hydrolysis of phosphate esters). Iron distribution is heavily regulated in mammals, and in cells iron is generally stored in the centre of metalloproteins (ferritins), partly because iron has a high potential for biological toxicity; in fact, free  $\text{Fe}^{2+}$  ions are efficient catalysts that can rapidly generate toxic oxygen free radicals within cells. Iron distribution is regulated, so restricting its availability to bacteria can help to prevent or limit infections. A major component of this regulation is the protein transferrin, which binds iron absorbed from the duodenum and carries it in the blood to cells. If an individual has an iron deficiency, the iron stores are depleted first, followed by a reduction in hemoglobin. As a result, red blood cells are small in size and diminished in number and the direct consequence is the occurrence of anemia. On the other hand, excessive iron can be toxic, because free fer-

rous iron reacts with peroxides to produce free radicals, which are highly reactive and can damage DNA, proteins, lipids and other cellular components. Thus, iron toxicity occurs when iron levels exceed the capacity of transferrin to bind the iron [6b]. Biologically relevant iron typically exists in Fe(II) and Fe(III) oxidation states. Both exist in low- and high-spin configurations and the facile interconversion between the low- and high-spin forms has important biochemical implications, as discussed in detail by Brady et al. [155]. The energy difference between low- and high-spin configurations for given oxidation state can be very small. Thus the modulation of spin state by ligand charges and differences in geometry can be important in catalytic mechanisms. A variety of Fe(III) salts are marketed as iron supplements and prescribed to treat iron-deficiency anemia, and iron mediates the anticancer activity (attack on DNA) of bleomycin [156].

Despite the importance of iron in biological chemistry, only limited studies of Fe NMR have been reported.  $^{57}\text{Fe}$ , the only isotope of iron suitable for NMR study, has spin  $I = 1/2$  but also a very low sensitivity when investigated at natural abundance (2.19%). High spin Fe(II) and Fe(III) centers are paramagnetic, so the diamagnetic, low-spin ferrous ion  $^{57}\text{Fe}^{2+}$  is the only NMR-observable iron isotope. However, use of  $^{57}\text{Fe}$ -enriched material and high fields combined with the very large chemical shift range (>11000 ppm) has yielded useful information especially about heme proteins. Ferrocenes and porphyrins have been used as model compounds to obtain chemical shift data and to gain insight on the relaxation mechanisms [157].  $^{57}\text{Fe}$  NMR spectra are available for myoglobins and cytochrome-*c* (Fig. 18) [158], and it has been established that this technique is a powerful probe for iron–ligand interactions in these proteins, particularly for porphyrin geometry [157a,159].

#### 3.9.2. Ruthenium and osmium

Both ruthenium and osmium have no known natural biological function. However, in the last 15 years ruthenium and osmium complexes have aroused great interest for their potential use as therapeutic anticancer agents [160]. Two Ru(III) complexes, namely *trans*-[RuCl<sub>4</sub>(Im)(DMSO)]ImH (NAMI-A) [161] and *trans*-[RuCl<sub>4</sub>(Ind)<sub>2</sub>]IndH (KP1019) [162] are undergoing clinical trials. Whilst KP1019 is cytotoxic to cancer cells, NAMI-A is relatively non-toxic but has antimetastatic activity. It has been proposed that the activity of Ru(III) complexes, which are usually relatively inert towards ligand substitution, is dependent on *in vivo* reduction to more labile Ru(II) analogues. Thus, the activity of Ru(II) complexes is currently being explored. In particular, since arenes are known to stabilize ruthenium in its 2+ oxidation state, the potential of Ru(II)-(η<sup>6</sup>-arene) complexes as anticancer agents is under investigation [163]. In addition, a variety of ruthenium derivatives have been reported with activity against bacteria, HIV, and parasitic infection. Radical scavenging properties have been identified for Ru(II) complexes that might offer therapeutic benefits in inflammatory diseases involving reactive oxygen species or NO [86]. Given the strict similarity with Ru(II), the possible design of Os(II)-(η<sup>6</sup>-arene) anticancer complexes has been recently taken into account [164].

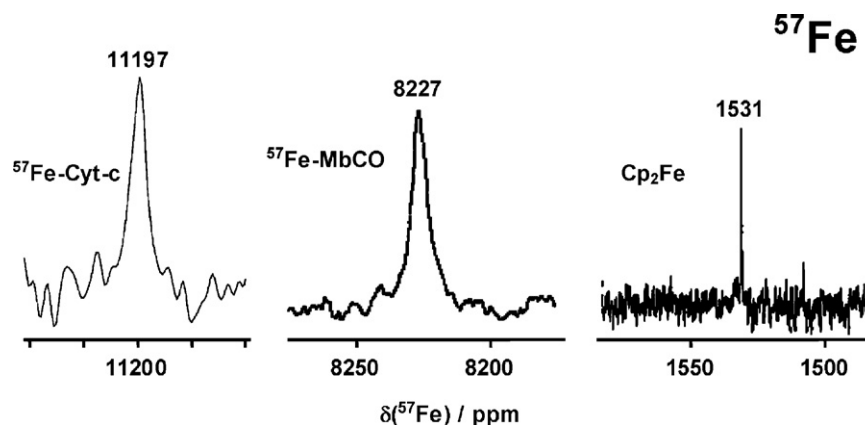


Fig. 18.  $^{57}\text{Fe}$  NMR spectra (referenced to external  $[\text{Fe}(\text{CO})_5]$  at 0.0 ppm) of  $^{57}\text{Fe}$ -cytochrome-*c* ( $^{57}\text{Fe}$ -Cyt-*c*, 3 mM in 50 mM phosphate buffer, pH 7, 298 K),  $^{57}\text{Fe}$ -carbonmonoxymyoglobin ( $^{57}\text{Fe}$ -MbCO, 15 mM in 50 mM phosphate buffer, pH 7.1, 296 K), and ferrocene ( $\text{Cp}_2\text{Fe}$ , 0.8 M in  $\text{C}_6\text{H}_6$ ) (adapted from Refs. [158c,158d]).

Both ruthenium NMR-active isotopes ( $^{99}\text{Ru}$ ,  $I=3/2$ ;  $^{101}\text{Ru}$ ,  $I=5/2$ ) are quadrupolar nuclei, the latter having a larger quadrupole moment. Therefore, the  $^{99}\text{Ru}$  nucleus is favored for NMR spectroscopy, despite the slightly lower natural abundance (12.72% vs. 17.07% for  $^{101}\text{Ru}$ ). Another problem encountered in  $^{99}\text{Ru}$  NMR is the low resonance frequency, resulting in acoustic ringing that causes distorted baselines. Very little is known about the dependence of  $\delta(^{99}\text{Ru})$  on structure and temperature, thus it is not surprising that relatively few  $^{99}\text{Ru}$  NMR spectroscopic studies have been performed [165]. In addition, due to the presence of unpaired electrons, Ru(III) compounds cannot be directly detected by  $^{99}\text{Ru}$  NMR spectroscopy, so  $^{99}\text{Ru}$ (II) is the only NMR-observable ruthenium isotope. To date,  $^{99}\text{Ru}$  NMR spectroscopy has been successfully employed mainly for Ru(II) complexes with highly symmetrical environments around the metal nucleus [166].

Like ruthenium, osmium has two magnetically receptive nuclei, although the  $^{189}\text{Os}$  isotope is not useful because of its spin  $I=5/2$  and large quadrupole moment. The  $^{187}\text{Os}$  isotope has spin  $I=1/2$  but has a natural abundance of only 1.64% and is the most insensitive nucleus in the periodic table, making its observation by conventional NMR techniques extremely difficult. In fact, for many years, the only known chemical shift was that of the reference compound  $[\text{OsO}_4]$  [167]. However, the advent of polarization transfer techniques, which require a non-zero scalar  $^nJ(\text{M}-\text{X})$  coupling, has improved the detection of low- $\gamma$  spin  $I=1/2$  nuclei.  $^{187}\text{Os}$  NMR data have been collected for several Os(II)-( $\eta^6$ -arene) complexes, using inverse 2D  $[^{31}\text{P},^{187}\text{Os}]-\{^1\text{H}\}$  and  $[^1\text{H},^{187}\text{Os}]$  NMR spectroscopy [168], showing the potential of this technique.

### 3.10. d-Block: Group 9 (Co, Rh)

#### 3.10.1. Cobalt and rhodium

Despite a very low biological abundance, cobalt plays a unique role in the metabolism of several living organisms [169]. Cobalt compounds contain the metal ion in the oxidation states 1+, 2+, and 3+. The importance of cobalt comes

from its participation in the  $\text{B}_{12}$  family of compounds, whose active forms are responsible for catalyzing a wide variety of processes related to nucleic acid, protein, and lipid syntheses, as well as for maintaining the normal function of epithelial and nervous cells [170]. Cobalamins also stand out as nature's most complex non-polymeric structures, and the first discovered biomolecule containing a metal-carbon bond. However, several different types of cobalt-containing enzymes have been identified other than vitamin  $\text{B}_{12}$  (Fig. 19) and its derivatives [171]. Cobalt complexes are also being investigated for their potential use in medicine as enzyme inhibitors and drug delivery devices [172].

$^{59}\text{Co}$  is a nucleus whose NMR observation should be, at least in principle, easy. It is 100% naturally abundant, possesses a relatively high magnetogyric ratio, and by virtue of the magnetic

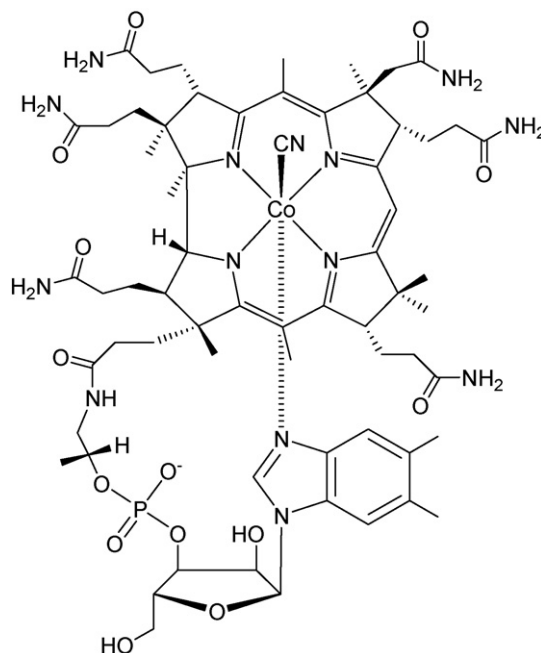


Fig. 19. Structure of vitamin  $\text{B}_{12}$ .



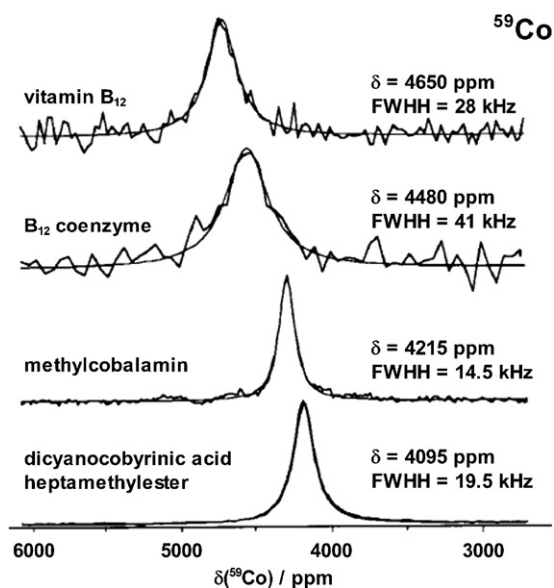


Fig. 20.  $^{59}\text{Co}$  NMR spectra of natural  $\text{B}_{12}$  derivatives in solution (externally referenced to 1 M aqueous  $[\text{Co}(\text{NH}_3)_6]\text{Cl}_3$ , and subsequently converted to ppm downfield from 1 M aqueous  $\text{K}_3[\text{Co}(\text{CN})_6]$  for the sake of literature consistency). Superimposed on the experimental traces are best Lorentzian fits characterized by the isotropic shift  $\delta$  and full-width-at-half-height (FWHH) values indicated on the right (adapted from Ref. [174]).

mixing of its occupied and excited d orbitals it may experience substantial paramagnetic deshieldings ( $>15000$  ppm) that can reveal even subtle changes in chemical environments. Complicating these measurements is the nuclear spin  $I=7/2$  of the isotope, associated with a quadrupole moment that provides an efficient relaxation mechanism and, consequently, leads to broadened resonances in solution [173].  $^{59}\text{Co}$  NMR spectroscopy has been used to study naturally occurring cobalamins. Targets of these investigations included vitamin  $\text{B}_{12}$ , the  $\text{B}_{12}$  coenzyme, methylcobalamin, and dicyanocobyrinic acid heptamethylester [174]. Illustrative  $^{59}\text{Co}$  NMR spectra are shown in Fig. 20. Similar studies have been carried out using solid-state  $^{59}\text{Co}$  NMR spectroscopy, showing that powder spectra with good signal-to-noise ratios can be recorded even at low magnetic field strengths. In fact, a number of circumstances combine to endow these solid-state spectra with a much higher quality than their solution counterparts [174]. Solid-state  $^{59}\text{Co}$  NMR spectroscopy has been successfully employed also to study a single-crystal of vitamin  $\text{B}_{12}$  [175] as well as in the analysis of vitamin  $\text{B}_{12}$  in its different polymorphic forms [176].

In contrast to cobalt, rhodium has no known biological function. Recently, rhodium complexes have been investigated for their possible applications in medicine as antitumor, antibacterial and antiparasitic agents [177]. As a monoisotopic species with  $I=1/2$  and a wide chemical shift range ( $\sim 8000$  ppm), the  $^{103}\text{Rh}$  nucleus is attractive for NMR studies. Unfortunately, low receptivity, negative magnetogyric ratio and very long relaxation times ( $>50$  s) are major drawbacks. A recent survey of  $^{103}\text{Rh}$  NMR spectroscopy has been published [178], but no studies of biological relevance appear to have been reported.

### 3.11. d-Block: Group 10 (Ni, Pd, Pt)

#### 3.11.1. Nickel and palladium

Nickel is often found in biological compounds as  $\text{Ni}(\text{II})$ . The role of nickel in biological systems has been appreciated only since 1975, when urease was shown to be a nickel enzyme [179]. Since then, six more nickel-containing enzymes have been discovered in bacteria and/or archaea: hydrogenase, methyl-S-coenzyme M reductase, carbon monoxide dehydrogenase, nickel superoxide dismutase, glyoxylase I, and a putative nickel *cis-trans* isomerase [180].

Nickel has one naturally occurring NMR-active isotope,  $^{61}\text{Ni}$ , with nuclear spin  $I=3/2$ . It is a quadrupolar nucleus characterized by low sensitivity to detection by NMR and low natural abundance. In addition, octahedral and tetrahedral  $\text{Ni}(\text{II})$  derivatives are paramagnetic, so it cannot be studied directly by  $^{61}\text{Ni}$  NMR spectroscopy.

Palladium is a non-essential element for life. Pharmaceutical interest in  $\text{Pd}(\text{II})$  compounds is driven by analogy to antitumor  $\text{Pt}(\text{II})$  complexes (see Section 3.11.2), as well as antiviral, antifungal and antimicrobial metallotherapeutics [181].

Palladium has one naturally occurring NMR-active isotope,  $^{105}\text{Pd}$ , with nuclear spin  $I=5/2$ . Although it has high natural abundance (22.23%), this quadrupolar nucleus is characterized by a low sensitivity to detection by NMR, low resonance frequency and extremely fast relaxation times ( $<10^{-5}$  s). As far as we know, no  $^{105}\text{Pd}$  NMR studies in solution have been reported.

#### 3.11.2. Platinum

Platinum is a relatively inert metal and has no natural biological role. Nevertheless, platinum complexes are now amongst the most widely used drugs for the treatment of cancer. The first and second generation compounds cisplatin and carboplatin are in widespread use to treat a variety of cancers, either as single agents or in combination with other drugs. Oxaliplatin, introduced into the clinic in 2002 has become an important option for the treatment of colorectal cancer and its possible use in the treatment of other cancers is a focus of intense investigation. The search for improved platinum-based drugs continues with the goals of reducing toxic side-effects and broadening the spectrum of activity to tumors resistant to cisplatin. A major focus of current research is in the investigation of “non-classical” platinum antitumor compounds, including *trans*- and polynuclear  $\text{Pt}(\text{II})$  derivatives as well as  $\text{Pt}(\text{IV})$  complexes, that act by a different mechanism to that of cisplatin to achieve a different profile of activity [2].

$^{195}\text{Pt}$  ( $I=1/2$ ) is a reasonably sensitive nucleus for NMR detection having a natural abundance of 33.7% and receptivity relative to  $^{13}\text{C}$  of 19.1. An attractive feature of  $^{195}\text{Pt}$  NMR for studies of platinum anticancer drugs is the very large chemical shift range ( $>15000$  ppm), which allows ready differentiation between  $\text{Pt}(\text{II})$  and  $\text{Pt}(\text{IV})$ , which tend to have chemical shifts at the high-field and low-field ends of the range, respectively. The resonances for square-planar  $\text{Pt}(\text{II})$  complexes span some 4000 ppm and ligand substitutions produce predictable chemical shift ranges. NMR methods have proved useful in the investigation of platinum drugs from the time that cisplatin was first

introduced into the clinic more than 30 years ago. Both 1D  $^{195}\text{Pt}$  and 2D [ $^1\text{H}$ ,  $^{15}\text{N}$ ] NMR techniques were used and made a major contribution in the understanding of the molecular mechanism of action of platinum-based anticancer drugs. This topic has been recently reviewed by several authors [16g,182], and will not be further discussed in this paper.

### 3.12. *d*-Block: Group 11 (Cu, Ag, Au)

#### 3.12.1. Copper

Copper is the third most abundant transition metal element in biological systems after iron and zinc. The bioinorganic chemistry of copper is dominated by 1+ and 2+ oxidation states. Almost all of the copper in humans is bound to either transport proteins (ceruloplasmin and copper-albumin), storage proteins (metallothioneins), or copper-containing enzymes, whereas unbound, free copper is not found in large quantities in the human body. A substantial number of copper metalloenzymes are found in the human body. Copper is essential for the proper functioning of these copper-dependent enzymes, including cytochrome-*c* oxidase (energy production), superoxide dismutase (antioxidant protection), tyrosinase (pigmentation), dopamine hydroxylase (catecholamine production), lysyl oxidase (collagen and elastin formation), clotting factor V (blood clotting), and ceruloplasmin (antioxidant protection, iron metabolism and copper transport). In addition to its enzymatic roles, copper is used for biological electron transport. The “blue copper” proteins (named after their intense blue color arising from a ligand-to-metal charge-transfer absorption band at  $\sim 600\text{ nm}$ ) that participate in electron transport include azurin and plastocyanin [6]. Most features of severe copper deficiency can be explained by a failure of one or more of these copper-dependent enzymes. For instance, depigmentation can be explained by a tyrosinase deficiency, and the defects of collagen and elastin causing abnormalities in the connective tissue and vascular system can be explained by a lysyl oxidase deficiency. Copper complexes are currently being investigated for their potential anticancer activity. Moreover, coordination with copper, either prior to administration or *in vivo*, often enhances the activity of various types of drugs such as antitumor and antiinflammatory agents [86].

The copper isotopes  $^{63}\text{Cu}$  and  $^{65}\text{Cu}$  have natural abundances of 69.09% and 30.91%, respectively, and nuclear spin  $I = 3/2$ . Thereby they couple strongly to local electric field gradients, and the quadrupole moments cause significant line-broadening when the charge is unevenly distributed. Consequently, only complexes with regular tetrahedral or cubic symmetry are NMR-active [183].  $^{63}\text{Cu}$  NMR spectroscopy is by far most used in copper chemistry because of both its higher receptivity and natural abundance compared to  $^{65}\text{Cu}$ .

For the past decades, the structures, electronic states, and reactivity of copper complexes have been widely investigated by various spectroscopic methods. UV–vis absorption, resonance Raman, and electron paramagnetic resonance spectroscopy are powerful tools for studying the structures and electronic states of Cu(II) complexes because of their characteristic absorptions

resulting from d–d transitions, ligand-to-metal charge-transfers, and unpaired electron on the copper(II) ion. On the other hand, these spectroscopic methods have not been applied extensively to studies of Cu(I) complexes because of featureless spectroscopic properties resulting from the closed shell  $d^{10}$  electron configuration. For diamagnetic Cu(I) complexes,  $^{63}\text{Cu}$  NMR spectroscopy appears to have the greatest potential for characterizing their structures and electronic states (also because most Cu(I) complexes prefer a tetrahedral configuration, which gives rise to a relatively sharp resonance line) [184], whereas the paramagnetism of Cu(II) center prevents its detection by  $^{63}\text{Cu}$  NMR spectroscopy.

#### 3.12.2. Silver and gold

Both silver and gold have no known natural biological role in humans, but interest in the biological and/or medicinal activities of Ag(I) and Au(I/III) compounds has increased in recent years. The antibacterial effects of silver compounds have long been known. Silver and silver compounds are widely used as antibacterial agents [185]. Chrysotherapy (therapeutic use of gold compounds) is established in modern medicine. In particular, some gold(I)-based drugs, such as myocrisin, solganol and auranofin, are currently being employed for the treatment of rheumatoid arthritis [186]. In addition, both Au(I) and Au(III) derivatives are emerging as a new class of metal-based anticancer agents [187].

All naturally occurring silver is found in two NMR-active isotopic forms,  $^{107}\text{Ag}$  and  $^{109}\text{Ag}$ , both having nuclear spin  $I = 1/2$ . Although  $^{107}\text{Ag}$  has a slightly higher natural abundance (51.82% vs. 48.18% for  $^{109}\text{Ag}$ ), the preferred isotope for NMR spectroscopic observation is  $^{109}\text{Ag}$ , due to its slightly higher receptivity. The two most serious difficulties encountered when performing silver NMR experiments are poor sensitivity and extremely long spin–lattice relaxation times. These properties stem from the very low gyromagnetic ratios for both  $^{107}\text{Ag}$  and  $^{109}\text{Ag}$ . NMR spectroscopy occupies a position of preeminence in probing metal-binding sites where the native metal ions, e.g. Zn(II), Ca(II), Fe(II), Mg(II), Cu(II) and Cu(I), can be substituted with spin  $I = 1/2$  metal isotopes. In spite of the attractiveness of Ag(I) as a redox stable analogue for Cu(I),  $^{109}\text{Ag}$  NMR has so far found limited applications in biological systems, owing mostly to the insensitivity of the investigated nucleus, making direct detection impractical for most biological systems [188]. Relatively few examples of Ag(I) complexes have been characterized by  $^{109}\text{Ag}$  NMR [189], and the only known metalloprotein studied by 2D [ $^1\text{H}$ ,  $^{109}\text{Ag}$ ] HMQC spectroscopy to date is the  $^{109}\text{Ag}$ -substituted yeast metallothionein (Fig. 21) [190].

The solution behavior of the anticancer agent  $[\text{Ag}(\text{d2pype})_2]\text{NO}_3$  (d2pype = 1,2-bis(di-2-pyridylphosphino)ethane) has been investigated by 2D [ $^{31}\text{P}$ ,  $^{109}\text{Ag}$ ] HMQC spectroscopy [191]. It was shown that the complex forms equilibrium mixtures of monomeric  $[\text{Ag}(\text{d2pype})_2]^+$ , dimeric  $[\{\text{Ag}(\text{d2pype})_2\}_2]^{2+}$  and trimeric  $[\{\text{Ag}(\text{d2pype})_2\}_3]^{3+}$  species in which the d2pype ligands coordinate in both bridging and chelated modes with the relative percentages of the species present depend on temperature and solvent.

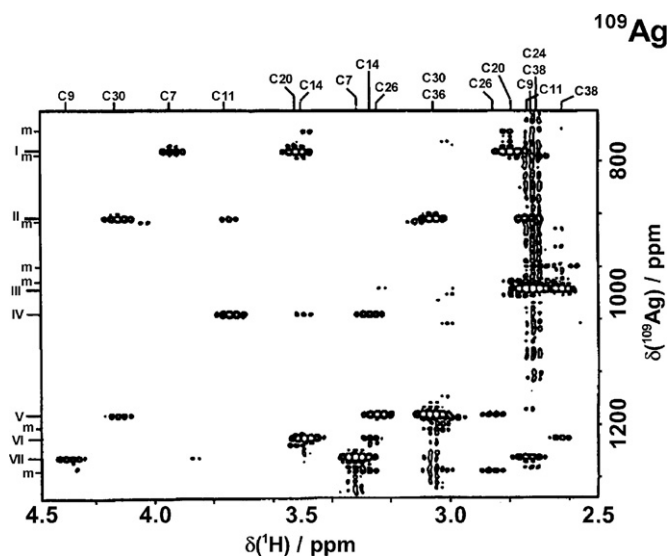


Fig. 21. 2D [ $^1\text{H}$ ,  $^{109}\text{Ag}$ ] HMQC spectrum (referenced to external 1 M  $\text{AgNO}_3$  at 0.0 ppm) of yeast  $^{109}\text{Ag}$ -metallothionein (6 mM in 18 mM phosphate buffer in  $\text{D}_2\text{O}$ , pH 6.5, 298 K). The spectrum shows the connectivities of all seven silver atoms with the cysteine  $\text{H}_\beta$  protons of the yeast  $\text{Ag}$ -metallothionein (adapted from Ref. [190]).

Gold has a single isotope,  $^{197}\text{Au}$ , which has a nuclear spin  $I=3/2$  and a large quadrupole moment. As a result of fast quadrupole relaxation, the resonances are extremely broad and weak. Due to the low NMR receptivity of  $^{197}\text{Au}$  combined with the fast relaxation, no NMR studies of gold have been described in the literature [192].

### 3.13. d-Block: Group 12 (Zn, Cd, Hg)

#### 3.13.1. Zinc

Zinc is an essential element in human and animal nutrition with a wide range of biological roles. Zinc plays catalytic, structural or regulatory roles in more than 200 zinc metalloenzymes that have been identified in biological systems. Among other things, these enzymes are involved in nucleic acid and protein metabolism and the production of energy. It is estimated that around 3000 proteins in the human body contain zinc prosthetic groups; in particular, zinc plays a structural role in the formation of the so-called zinc fingers. Zinc fingers are exploited by transcription factors for interacting with DNA and regulating the activity of genes. Another structural role of zinc is in the maintenance of the integrity of biological membranes resulting in their protection against oxidative injury. In addition, there are over a dozen types of cells in the human body that secrete zinc ions, and the roles of these secreted zinc signals in medicine and health are now being actively studied. Intriguingly, brain cells in the mammalian forebrain are one type of cell that secretes zinc, along with its other neuronal messenger substances [193]. Zinc exists under physiological conditions in the  $2+$  oxidation state. Over 95% of total body zinc is bound to proteins within cells and cell membranes. Plasma contains only 0.1% of total body zinc. Most of the zinc (75–88%) in blood is found in the red blood cell zinc metalloenzyme carbonic anhydrase. In the plasma, approximately

18% of zinc is bound to  $\alpha_2$ -macroglobulin, 80% to albumin and 2% to such proteins as transferrin and ceruloplasmin. As a metallothioretic agent, zinc has putative antiviral, fertility-enhancing and retino-protective activities. It is also used in the treatment of Wilson's disease, and it may exhibit immunomodulatory as well as antioxidant activity [194].

$^{67}\text{Zn}$ , the only naturally occurring NMR-active isotope of zinc (4.11%), has nuclear spin  $I=5/2$  and a large quadrupole moment which is responsible for high relaxation rates. This quadrupolar nucleus is characterized by a low sensitivity to detection by NMR and low resonance frequency. Despite these unfavorable spectroscopic properties,  $^{67}\text{Zn}$  NMR experiments in solution have been performed. The required concentration of  $\text{Zn}^{2+}$  is typically high,  $>0.1$  M, but lower concentrations can be utilized with isotopic enrichment. Also, due to the quadrupolar nature of the nuclide, even if solution NMR methods afforded observable zinc resonances in a metalloprotein, the resulting line-widths can obscure the determination of site-specific isotropic chemical shifts. With these nuclear properties, it is no wonder that the literature of  $^{67}\text{Zn}$  NMR is sparse, and of those reports only a few are relevant to biology.  $^{67}\text{Zn}$  NMR has been successfully applied to  $\text{Zn}^{2+}$ -enzyme or  $\text{Zn}^{2+}$ -protein systems, such as concanavalin, calmodulin, thermolysin, for studying the environment or behavior of  $\text{Zn}^{2+}$  interacting with the investigated biomolecule ([195] and references therein).

Historically, solid-state  $^{67}\text{Zn}$  NMR spectroscopy has been undesirable due to broad quadrupolar line-shapes and low sensitivity. In recent years, however, dramatic improvements in the solid-state NMR of quadrupolar nuclides have occurred. A general strategy for the observation of low  $\gamma$  half-integer quadrupolar nuclides has been developed. The methodology combines low-temperature (4–100 K) techniques with cross-polarization experiments while employing a Carr-Purcell-Meiboom-Gill spin-echo sequence, a strategy that affords sufficient sensitivity to examine  $\text{Zn}^{2+}$ -binding sites in metalloproteins by solid-state  $^{67}\text{Zn}$  NMR spectroscopy [196].

#### 3.13.2. Cadmium

Cadmium belongs to a category of heavy metal ions (cadmium, mercury, lead) that have increasingly attracted research attention over the years, due to their toxic manifestations in the environment and towards the various organisms living in it, including man [197]. Albeit non-essential in the human physiology, Cd(II) is largely associated with Zn(II), in competition with which a number of its toxic effects are believed to arise. As a toxic metal, Cd(II) is absorbed by the liver, ultimately finding its way to the kidney, the critical organ from the toxicity point of view [198].

In spite of the similar magnetic properties and natural occurrence of the two  $I=1/2$  cadmium isotopes,  $^{111}\text{Cd}$  (12.75%) and  $^{113}\text{Cd}$  (12.26%), the majority of the biological NMR studies have used  $^{113}\text{Cd}$  due to its slightly higher relative sensitivity. At natural abundance, the sensitivity of  $^{113}\text{Cd}$  is 7.6 times that of  $^{13}\text{C}$ , putting it on the fringe of accessibility for biological applications using modern high-field spectrometers. However, an approximate eightfold enhancement can be obtained by substitution with 96% isotopically enriched  $^{113}\text{Cd}$ , allowing reasonable

quality spectra to be acquired on as little as 0.5 mL of 0.5 mM of a  $^{113}\text{Cd}$ -substituted protein sample in a few hours of data accumulation.

Since the mid-1970s,  $^{113}\text{Cd}$  NMR spectroscopy has been employed by a large number of investigators in the study of a variety of metalloproteins and biological events in which the native Zn(II), Ca(II), Mg(II), Mn(II), Fe(II) or Cu(II) ions have been replaced by  $^{113}\text{Cd}$ (II). The adaptable ligand coordination number and geometry of Cd(II), which is quite similar to Zn(II), and factors such as its similar ionic radius (0.97 Å) to that of Ca(II) (0.99 Å) are the most commonly cited reasons why cadmium substitutes for such an extensive range of metal ions. Of even greater importance is the fact that, in a variety of cases where Zn(II) has been replaced by Cd(II) in native Zn(II) metalloenzymes and DNA-binding proteins, the wild-type activity has, at least to some extent, been retained, albeit at an altered pH maximum [199].

Mammalian metallothioneins (MTs) are considered unique small proteins because about one-third of their amino acids are cysteines. These supply sulfhydryl ligands that *in vivo* bind with high affinity to a number of metal ions of differing size and chemical properties, such as the essential metal ions  $\text{Zn}^{2+}$  and  $\text{Cu}^+$ , and the toxic metal ion  $\text{Cd}^{2+}$ . The 20 cysteines bind seven  $\text{Cd}^{2+}$  or  $\text{Zn}^{2+}$  ions or combinations of them in two metal-thiolate clusters.  $\text{Cu}^+$  forms substantially different complexes with MTs, the

structures of which are not yet well characterized [200].  $^{113}\text{Cd}$ , has frequently been used to probe the ligand environment of metal-binding sites.  $^{113}\text{Cd}$  chemical shifts are very sensitive to the nature, number, and geometric arrangement of the coordinating ligands. This is reflected by the almost 900 ppm range of chemical shifts observed in  $^{113}\text{Cd}$ -substituted metalloproteins (Fig. 22) [201]. The broad chemical shift dispersion of  $^{113}\text{Cd}$  resonances is useful not only in providing information about the ligand type(s) at a particular metal site, but also because systems containing multiple metal sites with identical ligand coordination environments have a high probability of yielding resolved  $^{113}\text{Cd}$  resonances (Fig. 23). The consistent correlation that exists between the  $^{113}\text{Cd}$  chemical shift in solution and the identity of the coordinating metal ligands (Fig. 22) is derived solely from Cd-substituted, structurally-defined metalloproteins.

Transferrins are known to bind the Cd(II) ion as tightly as Zn(II), Co(II) and Mn(II), and such a binding was investigated by  $^{113}\text{Cd}$  NMR spectroscopy. A sharp  $^{113}\text{Cd}$  signal due to the bound Cd(II) ion was observed at +21.6 and +11.7 ppm for ovotransferrin and human serum transferrin, respectively, and these chemical shift values are consistent with the involvement of only one histidine in each metal-binding set of the protein [202].

There is current interest in the antiviral activity of metal, especially zinc, cyclam (1,4,8,11-tetraazacyclotetradecane) complexes. Interest in cyclams arises from their anti-HIV

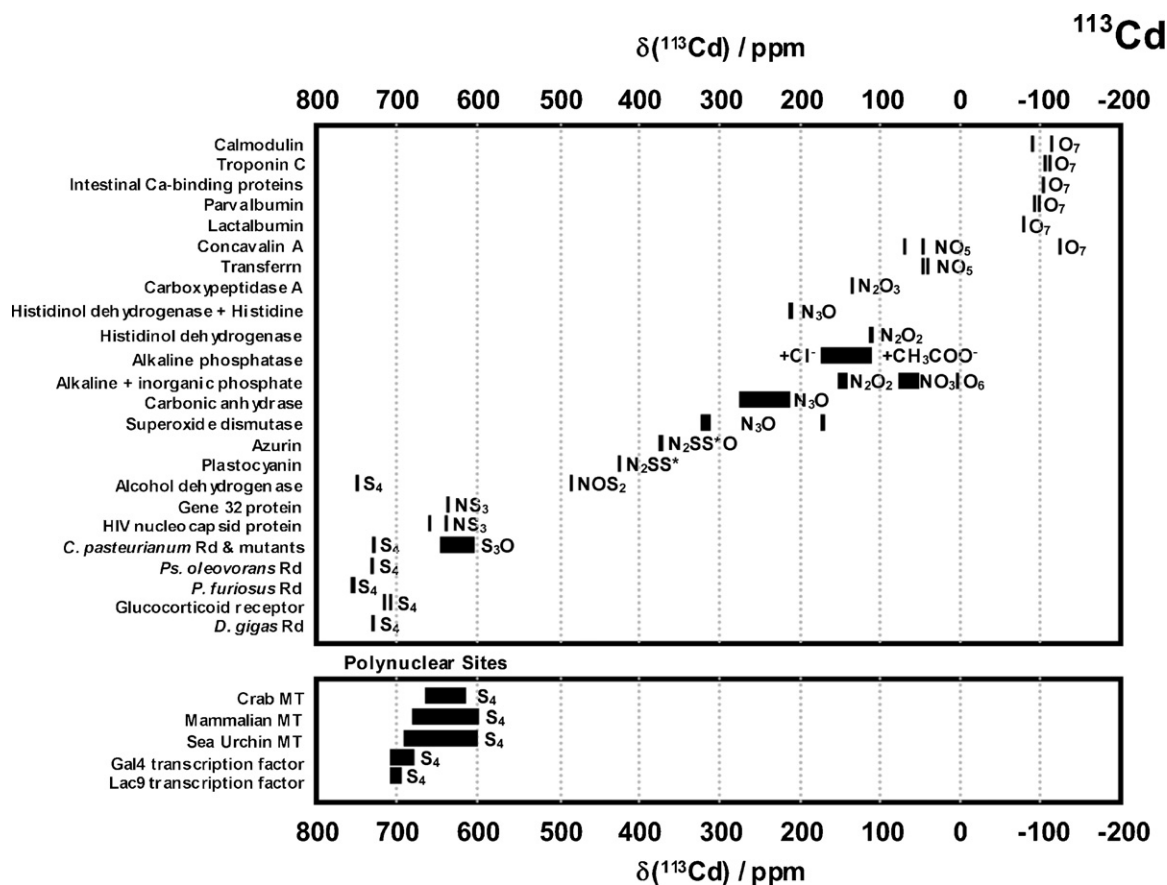


Fig. 22. Observed  $^{113}\text{Cd}$  chemical shifts for structurally characterized  $^{113}\text{Cd}$ -substituted metalloproteins: mononuclear (top) and polynuclear (bottom). All shifts are reported relative to external 0.1 M  $[\text{Cd}(\text{ClO}_4)_2]$ . The chemical shift position is correlated to ligand composition, where S represents sulfur from cysteine, S\* represents sulfur from methionine, O represents oxygen from carboxylate or water, and N represents nitrogen from histidine (adapted from Ref. [201a]).



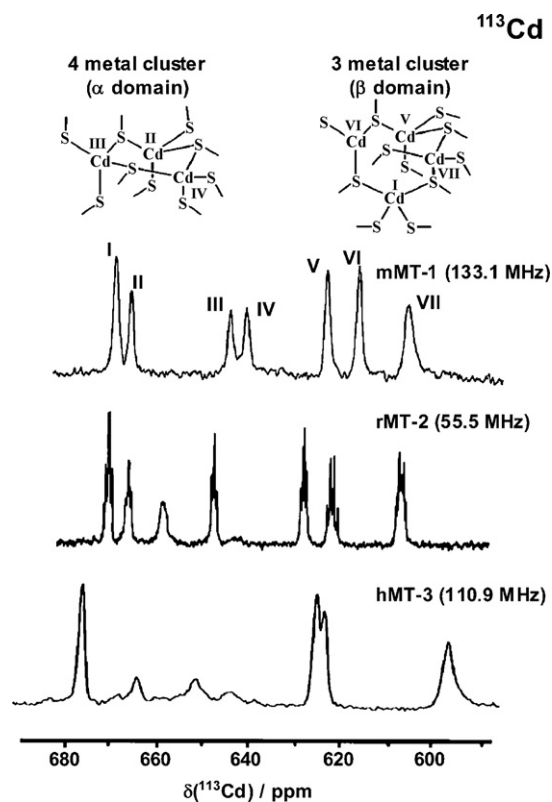


Fig. 23.  $^{113}\text{Cd}$  NMR spectra of mammalian MTs (mouse MT-1, human MT-3, rabbit MT-2) acquired at the indicated frequencies. Schematic structures of the two metal clusters are reported (adapted from Ref. [201a]).

activity. Their biological activity appears to be dependent on recognition of membrane proteins (viral coreceptors) and, therefore, on their configurations. In a recent study, Cd(II) has been used as a probe for Zn(II) on account of its useful NMR properties. Insights into the various configurations Cd–cyclam complexes were provided by  $^{113}\text{Cd}$  NMR spectroscopy [203].

### 3.13.3. Mercury

Mercury has no known natural biological role. Hg(0) is volatile and relatively non-toxic, whereas Hg(II) is toxic to most living organisms because of its avid coordination to thiol groups within biological systems. Hg(II) is known to undergo biological methylation to methylmercury and dimethylmercury, both of which are extremely toxic to humans [204]. Hg(II) is a virulent cumulative poison, readily absorbed through the respiratory tract, the gastrointestinal tract or through the skin.

Mercury has two NMR-active isotopes,  $^{199}\text{Hg}$  and  $^{201}\text{Hg}$ , the latter being quadrupolar ( $I = 3/2$ ). The  $I = 1/2$  isotope,  $^{199}\text{Hg}$ , with a natural abundance of 16.84%, has a chemical shift range of 2500 ppm and a relative sensitivity 5.4 times that of  $^{13}\text{C}$  and 8 times that of  $^{113}\text{Cd}$  for an equal number of nuclei.  $^{199}\text{Hg}$  NMR spectroscopy is in principle an excellent probe of organomercury adducts [205], but the inherent insensitivity of  $^{199}\text{Hg}$  makes the study of biological materials difficult. With conventional NMR direct detection techniques, including large (10–15 mm) sample tubes and long accumulation times, concentrations exceeding the solubility limits of most proteins and nucleic acids would

be necessary to obtain  $^{199}\text{Hg}$  NMR spectra [206]. A variety of indirect detection techniques have been devised to improve the observation of this insensitive nucleus [205,207].

Like Cd(II) (see Section 3.13.2),  $^{199}\text{Hg}$  NMR spectroscopy can be used to probe metal-binding sites where the native metal ions can be substituted by Hg(II) itself.  $^{199}\text{Hg}$  NMR spectra of  $^{199}\text{Hg}$ -substituted metalloproteins, e.g. carbonic anhydrase, azurin, plastocyanin, rusticyanin, rubredoxin, Gal4, MerR and MerP, and a number of mercury model complexes have been reported [208]. Much of these data are a result of the recent efforts of O'Halloran and co-workers aimed at defining the metal coordination environments in proteins involved in bacterial mercury resistance, and have revealed  $^{199}\text{Hg}$  chemical shifts indicative of certain coordination environments [208b].  $\{\text{HgS}_3\}$  centers have chemical shifts of ca.  $-100$  ppm and  $\{\text{HgS}_4\}$  centers at approximately  $-250$  ppm, with  $\{\text{HgN}_4\}$  sites at the other extreme of chemical shift at about  $-1200$  ppm (relative to  $[\text{Hg}(\text{CH}_3)_2]$ ). In addition,  $^{199}\text{Hg}$  exhibits scalar couplings to  $^1\text{H}$ ,  $^{13}\text{C}$  and  $^{15}\text{N}$  that are slightly larger than those observed with  $^{113}\text{Cd}$ , permitting heteronuclear correlation experiments to be carried out, which are often able to confirm the ligand type(s) and stoichiometry. The  $^{199}\text{Hg}$  nucleus exhibits  $T_1$  values in  $^{119}\text{Hg}$ -substituted plastocyanin and  $^{199}\text{Hg}$ -substituted azurin of 10 and 13 ms, respectively, which are approximately 10 times smaller than values obtained for  $^{113}\text{Cd}$  in the identical  $^{113}\text{Cd}$ -substituted proteins [208b]. Although the number of applications where the  $^{199}\text{Hg}$  ion can substitute isostructurally for the native metal ions in metalloproteins is limited owing to the 1.10 Å ionic radius and preference for either digonal or trigonal coordination geometry of the Hg(II) ion, it is clear that  $^{199}\text{Hg}$  NMR will continue to make important contributions in studies of selected metalloproteins.

### 3.14. f-Block: lanthanides

The main applications of lanthanides are as MRI paramagnetic contrast agents, while interest in the radioisotopes of lanthanides for radionuclide therapy is becoming more evident. The ability of lanthanide complexes to catalyze DNA hydrolysis (artificial nucleases) has been reviewed [209]. Further development of MRI contrast agents focuses mainly on gadolinium chelated by polydentate aminocarboxylate and related ligands. Gadolinium also has potential for use in neutron capture therapy with the advantage that its uptake can be monitored by MRI [210]. There are two main goals for future development. One is to control biological behavior (cellular uptake and retention, tissue targeting, *in vivo* stability) by incorporating Gd into bioconjugates, such as lipids with acid labile bonds (dota-palmitic acid micelles, hydroxymethyl dota derivatives, enhanced stability dtpa derivatives, and polymers/dendrimers). The other is to improve the efficiency with which the complexes induce spin relaxation in protons of water molecules, by designing chelators to control exchange rates of coordinated, or hydrogen-bonded water molecules, and by controlling the mobility and rotation (e.g. through molecular size) of complexes. These two goals can be combined by designing agents whose spin relaxation properties are dependent on the physiological environment, so that

MRI scans can provide biochemical/physiological as well as structural information.  $\beta$ -Emitting radionuclides of lanthanide elements, and bifunctional chelators for attaching them to carrier molecules have been also reviewed. Lanthanide complexes are also being evaluated for their antitumor cytotoxic effects and their ability to catalyse DNA hydrolysis [86].

The paramagnetic properties of trivalent lanthanide cations (Ln(III)) have been exploited in NMR spectroscopy for a long time. Applications have been both qualitative, to bring about simplification of the spectrum, and quantitative, by comparison of the lanthanide-induced shift and relaxation rate enhancements with values calculated for a proposed structure. Currently the main application of Ln(III) complexes in this field is as chiral shift reagents for the NMR separation of enantiomers, as well as for the separation of NMR signals from intracellular and extracellular alkali metal ions [211]. At the same time there has been an increasing interest in Ln(III) complexes for application as contrast agents [212]. Since lanthanides have several NMR-active isotopes they are important tools in structural analysis. This topic has been widely reviewed and will not be further discussed in this paper [213].

#### 4. NMR spectroscopy of biologically relevant non-metals

##### 4.1. *p*-Block: Group 16 (O, S, Se)

###### 4.1.1. Oxygen

One of the main reasons for studying oxygen is its ubiquity in biology. Indeed, oxygen controls or participates in nearly every biological process, especially those involving aerobic metabolism. Oxygen occupies a key position both at structural and physiological levels. In all macromolecules, including peptides, proteins, DNA and RNA (especially ribosomes) and carbohydrates, oxygen has a major role in the molecular conformation observed, such as the secondary, tertiary and quaternary structure. In proteins that are stabilized through multiple hydrogen bonds, changes which occur between ground and transition states can also induce an important effect on enzyme catalysis [214]. It is therefore not surprising that oxygen atoms are involved in triggering, signaling and activation mechanisms.

$^{17}\text{O}$  is the only NMR-active oxygen isotope ( $I=5/2$ ) and its application in NMR has been hindered by several of its intrinsic nuclear properties resulting in low sensitivity and complex spectra. Amongst these are (i) the small gyromagnetic ratio, so that the resonance frequency is about one-seventh that of protons; (ii) a low natural abundance of 0.037% leading to an extremely low absolute sensitivity so that isotopic enrichment is usually necessary; (iii) a nuclear quadrupole moment; and (iv) in a number of cases a large electric field gradient is experienced.  $^{17}\text{O}$  exhibits a large NMR chemical shift range depending on the chemical function and the local environment, with the shift being distributed on *ca.* 1000 ppm [215].

$^{17}\text{O}$  solution NMR spectroscopy is a useful technique to solve structural problems for small organic molecules. The fast reorientation of the molecules in solution results in narrow spec-

tral lines due to the averaging of the quadrupolar interaction. Rapid quadrupolar relaxation of  $^{17}\text{O}$  has, however, prevented successful applications of solution  $^{17}\text{O}$  NMR spectroscopy to biological macromolecules [216]. The large quadrupolar interaction of oxygen-containing functional groups can cause highly effective relaxation, which leads to strong broadening of the NMR signals, which can be severe for large molecules. Amongst the few reported studies,  $^{17}\text{O}$  NMR spectroscopy has been successfully used to study synthetic oxygen carriers related to biological systems, such as a synthetic single-face hindered iron porphyrin–dioxygen complex [217], metal–nucleotide interactions [218], and nucleic acid dynamics [219].

In order to overcome problems related to the detection of  $^{17}\text{O}$  NMR signals, lanthanide-induced  $^{17}\text{O}$  solid-state NMR has recently been seen as an alternative for structural studies to  $^{17}\text{O}$  solution NMR, since the relaxation times are much longer and the intrinsic spectral resolution is not limited by molecular weight [215].

One unique NMR property of  $^{17}\text{O}$  is the independence of  $^{17}\text{O}$  relaxation times on the magnetic field strength, and this makes it possible to achieve a large sensitivity gain for *in vivo*  $^{17}\text{O}$  NMR applications at high fields. *In vivo*  $^{17}\text{O}$  NMR has two major applications for studying brain function and cerebral bioenergetics [220]. The first application is to measure the cerebral blood flow (CBF) through monitoring the washout of inert  $\text{H}_2^{17}\text{O}$  tracer in brain tissue following an intravascular bolus injection of the  $^{17}\text{O}$ -labelled water. The second application, perhaps the most important one, is to determine the cerebral metabolic rate of oxygen utilization (CMRO2) through monitoring the dynamic changes of metabolically generated  $\text{H}_2^{17}\text{O}$  from inhaled  $^{17}\text{O}$ -labeled oxygen gas in the brain tissue. Unlike the CBF measurements, the amount of the metabolically generated  $\text{H}_2^{17}\text{O}$  during an inhalation of  $^{17}\text{O}_2$  is small. This could affect the reliability of CMRO2 measurement using *in vivo*  $^{17}\text{O}$  approaches. With the dramatic  $^{17}\text{O}$  sensitivity gain realized at high fields, it was possible to obtain a three-dimensional  $^{17}\text{O}$  chemical shift imaging from the natural abundance  $\text{H}_2^{17}\text{O}$  in a rat brain with excellent signal-to-noise ratio as well as good temporal and spatial resolutions (11 s of data acquisition and  $\sim 0.1$  ml chemical shift imaging voxel size) at 9.4 T [220a]. Fig. 24 shows one example of three adjacent slices of  $^{17}\text{O}$  chemical shift imaging of the natural abundance  $\text{H}_2^{17}\text{O}$  from a representative rat brain acquired by an  $^{17}\text{O}$  surface coil and the 3D Fourier series window spectroscopic imaging technique at 9.4 T. One great merit of *in vivo*  $^{17}\text{O}$  NMR for the determination of CMRO2 is that only the metabolic  $\text{H}_2^{17}\text{O}$  is detectable. This merit dramatically simplifies both CMRO2 measurement and quantification compared to other established methods. There are two major NMR approaches for monitoring  $\text{H}_2^{17}\text{O}$  *in vivo*, namely a direct approach by using  $^{17}\text{O}$  NMR detection and an indirect approach by using  $^1\text{H}$  NMR detection for measuring the changes in  $T_2$ - or  $T_1$ -weighted proton NMR signals caused by the  $^{17}\text{O}$ – $^1\text{H}$  scalar coupling and proton chemical exchange. Both approaches are suitable for CBF measurements. However, recent studies indicate that the direct *in vivo*  $^{17}\text{O}$  NMR approach at high/ultrahigh fields appears to offer significant advantages for quantifying and imaging CMRO2 [220b].

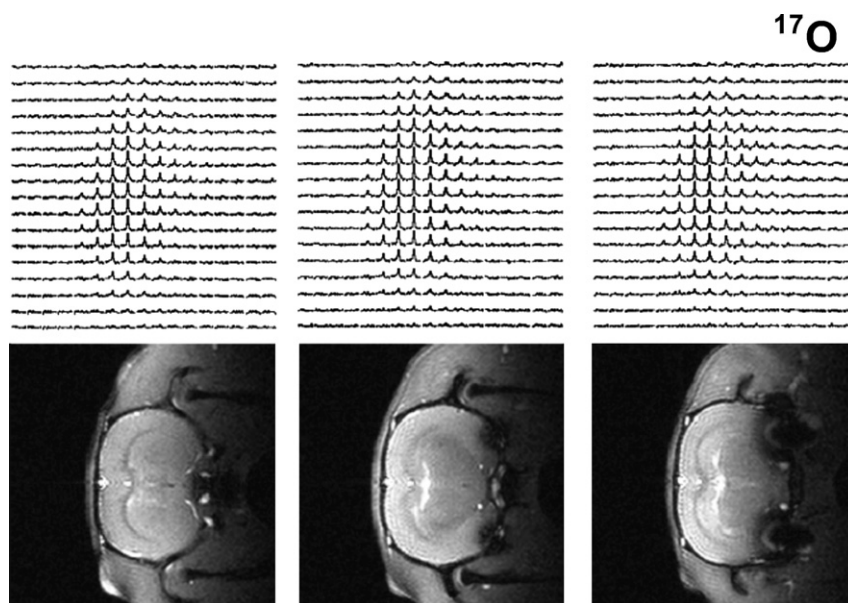


Fig. 24. Three-dimensional coronal  $^{17}\text{O}$  MRI (Fourier series window) images of natural abundance  $\text{H}_2^{17}\text{O}$  in the rat brain acquired at 9.4 T. Three adjacent coronal  $^{17}\text{O}$  images (0.1 ml voxel size; total acquisition time of 11 s) and the corresponding proton anatomical images are presented herein (adapted from Ref. [220a]).

#### 4.1.2. Sulfur

Sulfur is essential for all living cells. Sulfur may also serve as a chemical food source for some primitive organisms: some forms of bacteria use hydrogen sulfide ( $\text{H}_2\text{S}$ ) in place of water as the electron donor in a primitive photosynthesis-like process. Sulfide forms a part of iron–sulfur clusters and the bridging ligand in the  $\text{Cu}_A$  site of cytochrome-*c* oxidase, involved in utilization of oxygen by all aerobic life. In plants and animals the amino acids cysteine and methionine contain sulfur, as do all polypeptides, proteins, and enzymes which contain these amino acids. Homocysteine and taurine are other sulfur-containing acids which are similar in structure, but which are not coded for by DNA, and are not part of the primary structure of proteins. Glutathione ( $\gamma\text{-Glu-Cys-Gly}$ ) is an important sulfur-containing tripeptide which plays a role in cells as a source of chemical reduction potential in the cell, through its sulfhydryl group. Many important cellular enzymes use prosthetic groups ending with sulfhydryl groups to handle reactions involving acyl-containing biochemicals: two common examples from basic metabolism are coenzyme A and alpha-lipoic acid. Disulfide bonds (S–S bonds) formed between cysteine residues in peptide chains are very important in protein assembly and structure. These strong covalent bonds between peptide chains give proteins a great deal of extra toughness and resilience [221].

$^{33}\text{S}$  is the only naturally occurring isotope of sulfur with a non-zero nuclear spin ( $I=3/2$ ). Since it has a moderate quadrupole moment, a low natural abundance and a low magnetogyric ratio, it is clearly an intrinsically insensitive nucleus. It was shown that the enormous diversity of chemical environments for sulfur is reflected in a chemical shift range of over 1000 ppm and line-widths varying between 0.03 and >5000 Hz. Since  $^{33}\text{S}$  has a large quadrupole moment, nuclear relaxation is dominated by the quadrupolar mechanism and, consequently,  $^{33}\text{S}$  NMR signals are very broad unless the electronic sur-

rounding of sulfur is highly symmetric. However, despite these drawbacks, a number of studies using sulfur NMR spectroscopy have been reported [222], but none of them are strictly related to biological studies.

The potential of  $^{33}\text{S}$  NMR spectroscopy for biochemical investigations on taurine has been explored [223]. Taurine (2-aminoethanesulfonic acid) is a naturally occurring  $\beta$ -amino acid widely distributed in the biosphere. Despite the intensive studies, many mechanisms of the biochemical reactions involving taurine remain unknown or uncertain, probably because of the difficulty in detecting taurine in intact tissues. In this work,  $^{33}\text{S}$  NMR spectra of biological tissues were reported for the first time, and this appears to be one of the few biologically relevant applications of this technique. As shown in Fig. 25, in the chemical shift range  $-240$  to  $+300$  ppm the  $^{33}\text{S}$  spectrum of *L. lithophaga* homogenates exhibits a single signal that was assigned to the  $^{-33}\text{SO}_3^-$  group of taurine on the basis of its chemical shift value ( $-6.8$  ppm). The assignment was confirmed by adding pure taurine to the sample. In the spectral range examined, no  $^{33}\text{S}$  NMR signals were detected from other sulfur-containing biological molecules, for instance, cystine, cysteine, methionine, and hypotaurine.

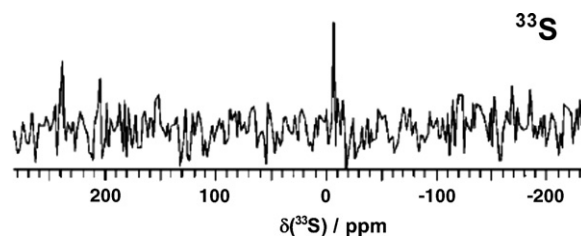


Fig. 25. *In vivo*  $^{33}\text{S}$  NMR spectrum (referred to the  $^{33}\text{S}$  signal of 1 M  $\text{Na}_2\text{SO}_4$  in  $\text{H}_2\text{O}$  in a coaxial cell) of an *L. lithophaga* homogenate. The peak at  $-6.8$  ppm is assigned to the amino acid taurine (adapted from Ref. [223]).



### 4.1.3. Selenium

Selenium is a trace element essential for mammals. Low molecular weight selenium compounds present in the human body include as selenocysteine (or selenocystine) and selenomethionine, with much lower abundance of their metabolic precursors. Selenium indeed displays many similarities with its congener sulfur, *i.e.* they have rather similar electronegativities and atom sizes and they have the same major oxidation states. There are thus many sulfur compounds that have selenium analogs. However, in spite of these similarities, there are nonetheless clearly differences between the two elements, and substitution for one another results in compounds with quite diverse chemical properties [224]. Diseases associated with selenium deficiency include asthma, Keshan disease, and HIV. Therefore, selenium-based agents are currently being investigated for their potential therapeutic applications. Moreover, selenium compounds have been shown to be of value as cancer chemopreventive agents [225].

The element selenium has six natural isotopes, but only one of them,  $^{77}\text{Se}$ , is NMR-active having a nuclear spin quantum number  $I=1/2$ , and high-resolution NMR spectroscopy is possible.  $^{77}\text{Se}$  is approximately three times more sensitive than  $^{13}\text{C}$ , and taking into account that longitudinal relaxation times are in the range of seconds and that NOE effects are nearly always absent, the sensitivities of  $^{13}\text{C}$  and  $^{77}\text{Se}$  are comparable in routine NMR experiments [226].

$^{77}\text{Se}$  NMR spectroscopy has been successfully employed in several cases: the characterization of selenium-based metallo-drugs [227], the determination of spin–lattice relaxation times for several classes of biologically relevant selenium compounds [228], and the identification of seleno-proteins [229].

## 4.2. *p*-Block: Halogens (F, Cl, Br, I)

### 4.2.1. Fluorine

Fluorine is an essential element, and as fluoride is an important trace element affecting bones and teeth [230].

$^{19}\text{F}$  has many favorable NMR characteristics, including a nuclear spin  $I=1/2$ , 100% natural abundance, high sensitivity and large chemical shift range ( $\sim 500$  ppm) [231]. While fluorine occurs in the body, it is present mostly in the form of solid fluorides in bones and teeth. Endogenous fluorine has a very short  $T_2$  relaxation time [230] and the resulting signal is below the limits of NMR detection in most biological systems of interest. On the other hand, as a number of fluorinated drugs are currently in clinical use, such as 5-fluorouracil, flurbiprofen, isoflurane, fluoxetine, haloperidol [232],  $^{19}\text{F}$  NMR offers a powerful method of monitoring their pharmacokinetics and metabolism.  $^{19}\text{F}$  NMR spectroscopy is a versatile non-invasive analytical technique to detect, identify and quantify metabolites of fluorinated drugs both *in vitro* and *in vivo*, in order to study their physiology and pharmacology. Several reviews have been recently published on this topic [16h,232,233]. An example is given in Fig. 26, where  $^{19}\text{F}$  NMR spectroscopy is used to follow the degradative pathway (depicted in Fig. 27) of capecitabine. Capecitabine is a pro-drug

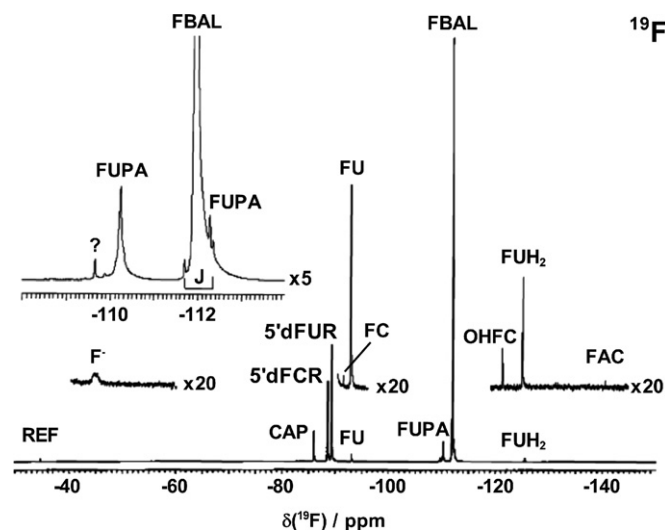


Fig. 26.  $^{19}\text{F}$  NMR spectrum at 282 MHz with proton decoupling of a urine sample from a patient treated orally with capecitabine at a dose of 2900 mg/day administered twice daily at 12 h interval. Urine fraction 0–12 h collected after the first dose of 1450 mg and 14-fold concentrated, pH of the sample: 5.5. The chemical shifts are expressed relative to the resonance peak of trifluoroacetic acid (5% (w/v) aqueous solution) used as external reference (REF). Assignments:  $\text{F}^-$ , fluoride ion; CAP, capecitabine; 5'dFCR, 5'-deoxy-5-fluorocytidine; 5'dFUR, 5'-deoxy-5-fluorouridine; FC, 5-fluorocytosine; FU, 5-fluorouracil; ?, unknown; FUPA,  $\alpha$ -fluoro- $\beta$ -ureidopropionic acid; FBAL,  $\alpha$ -fluoro- $\beta$ -alanine; FHPA, 2-fluoro-3-hydroxypropanoic acid; OHFC, 6-hydroxy-5-fluorocytosine;  $\text{FUH}_2$ , 5,6-dihydro-5-fluorouracil; FAC, fluoroacetic acid. J,  $^1\text{J}(^{13}\text{C}-^{19}\text{F})$  coupling constant (adapted from Ref. [16h]).

of the anticancer agent 5-fluorouracil, designed to be used as an oral formulation to overcome toxic side-effects of 5-fluorouracil without compromising its antitumor efficacy [234].

Two non-invasive  $^{19}\text{F}$  NMR methodologies have been exploited to measure the heterogeneous distribution of hypoxia in tumors. The first is  $^{19}\text{F}$  NMR measurements of tumor oxygenation following the administration of perfluorocarbon emulsions, and the second involves  $^{19}\text{F}$  NMR measurements of the retention of fluorinated 2-nitroimidazoles by hypoxic tumor tissues [235].

### 4.2.2. Chlorine

Chlorine is an essential element for all living organisms largely as chloride ( $\text{Cl}^-$ ), but hypochlorite ( $\text{ClO}^-$ ) is produced in some cell compartments (to destroy invading organisms). Together with  $\text{Na}^+$ ,  $\text{Cl}^-$  is a major extracellular electrolyte. In conjunction with monovalent alkali metals and  $\text{H}^+$  ions, it controls transmembrane potentials and regulates the equilibrium of cellular electrolytes and osmotic pressures. A defect in  $\text{Cl}^-$  transport causes cystic fibrosis, a genetic disorder resulting in a defect in the transmembrane chloride channel [37].

All naturally occurring chlorine is found in two NMR-active isotopic forms,  $^{35}\text{Cl}$  and  $^{37}\text{Cl}$ , both having nuclear spin  $I=3/2$ . Given its higher natural abundance (75.53%) and higher receptivity,  $^{35}\text{Cl}$  is the preferred isotope for NMR spectroscopic observation. Their relaxation is normally dominated by the contributions from interaction of their quadrupole moments with time-dependent electric field gradients at the nucleus.



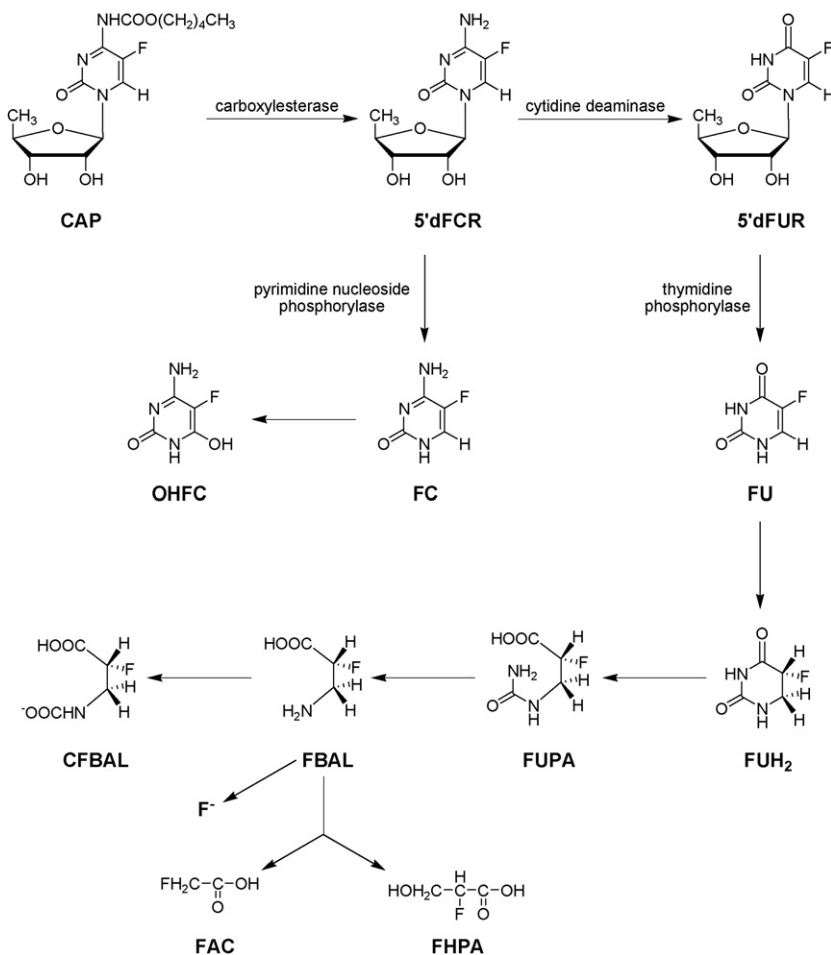


Fig. 27. Catabolic pathway of capecitabine. All the compounds (except CFBAL) are represented in neutral form. CAP, capecitabine; 5'dFCR, 5'-deoxy-5-fluorocytidine; 5'dFUR, 5'-deoxy-5-fluorouridine; FU, 5-fluorouracil; FUH<sub>2</sub>, 5,6-dihydro-5-fluorouracil; FUPA, α-fluoro-β-ureidopropionic acid; FBAL, α-fluoro-β-alanine; CFBAL, N-carboxy-α-fluoro-β-alanine; F<sup>-</sup>, fluoride ion; FHPA, 2-fluoro-3-hydroxypropanoic acid; FAC, fluoroacetic acid; FC, 5-fluorocytosine; OHFC, 6-hydroxy-5-fluorocytosine.

Although both the natural abundance and receptivity are favorable, recording <sup>35</sup>Cl NMR spectra is often difficult as it gives rise to rather broad signals. Therefore, a very few papers report on the use of <sup>35</sup>Cl NMR techniques for specific biological purposes. Chlorine NMR studies of chloride binding to proteins have been used to investigate a number of interesting properties associated with the proteins [236]. However, the major use of the method has generally been restricted to that of a titration indicator.

ATP binds to mammalian metallothionein-2 (MT-2), and this interaction and the associated conformational change of the protein affect the sulfhydryl reactivity and zinc transfer potential of MT. <sup>35</sup>Cl NMR spectroscopy has further identified chloride as an additional biological MT ligand, which can interfere with the interaction of ATP with MT [237].

<sup>35</sup>Cl NMR spectroscopy has been also used to investigate transmembrane Cl<sup>-</sup> transport [238], the chloride binding by the AML1/Runx1 transcription factor [239], and to demonstrate, by means of <sup>35</sup>Cl and <sup>37</sup>Cl relaxation measurements, that human α<sub>2</sub>-macroglobulin tetramer possesses a unique pair of zinc-binding sites [240].

#### 4.2.3. Bromine and iodine

Bromine is currently not thought to be an essential element for man, although it is present in blood at micromolar concentrations. As hypobromite (BrO<sup>-</sup>), it has a potential role in the destruction of pathogenic organisms. Iodine is an essential micronutrient for humans, where it is required for incorporation into the thyroid hormones thyroxine and triiodothyronine.

<sup>79/81</sup>Br and <sup>127</sup>I are magnetically active isotopes, and are characterized by a high sensitivity to detection by NMR spectroscopy. Bromine has two naturally occurring isotopes, <sup>79</sup>Br and <sup>81</sup>Br, with nuclear spin  $I = 3/2$ . Although <sup>79</sup>Br has a slightly higher natural abundance (50.54% vs. 49.46% for <sup>81</sup>Br), the preferred isotope for NMR spectroscopic observation is <sup>81</sup>Br, due to its higher receptivity. The chemical shift range of the bromine nucleus is approximately 800 ppm. <sup>127</sup>I is the only NMR-active isotope of iodine at 100% natural abundance, with nuclear spin  $I = 5/2$  and a chemical shift range of approximately 6000 ppm [236].

Only a few <sup>81</sup>Br and <sup>127</sup>I NMR experiments of biological relevance have been reported. There has been considerable interest in the application of NMR probes to the study of the conforma-

tion of proteins. The NMR halide probe method [241] detects changes in the halide nuclear transverse relaxation time ( $T_2$ ) as a result of halide exchange between symmetrically solvated free halide ion (long  $T_2$ ) and a probe site where the quadrupolar halide nucleus is bound tightly to a specific region within a protein (short  $T_2$ ). The resulting relaxation time is dependent on the relative concentrations of free and bound sites, and the physical environment of the bound halide. In its most common application, a solution of protein is prepared in aqueous sodium halide, and specific binding sites on the protein may be titrated with a metal such as mercury which binds only to these sites and which subsequently complexes halide from the solution. The application of the bromide ion as an NMR probe has been investigated, as it has some advantages over the more commonly used chloride ion, the most important being its ability to yield values for the free-to-bound exchange rate constant of the probe itself, in addition to the correlation time for reorientation of the bound probe. The exchange rates are fast, near the diffusion limit, and are sensitive to protein conformational effects near the binding site [242].

$^{127}\text{I}$  NMR spectroscopy has only rarely been utilized for studies of fluid systems partly because, for covalent environments, the  $^{127}\text{I}$  NMR signal is generally broadened beyond detection. The iodide ion, on the other hand, may be conveniently studied. For example,  $^{127}\text{I}^-$  has been used as a probe for the anion binding properties of human serum albumin [243]. Analogous studies have been performed to investigate the binding of iodide to some peroxidases [244].

## 5. Conclusions

Although there is enormous potential for the application of inorganic chemistry for the design of novel therapeutic and diagnostic agents, progress is hampered by the lack of methods for their speciation in solution. The nature of the species will determine their biological activity. Our review has illustrated the challenges involved in making NMR studies of many elements of interest. Although a few have readily observable spin  $I = 1/2$  nuclei available for study (*e.g.* Cd, Ag, Pt), their sensitivity is not sufficient for investigations at biologically relevant concentration (micromolar or below), and signal broadening *via* relaxation mechanisms such as chemical shift anisotropy can be a problem. Nevertheless, in favorable circumstances, NMR spectroscopy can provide valuable insight into the biological chemistry of these elements. The problem of line-broadening of resonances from quadrupolar nuclei in low-symmetry environments greatly hinders NMR studies of a range of biologically important elements, but again under favorable conditions, NMR can also provide insight into both the thermodynamics and kinetics of their bonding sites. There is a need for the continued development of new NMR methods to study a wide range of nuclei, especially to decrease the line-widths of peaks from quadrupolar nuclei and increase the effective sensitivity of detection. Such advances could potentially be of direct benefit to the design of new medicines.

## Acknowledgements

We thank the EC (Marie Curie Fellowship for LR) and Körber Foundation for financial support.

## References

- [1] J. McMaster, Annu. Rep. Prog. Chem. Sect. A: Inorg. Chem. 98 (2002) 593.
- [2] P.J. Sadler, C. Muncie, M.A. Shipman, in: I. Bertini, H.B. Gray, E.I. Stiefel, J.S. Valentine (Eds.), Biological Inorganic Chemistry: Structure & Reactivity, University Science Books, Mill Valley, CA, 2007, p. 95.
- [3] M. Park, Q. Li, N. Shcheynikov, S. Muallem, W. Zeng, Cell Cycle 4 (2005) 24.
- [4] C. Camilleri, S.J. Markich, B.N. Noller, C.J. Turley, G. Parker, R.A. van Dam, Chemosphere 50 (2002) 355.
- [5] A. Levina, P.A. Lay, Coord. Chem. Rev. 249 (2005) 281.
- [6] (a) I. Bertini, H.B. Gray, E.I. Stiefel, J.S. Valentine (Eds.), Biological Inorganic Chemistry: Structure & Reactivity, University Science Books, Mill Valley, CA, 2007; (b) J.J.R. Fraústo da Silva, R.J.P. Williams, Biological Chemistry of the Elements, Oxford University Press, Oxford, 2001.
- [7] N.K. Karpowich, H.H. Huang, P.C. Smith, J.F. Hunt, J. Biol. Chem. 278 (2003) 8429.
- [8] D.G. Gourley, A.W. Schüttelkopf, L.A. Anderson, N.C. Price, D.H. Boxer, W.N. Hunter, J. Biol. Chem. 276 (2001) 20641.
- [9] C. Andreini, L. Banci, I. Bertini, A. Rosato, J. Proteome Res. 5 (2006) 196.
- [10] G.V. Kryukov, S. Castellano, S.V. Novoselov, A.V. Lobanov, O. Zehab, R. Guigó, V.N. Gladyshev, Science 300 (2003) 1439.
- [11] T. Storr, K.H. Thompson, C. Orvig, Chem. Soc. Rev. 35 (2006) 534.
- [12] K.H. Thompson, C. Orvig, in: H.B. Kraatz, N. Metzler-Nolte (Eds.), Concepts and Model Systems in Bioinorganic Chemistry, Wiley-VCH, Weinheim, 2006, p. 25.
- [13] B.J. Stockman, Prog. Nucl. Magn. Reson. Spectrosc. 33 (1998) 109.
- [14] (a) J.S. Cohena, J.W. Jaroszewski, O. Kaplan, J. Ruiz-Cabellod, S.W. Collier, Prog. Nucl. Magn. Reson. Spectrosc. 28 (1995) 53; (b) I.C.P. Smith, L.C. Stewart, Prog. Nucl. Magn. Reson. Spectrosc. 40 (2002) 1; (c) M. Dadiani, E. Furman-Haran, H. Degani, Prog. Nucl. Magn. Reson. Spectrosc. 49 (2006) 27.
- [15] (a) G. Wu, Biochem. Cell Biol. 76 (1998) 429; (b) L.K. Thompson, Curr. Opin. Struct. Biol. 12 (2002) 661; (c) D. Basting, I. Lehner, M. Lorch, C. Glaubitz, Naunyn Schmiedeberg's Arch Pharmacol. 372 (2006) 451; (d) A. Naito, I. Kawamura, Biochim. Biophys. Acta, Biomembr. 1768 (2007) 1900.
- [16] (a) P.B. Barker, D.D.M. Lin, Prog. Nucl. Magn. Reson. Spectrosc. 49 (2006) 99; (b) R.A. Wind, J.Z. Hu, Prog. Nucl. Magn. Reson. Spectrosc. 49 (2006) 207; (c) M. Rivera, G.A. Caignan, Anal. Bioanal. Chem. 378 (2004) 1464; (d) W. Bermel, I. Bertini, I.C. Felli, M. Piccioli, R. Pierattelli, Prog. Nucl. Magn. Reson. Spectrosc. 48 (2006) 25; (e) P.-G. Henry, G. Adriany, D. Deelchand, R. Gruetter, M. Marjanska, G. Öz, E.R. Seaquist, A. Shestov, K. Ugurbil, Magn. Reson. Imaging 24 (2006) 527; (f) R. Marek, A. Lycka, Curr. Org. Chem. 6 (2002) 35; (g) S.J. Berners-Price, L. Ronconi, P.J. Sadler, Prog. Nucl. Magn. Reson. Spectrosc. 49 (2006) 65; (h) R. Martino, V. Gilard, F. Desmoulin, M. Malet-Martino, J. Pharm. Biomed. Anal. 38 (2005) 871.
- [17] J. Mason, Chem. Rev. 87 (1987) 1299.
- [18] I. Bertini, C. Luchinat, G. Parigi, Solution NMR of Paramagnetic Molecules: Applications to Metallobiomolecules and Models, Elsevier Science B.V., Amsterdam, 2001.

- [19] L. Que, H.M. Harold, S.S. David, B.P. Murch, P.A. Arafa, M. Isam, *Inorg. Chem.* 26 (1987) 2779.
- [20] I. Bertini, P. Turano, A.J. Villa, *Chem. Rev.* 93 (1993) 2833.
- [21] M.L. Weiner, in: N.J. Birch, C. Padgham, M.S. Hughes (Eds.), *Lithium in Medicine and Biology*, Marius Press, Carnforth, 1993, p. 15.
- [22] D.K. Anderson, L.D. Prockop, in: F.N. Johnson (Ed.), *Lithium Research and Therapy*, Academic Press, London, 1975, p. 267.
- [23] M. Maj, *Bipolar Disord.* 5 (2003) 180.
- [24] J.W. Akitt, in: J. Mason (Ed.), *Multinuclear NMR Spectroscopy*, Plenum Press, New York, 1987, p. 189.
- [25] N. Bansal, M.J. Germann, I. Lazar, C. Malloy, A.D. Sherry, *J. Magn. Reson. Imaging* 2 (1992) 385.
- [26] (a) R.A. Komoroski, *NMR Biomed.* 18 (2005) 67;  
(b) R.A. Komoroski, *Magn. Reson. Imaging* 18 (2000) 103.
- [27] J.C. Soares, F. Boada, S. Spencer, A.G. Mallinger, C.S. Dippold, K. Forster Wells, E. Frank, M.S. Keshavan, S. Gershon, D.J. Kupfer, *Biol. Psychiatry* 49 (2001) 437.
- [28] A. Frazer, J. Mendels, S.K. Secunda, C.M. Cochrane, C.P. Bianchi, *J. Psychiatr. Res.* 10 (1973) 1.
- [29] E. Pierson, K. Luterbach, E. Rzepka, S. Ramaprasad, *Magn. Reson. Imaging* 22 (2004) 123.
- [30] (a) A. Nakano, Q.S. Xie, J.V. Mallen, L. Echegoyen, G.W. Gokel, *J. Am. Chem. Soc.* 112 (1990) 1287;  
(b) F.G. Riddell, M.K. Hayer, *Biochim. Biophys. Acta* 817 (1985) 313;  
(c) T.L. Knubovets, A.V. Revazov, L.A. Sibeldina, U. Eichhoff, *Magn. Reson. Med.* 26 (1987) 4953.
- [31] S. Forsen, B. Lindman, in: K.R. Harris, B.E. Mann (Eds.), *NMR and Periodic Table*, Academic Press, London, 1978, p. 129.
- [32] M. Lupu, D. Ojcius, J.L. Perfettini, J. Patry, J.L. Dimicoli, J. Mispelter, *Biochimie* 85 (2003) 849.
- [33] S.J. Kohler, N.H. Kolodny, *Prog. Nucl. Magn. Reson. Spectrosc.* 24 (1992) 411.
- [34] A.M. Torres, D.J. Philp, R. Kemp-Harper, C. Garvey, P.W. Kuchel, *Magn. Reson. Chem.* 43 (2005) 217.
- [35] (a) N.V. Hud, P. Schultze, V. Sklenar, J. Feigon, *J. Mol. Biol.* 285 (1999) 233;  
(b) S. Basu, A.A. Szweczek, M. Cocco, S.A. Strobel, *J. Am. Chem. Soc.* 122 (2000) 3240.
- [36] A. Wong, R. Ida, G. Wu, *Biochem. Biophys. Res. Commun.* 337 (2005) 363.
- [37] J.A. Cowan, *Inorganic Biochemistry: An Introduction*, Wiley-VCH, New York, 1997.
- [38] H.J. Guttman, S. Cayley, M. Li, C.F. Anderson, M.T. Record Jr., *Biochemistry* 34 (1995) 1393.
- [39] Q. Xu, H. Deng, W.H. Braunlin, *Biochemistry* 32 (1993) 13130.
- [40] Y. Sea, M. Murakami, E. Suzuki, S. Kuki, K. Nagayama, H. Watari, *Biochemistry* 29 (1990) 599.
- [41] (a) R.M. Wellard, B.P. Shehan, W.R. Adam, D.J. Craik, *Magn. Reson. Med.* 29 (1993) 68;  
(b) S.A. Rashid, W.R. Adam, D.J. Craik, B.P. Shehan, R.M. Wellard, *Magn. Reson. Med.* 17 (1991) 213.
- [42] T. Ogino, G.I. Shulman, M.J. Avison, S.R. Gullanst, J.A. den Hollander, R.G. Shulman, *Proc. Natl. Acad. Sci. U.S.A.* 82 (1985) 1099.
- [43] W.D. Love, G.E. Burch, *J. Lab. Clin. Med.* 41 (1953) 351.
- [44] (a) J.L. Allis, C.D. Snaith, A.-M.L. Seymour, G.K. Radda, *FEBS Lett.* 242 (1989) 215;  
(b) J.L. Allis, Z.H. Endre, G.K. Radda, *Ren. Physiol. Biochem.* 12 (1989) 171.
- [45] V.V. Kupriyanov, L.C. Stewart, B. Xiang, J. Kwak, R. Deslauriers, *Circ. Res.* 76 (1995) 839.
- [46] V.V. Kupriyanov, B. Xiang, J.K. Sun, O. Jilkina, G.P. Dai, R. Deslauriers, *Magn. Reson. Med.* 46 (2001) 963.
- [47] K. Drewnowska, C.M. Baumgarten, *Am. J. Physiol.* 260 (1991) C122.
- [48] O. Jilkina, B. Kuzio, J. Rendell, B. Xiang, V.V. Kupriyanov, *J. Mol. Cell. Cardiol.* 41 (2006) 893.
- [49] D.G. Davis, E. Murphy, R.E. London, *Biochemistry* 27 (1988) 3547.
- [50] L.L. Soong, G.E. Leroi, A.I. Popov, *Inorg. Chem.* 29 (1990) 1366.
- [51] J. Goodman, J.J. Neil, J.J.H. Ackerman, *NMR Biomed.* 18 (2005) 125.
- [52] W. Lin, D. Mota de Freitas, Q. Zhang, K.W. Olsen, *Arch. Biochem. Biophys.* 369 (1999) 78.
- [53] (a) P.E. Pfeffer, D.B. Rolin, D. Brauer, S.-I. Tu, T.F. Kumosinski, *Biochim. Biophys. Acta* 1054 (1990) 169;  
(b) Y. Li, J. Neil, J.J. Ackerman, *NMR Biomed.* 8 (1995) 183.
- [54] J. Lake, *Annu. Rev. Biochem.* 54 (1985) 507.
- [55] S.M. Linn, R.J. Roberts, *Nucleases*, Cold Spring Harbor Laboratory Press, New York, 1993.
- [56] E.I. Ochiai, *General Principles of Biochemistry of the Elements*, Plenum Press, New York, 1987.
- [57] P. Delva, in: M. Gielen, E.R.T. Tiekink (Eds.), *Metallotherapeutic Drugs and Metal-Based Diagnostic Agents: The Use of Metals in Medicine*, Wiley-VCH, Weinheim, 2005, p. 51.
- [58] W.H. Braunlin, *Adv. Biophys. Chem.* 5 (1995) 89.
- [59] J.A. Cowan, *Inorg. Chem.* 30 (1991) 2740.
- [60] M.-D. Tsai, T. Drakenberg, E. Thulin, S. Forsen, *Biochemistry* 26 (1987) 3635.
- [61] H. Yan, M.-D. Tsai, *Biochemistry* 30 (1991) 5539.
- [62] W. Xian, J.X. Tang, P.A. Janmey, W.H. Braunlin, *Biochemistry* 38 (1999) 7219.
- [63] M. Barbagallo, L.J. Dominguez, in: M. Gielen, E.R.T. Tiekink (Eds.), *Metallotherapeutic Drugs and Metal-Based Diagnostic Agents: The Use of Metals in Medicine*, Wiley-VCH, Weinheim, 2005, p. 109.
- [64] S.J. Lippard, J.M. Berg, *Principles of Bioinorganic Chemistry*, University Science Books, Mill Valley, CA, 1994.
- [65] H.J. Vogel, S. Forsen, *Biol. Magn. Reson.* 7 (1987) 249.
- [66] T. Andersson, T. Drakenberg, S. Forsen, E. Thulin, M. Swärd, *J. Am. Chem. Soc.* 104 (1982) 576.
- [67] T. Andersson, T. Drakenberg, S. Forsen, E. Thulin, *Eur. J. Biochem.* 126 (1982) 501.
- [68] J.M. Aramini, T. Drakenberg, T. Hiraoki, Y. Ke, K. Nitta, H.J. Vogel, *Biochemistry* 31 (1992) 6761.
- [69] G. Rana, K. Vyakaranam, J.A. Maguire, N.S. Hosmane, in: M. Gielen, E.R.T. Tiekink (Eds.), *Metallotherapeutic Drugs and Metal-Based Diagnostic Agents: The Use of Metals in Medicine*, Wiley-VCH, Weinheim, 2005, p. 19.
- [70] R.F. Barth, *J. Neuro-Oncol.* 62 (2003) 1.
- [71] (a) P. Bendel, *NMR Biomed.* 18 (2005) 74;  
(b) P. Bendel, W. Sauerwein, *Med. Phys.* 28 (2001) 178.
- [72] E. Tsilikounas, C.A. Kettner, W.W. Bachovchin, *Biochemistry* 32 (1993) 12651.
- [73] P.-P.P. Zhu Tang, M.P. Schweizer, K.M. Bradshaw, W.F. Bauer, *Biochem. Pharmacol.* 49 (1995) 625.
- [74] G.W. Pettigrew, G.R. Moore, *Cytochromes-c Biological Aspects*, Springer-Verlag, Berlin, 1987.
- [75] G. Taler, U. Eliav, G. Navon, *J. Magn. Reson.* 141 (1999) 228.
- [76] G. Taler, A. Schejter, G. Navon, *Inorg. Chim. Acta* 273 (1998) 388.
- [77] J.P. André, H.R. Mäcke, *J. Inorg. Biochem.* 97 (2003) 315.
- [78] D. Malakoff, *Science* 288 (2000) 1323.
- [79] T. Salifoglou, in: M. Gielen, E.R.T. Tiekink (Eds.), *Metallotherapeutic Drugs and Metal-Based Diagnostic Agents: The Use of Metals in Medicine*, Wiley-VCH, Weinheim, 2005, p. 65.
- [80] W.R. Harris, L. Messori, *Coord. Chem. Rev.* 228 (2002) 237.
- [81] (a) J.M. Aramini, H.J. Vogel, *J. Am. Chem. Soc.* 115 (1993) 245;  
(b) J.M. Aramini, H.J. Vogel, *J. Am. Chem. Soc.* 116 (1994) 6971;  
(c) J.M. Aramini, D.D. McIntyre, H.J. Vogel, *J. Am. Chem. Soc.* 116 (1994) 11506;  
(d) J.M. Aramini, H.J. Vogel, *J. Am. Chem. Soc.* 116 (1994) 1988.
- [82] J.M. Aramini, M.W. Germann, H.J. Vogel, *J. Am. Chem. Soc.* 115 (1993) 9750.
- [83] I. Dellavia, J. Blixt, C. Dupressoir, C. Detellier, *Inorg. Chem.* 33 (1994) 2823.
- [84] P. Yu, B.L. Phillips, M.M. Olmstead, W.H. Casey, *J. Chem. Soc., Dalton Trans.* (2002) 2119.
- [85] R.L. Hayes, in: H.G. Seiler, H. Sigel, A. Sigel (Eds.), *Handbook of Toxicity of Inorganic Compounds*, Marcel Dekker, New York, 1988, p. 297.

- [86] P.J. Blower, *Annu. Rep. Prog. Chem. Sect. A: Inorg. Chem.* 98 (2002) 615.
- [87] M.J. Clarke, F. Zhu, D.R. Frasca, *Chem. Rev.* 99 (1999) 2511.
- [88] M. Thiel, T. Schilling, D.C. Gey, R. Ziegler, P. Collery, B.K. Keppler, *Contrib. Oncol.* 54 (1999) 439.
- [89] L.R. Bernstein, T. Tanner, C. Godfrey, B. Noll, *Met.-Based Drugs* 7 (2000) 33.
- [90] J.J. Delpuech, *NMR of Newly Accessible Nuclei*, vol. 2, Academic Press, London, 1983.
- [91] J.F. Hinton, R.W. Briggs, in: R.K. Harris, B.E. Mann (Eds.), *NMR and the Periodic Table*, Academic Press, New York, 1978 (Chapter 9).
- [92] J. Burgess, *Chem. Soc. Rev.* (1996) 85.
- [93] I. Bertini, C. Luchinat, L. Messori, *J. Am. Chem. Soc.* 105 (1983) 1347.
- [94] I. Bertini, L. Messori, G.C. Pellacani, M. Sola, *Inorg. Chem.* 27 (1988) 761.
- [95] J.M. Aramini, P.H. Krygsmann, H.J. Vogel, *Biochemistry* 33 (1994) 3304.
- [96] J.P. Loria, T. Nowak, *Biochemistry* 37 (1998) 6967.
- [97] D.S. Resiga, T. Nowak, *J. Biol. Chem.* 278 (2003) 40943.
- [98] R. Haselhorst, K. Scheffler, L. Faletti, A. Kaspar, C. Prunte, J. Seelig, *Magn. Reson. Med.* 40 (1998) 170.
- [99] E. Lukevics, L. Ignatovich, in: M. Gielen, E.R.T. Tiekink (Eds.), *Metallotherapeutic Drugs and Metal-Based Diagnostic Agents: The Use of Metals in Medicine*, Wiley-VCH, Weinheim, 2005, p. 279.
- [100] M.J. DiMartino, J.C. Lee, M. Badger, K.A. Muirhead, K. Mirabelli, N. Hanna, *J. Pharmacol. Exp. Ther.* 236 (1986) 103.
- [101] Y. Takeuchi, M. Nishikawa, K. Tanaka, T. Takayama, M. Imanari, M. Deguchi, T. Fujito, Y. Sugisaka, *Chem. Commun.* (2000) 687.
- [102] J.T. Byrd, M.O. Andrae, *Science* 218 (1982) 506.
- [103] (a) M. Gielen, *Coord. Chem. Rev.* 151 (1996) 41;  
(b) M. Nath, S. Pokharia, R. Yadav, *Coord. Chem. Rev.* 215 (2001) 99;  
(c) L. Ronconi, C. Marzano, U. Russo, S. Sitran, R. Graziani, D. Fregona, *J. Inorg. Biochem.* 91 (2002) 413.
- [104] M. Gielen, E.R.T. Tiekink, in: M. Gielen, E.R.T. Tiekink (Eds.), *Metallotherapeutic Drugs and Metal-Based Diagnostic Agents: The Use of Metals in Medicine*, Wiley-VCH, Weinheim, 2005, p. 421.
- [105] J.C. Meurice, M. Vallier, M. Ratier, J.G. Duboudin, M. Petraud, *J. Chem. Soc., Perkin Trans. 2* (1996) 1331.
- [106] J.C. Martins, M. Biesemans, R. Willem, *Prog. Nucl. Magn. Reson. Spectrosc.* 36 (2000) 271.
- [107] L. Pellerito, L. Nagy, *Coord. Chem. Rev.* 224 (2002) 111.
- [108] I. Kessel, J.T. O'Connon, *Getting the Lead Out: The Complete Resource on How to Prevent and Cope with Lead Poisoning*, Plenum Press, New York, 1997.
- [109] S. Hassfjell, *Appl. Radiat. Isot.* 55 (2001) 433.
- [110] Z.S. Yao, K. Garmestani, K.J. Wong, L.S. Park, E. Dadachova, A. Yordanov, T.A. Waldmann, W.C. Eckelman, C.H. Paik, J.A. Carrasquillo, *J. Nucl. Med.* 42 (2001) 1538.
- [111] A.E. Martell, R.J. Motekaitis, *Determination and Use of Stability Constants*, VCH Publishers, New York, 1988.
- [112] E.S. Claudio, M.A. ter Horst, C.E. Forde, C.L. Stern, M.K. Zart, H.A. Godwin, *Inorg. Chem.* 39 (2000) 1391.
- [113] G.W. Goldstein, *Neurotoxicology* 14 (1993) 97.
- [114] J.M. Aramini, T. Hiraoki, M. Yazawa, T. Yuan, M. Zhang, H.J. Vogel, *J. Biol. Inorg. Chem.* 1 (1996) 39.
- [115] R.J. Andersen, R.C. DiTargiani, R.D. Hancock, C.L. Stern, D.P. Goldberg, H.A. Godwin, *Inorg. Chem.* 45 (2006) 6574.
- [116] (a) O.M. Ni Dhubhghaill, P.J. Sadler, *Struct. Bond.* 78 (1991) 129;  
(b) P.C. Ho, in: M. Gielen, E.R.T. Tiekink (Eds.), *Metallotherapeutic Drugs and Metal-Based Diagnostic Agents: The Use of Metals in Medicine*, Wiley-VCH, Weinheim, 2005, p. 297.
- [117] S. Yan, L. Jin, H. Sun, in: M. Gielen, E.R.T. Tiekink (Eds.), *Metallotherapeutic Drugs and Metal-Based Diagnostic Agents: The Use of Metals in Medicine*, Wiley-VCH, Weinheim, 2005, p. 441.
- [118] N. Burford, M.D. Eelman, in: M. Gielen, E.R.T. Tiekink (Eds.), *Metallotherapeutic Drugs and Metal-Based Diagnostic Agents: The Use of Metals in Medicine*, Wiley-VCH, Weinheim, 2005, p. 529.
- [119] N. Yang, J.A. Tanner, B.-J. Zheng, R.M. Watt, M.-L. He, L.-Y. Lu, J.-Q. Jiang, K.-T. Shum, Y.-P. Lin, K.-L. Wong, M.C.M. Lin, H.-F. Kung, H. Sun, J.-D. Huang, *Angew. Chem. Int. Ed.* 46 (2007) 6464.
- [120] B. Sredni, R.R. Caspi, A. Klein, Y. Kalechman, Y. Danziger, M. Ben Ya'akov, T. Tamari, F. Shalit, M. Albeck, *Nature* 330 (1987) 173.
- [121] A.K. Singh, S. Sharma, *Coord. Chem. Rev.* 209 (2000) 49.
- [122] A. Albeck, H. Weitman, B. Sredni, M. Albeck, *Inorg. Chem.* 37 (1998) 1704.
- [123] G. Paganelli, S. Zoboli, M. Cremonesi, L. Bodei, M. Ferrari, C. Grana, M. Bartolomei, F. Orsi, C. De Cicco, H.R. Maacke, M. Chinol, F. de Braud, *Eur. J. Nucl. Med.* 28 (2001) 426.
- [124] C. Brevard, P. Granger, *Handbook of High Resolution Multinuclear NMR*, John Wiley and Sons, New York, 1981.
- [125] P.S. Pregosin, *Transition Metal Nuclear Magnetic Resonance*, Elsevier, New York, 1991.
- [126] R.E. White, T.P. Hanusa, *Organometallics* 25 (2006) 5621.
- [127] S. Yaghoubi, C.W. Schwieter, J.P. McCue, *Biol. Trace Elem. Res.* 78 (2000) 205.
- [128] E. Dubler, in: M. Gielen, E.R.T. Tiekink (Eds.), *Metallotherapeutic Drugs and Metal-Based Diagnostic Agents: The Use of Metals in Medicine*, Wiley-VCH, Weinheim, 2005, p. 125.
- [129] P.M. Abeyasinghe, M.M. Harding, *Dalton Trans.* (2007) 3474.
- [130] R.G. Kidd, R.W. Matthews, H.G. Spinney, *J. Am. Chem. Soc.* 94 (1972) 6686.
- [131] (a) P.G. Gassman, W.H. Campbell, D.W. Macomber, *Organometallics* 3 (1984) 385;  
(b) W.C. Finch, E.V. Anslyn, R.H. Grubbs, *J. Am. Chem. Soc.* 110 (1988) 2406.
- [132] R.C. Maurya, S. Rajput, *J. Mol. Struct.* 833 (2007) 133.
- [133] A. Butler, M.J. Danzitz, *J. Am. Chem. Soc.* 109 (1987) 1864.
- [134] (a) K.H. Thompson, C. Orvig, *Coord. Chem. Rev.* 219–221 (2001) 1033;  
(b) K.H. Thompson, C. Orvig, *J. Inorg. Biochem.* 100 (2006) 1925.
- [135] A. Gorzszás, K. Getty, I. Andersson, L. Pettersson, *Dalton Trans.* (2004) 2873.
- [136] P. Caravan, L. Gelmini, N. Glover, F.G. Herring, H. Li, J.H. McNeill, S.J. Rettig, I.A. Setyawati, E. Shuter, Y. Sun, A.S. Tracey, V.G. Yuen, C. Orvig, *J. Am. Chem. Soc.* 117 (1995) 12759.
- [137] V.G. Yuen, P. Caravan, L. Gelmini, N. Glover, J.H. McNeill, I.A. Setyawati, Y. Zhou, C. Orvig, *J. Inorg. Biochem.* 68 (1997) 109.
- [138] F. Yraola, S. Garcia-Vicente, L. Martí, F. Albericio, A. Zorzano, M. Royo, *Chem. Biol. Drug. Des.* 69 (2007) 423.
- [139] (a) A. Butler, H. Eckert, *J. Am. Chem. Soc.* 111 (1989) 2802;  
(b) J.A. Saponja, H.J. Vogel, *J. Inorg. Biochem.* 62 (1996) 253.
- [140] T.C. Delgado, A.I. Tomaz, I. Correia, J. Costa Pessoa, J.G. Jones, C.F.G.C. Geraldes, M.M.C.A. Castro, *J. Inorg. Biochem.* 99 (2005) 2328.
- [141] M. Aureliano, T. Tiago, R.M.C. Gandara, A. Sousa, A. Moderno, M. Kaliva, A. Salifoglou, R.O. Duarte, J.J.G. Moura, *J. Inorg. Biochem.* 99 (2005) 2355.
- [142] J.B. Vincent, *Acc. Chem. Res.* 33 (2000) 503.
- [143] C. Beedham, *Drug Metab. Rev.* 16 (1985) 119.
- [144] A. Kletzin, M.W. Adams, *FEMS Microbiol. Rev.* 18 (1996) 5.
- [145] K. Nomiya, H. Torii, T. Hasegawa, Y. Nemoto, K. Nomura, K. Hashino, M. Uchida, Y. Kato, K. Shimizu, M. Oda, *J. Inorg. Biochem.* 86 (2001) 657.
- [146] A. Hafner, L.S. Hegedus, G. deWeck, B. Hawkins, K.H. Dotz, *J. Am. Chem. Soc.* 110 (1988) 8413.
- [147] G.-S. Kim, D.A. Judd, C.L. Hill, R.F. Schinazi, *J. Med. Chem.* 37 (1994) 816.
- [148] G.H. Reed, R.R. Poyner, *Met. Ions Biol. Syst.* 37 (2000) 183.
- [149] J.D. Crowley, D.A. Traynor, D.C. Weatherburn, *Met. Ions Biol. Syst.* 37 (2000) 209.
- [150] M.J. Horsburgh, S.J. Wharton, M. Karavolos, S.J. Foster, *Trends Microbiol.* 10 (2002) 496.
- [151] J.H. Freeland-Graves, T. Bose, A. Karbassian, in: M. Gielen, E.R.T. Tiekink (Eds.), *Metallotherapeutic Drugs and Metal-Based Diagnostic Agents: The Use of Metals in Medicine*, Wiley-VCH, Weinheim, 2005, p. 159.



- [152] J.E. Sheats, R.S. Czernuszewicz, G.C. Dismukes, A.L. Rheingold, V. Petrouleas, J.A. Stubbe, W.H. Armstrong, R.H. Beer, S.J. Lippard, *J. Am. Chem. Soc.* 109 (1987) 1435.
- [153] O.O. Sogbein, J.F. Valliant, in: M. Gielen, E.R.T. Tiekink (Eds.), *Metallotherapeutic Drugs and Metal-Based Diagnostic Agents: The Use of Metals in Medicine*, Wiley-VCH, Weinheim, 2005, p. 333.
- [154] V.A. Mikhalev, *Radiochemistry* 47 (2005) 319.
- [155] G.W. Brady, C.R. Kurkjian, E.F. Lyden, M.B. Robin, P. Saltman, T. Spiro, A. Terzis, *Biochemistry* 7 (1968) 2185.
- [156] X. Wu, M.L. Go, in: M. Gielen, E.R.T. Tiekink (Eds.), *Metallotherapeutic Drugs and Metal-Based Diagnostic Agents: The Use of Metals in Medicine*, Wiley-VCH, Weinheim, 2005, p. 179.
- [157] (a) L. Baltzer, M. Landergren, *J. Am. Chem. Soc.* 112 (1990) 2804;  
(b) L. Baltzer, E.D. Becker, B.A. Averill, J.M. Hutchinson, O.A. Gansow, *J. Am. Chem. Soc.* 106 (1984) 2444;  
(c) E.J.M. Meier, W. Kozminski, A. Linden, P. Lustenberger, W. von Philipsborn, *Organometallics* 15 (1996) 2469.
- [158] (a) L. Baltzer, E.D. Becker, R.G. Tschudin, O.A. Gansow, *J. Chem. Soc., Chem. Commun.* (1985) 1040;  
(b) H.C. Lee, J.K. Gard, T.L. Brown, E. Oldfield, *J. Am. Chem. Soc.* 107 (1985) 4087;  
(c) L. Baltzer, *J. Am. Chem. Soc.* 109 (1987) 3479;  
(d) J. Chung, H.C. Lee, E. Oldfield, *J. Magn. Reson.* 90 (1990) 148.
- [159] (a) L. Baltzer, M. Landergren, *J. Chem. Soc., Chem. Commun.* (1987) 32;  
(b) I.P. Gerathanassis, C.G. Kalodimos, G.E. Hawkes, P. Haycock, *J. Magn. Reson.* 131 (1998) 163.
- [160] L. Ronconi, P.J. Sadler, *Coord. Chem. Rev.* 251 (2007) 1633.
- [161] G. Sava, E. Alessio, A. Bergamo, G. Mestroni, in: M.J. Clarke, P.J. Sadler (Eds.), *Topics in Biological Inorganic Chemistry—Metallopharmaceuticals I*, Springer-Verlag, Berlin, 1999, p. 143.
- [162] M. Galanski, V.B. Arion, M.A. Jakupc, B.K. Keppler, *Curr. Pharm. Des.* 9 (2003) 2078.
- [163] (a) Y.K. Yan, M. Melchart, A. Habtemariam, P.J. Sadler, *Chem. Commun.* (2005) 4764;  
(b) P.J. Dyson, G. Sava, *Dalton Trans.* (2006) 1929;  
(c) A.V. Rudnev, S.S. Aleksenko, O. Semenova, C.G. Hartinger, A.R. Timerbaev, B.K. Keppler, *J. Sep. Sci.* 28 (2005) 121.
- [164] A.F.A. Peacock, A. Habtemariam, R. Fernandez, V. Walland, F.P.A. Fabiani, S. Parsons, R.E. Aird, D.I. Jodrell, P.J. Sadler, *J. Am. Chem. Soc.* 128 (2006) 1739.
- [165] S. Gaemers, J. van Slageren, C.M. O'Connor, J.G. Vos, R. Hage, C.J. Elsevier, *Organometallics* 18 (1999) 5238.
- [166] (a) X. Xiaoming, T. Matsumura-Inoue, S. Mizutani, *Chem. Lett.* (1997) 241;  
(b) G. Orellana, A. Kirsch-De Mesmaeker, N.J. Turro, *Inorg. Chem.* 29 (1990) 882;  
(c) P.J. Steel, F. Lahousse, D. Lerner, C. Marzin, *Inorg. Chem.* 22 (1983) 1488.
- [167] J. Kaufmann, A. Schwenk, *Phys. Lett.* 24A (1967) 115.
- [168] (a) R. Benn, E. Joussen, H. Lehmkuhl, F. Lopez Ortiz, A. Rufinska, *J. Am. Chem. Soc.* 111 (1989) 8754;  
(b) R. Benn, H. Brenneke, E. Joussen, H. Lehmkuhl, F. Lopez Ortiz, *Organometallics* 9 (1990) 756;  
(c) A.G. Bell, W. Kozminski, A. Linden, W. von Philipsborn, *Organometallics* 15 (1996) 3124.
- [169] R.S. Young, *Cobalt in Biology and Biochemistry*, Academic Press, New York, 1979.
- [170] D. Dolphin, B<sub>12</sub>, John Wiley and Sons, New York, 1982.
- [171] M. Kobayashi, S. Shimizu, *Eur. J. Biochem.* 161 (1999) 1.
- [172] H. Chao, L.-N. Ji, in: M. Gielen, E.R.T. Tiekink (Eds.), *Metallotherapeutic Drugs and Metal-Based Diagnostic Agents: The Use of Metals in Medicine*, Wiley-VCH, Weinheim, 2005, p. 201.
- [173] C.L. Drennan, S. Huang, J.T. Drummond, R.G. Matthews, M.L. Ludwig, *Science* 266 (1994) 1669.
- [174] A. Medek, V. Frydman, L. Frydman, *Proc. Natl. Acad. Sci. U.S.A.* 94 (1997) 14237.
- [175] W.P. Power, C.W. Kirby, N.J. Taylor, *J. Am. Chem. Soc.* 120 (1998) 9428.
- [176] A. Medek, L. Frydman, *J. Am. Chem. Soc.* 122 (2000) 684.
- [177] F.P. Pruchnik, in: M. Gielen, E.R.T. Tiekink (Eds.), *Metallotherapeutic Drugs and Metal-Based Diagnostic Agents: The Use of Metals in Medicine*, Wiley-VCH, Weinheim, 2005, p. 379.
- [178] J.M. Ernsting, S. Gaemers, C.J. Elsevier, *Magn. Reson. Chem.* 42 (2004) 721.
- [179] N.E. Dixon, T.C. Gazzola, R.L. Blakeley, B. Zermer, *J. Am. Chem. Soc.* 97 (1975) 4131.
- [180] R.K. Watt, P.W. Ludden, *Cell Mol. Life Sci.* 56 (1999) 604.
- [181] A. Garoufis, in: M. Gielen, E.R.T. Tiekink (Eds.), *Metallotherapeutic Drugs and Metal-Based Diagnostic Agents: The Use of Metals in Medicine*, Wiley-VCH, Weinheim, 2005, p. 399.
- [182] (a) F. Li, H. Sun, in: M. Gielen, R. Willem, B. Wrackmeir (Eds.), *Physical Organometallic Chemistry*, vol. 4, John Wiley and Sons, New York, 2004, p. 163;  
(b) J. Vinje, E. Sletten, *Anti-Cancer Agents Med. Chem.* 7 (2007) 35.
- [183] P. Kroneck, O. Lutz, A. Nolle, H. Oehler, *Z. Naturforsch. A* 35 (1980) 221.
- [184] M. Kujime, T. Kurahashi, M. Tomura, H. Fujii, *Inorg. Chem.* 46 (2007) 541.
- [185] A.D. Russell, W.B. Hugo, *Prog. Med. Chem.* 31 (1994) 351.
- [186] C.F. Shaw III, *Chem. Rev.* 99 (1999) 2589.
- [187] (a) E.R.T. Tiekink, *Crit. Rev. Oncol. Hematol.* 42 (2002) 225;  
(b) L. Messori, G. Marcon, in: A. Sigel, H. Sigel (Eds.), *Metal Ions in Biological Systems—Metal Complexes in Tumor Diagnosis and as Anti-cancer Agents*, FontisMedia S.A./Marcel Dekker Inc., Basel, 2004, p. 385;  
(c) P.J. Barnard, S.J. Berners-Price, *Coord. Chem. Rev.* 251 (2007) 1889;  
(d) D. Saggioro, M.P. Rigobello, L. Paloschi, A. Folda, S.A. Moggach, S. Parsons, L. Ronconi, D. Fregona, A. Bindoli, *Chem. Biol.* 14 (2007) 1128.
- [188] J. Mason, *Multinuclear NMR Spectroscopy*, Plenum Press, New York, 1987.
- [189] G.H. Penner, X. Liu, *Prog. Nucl. Magn. Reson. Spectrosc.* 49 (2006) 151.
- [190] S.S. Narula, R.K. Mehra, D.R. Winge, I.M. Armitage, *J. Am. Chem. Soc.* 113 (1991) 9354.
- [191] S.J. Berners-Price, R.J. Bowen, P.J. Harvey, P.C. Healy, G.A. Koutsantonis, *J. Chem. Soc., Dalton Trans.* (1998) 1743.
- [192] K. Zangger, I.M. Armitage, *Met.-Based Drugs* 6 (1999) 239.
- [193] J.M. Berg, Y. Shi, *Science* 271 (1996) 1081.
- [194] J.V. Higdon, E. Ho, in: M. Gielen, E.R.T. Tiekink (Eds.), *Metallotherapeutic Drugs and Metal-Based Diagnostic Agents: The Use of Metals in Medicine*, Wiley-VCH, Weinheim, 2005, p. 237.
- [195] T. Shimizu, M. Hatano, *Inorg. Chem.* 24 (1985) 2003.
- [196] A.S. Lipton, J.A. Sears, P.D. Ellis, *J. Magn. Reson.* 151 (2001) 48.
- [197] J.E. Fergusson, *The Heavy Elements: Chemistry Environmental Impact and Health Effects*, Pergamon Press, Oxford, 1990.
- [198] C. Bevan, E. Kinne-Saffran, E.C. Foulkes, R.K.H. Kinne, *Toxicol. Appl. Pharmacol.* 101 (1989) 461.
- [199] (a) I.M. Armitage, A.J.M. Schoot Uiterkamp, J.F. Chlebowski, J.E. Coleman, *J. Magn. Reson.* 29 (1978) 375;  
(b) J.E. Coleman, D.P. Giedroc, in: R.B. King (Ed.), *Encyclopedia of Inorganic Chemistry*, John Wiley and Sons, Chichester, 1994.
- [200] J. Chan, Z. Huang, M.E. Merrifield, M.T. Salgado, M.J. Stillman, *Coord. Chem. Rev.* 233–234 (2002) 319.
- [201] (a) G. Öz, D.L. Pountney, I.M. Armitage, *Biochem. Cell Biol.* 76 (1998) 223;  
(b) I.M. Armitage, R.T. Pajer, A.J.M. Schoot Uiterkamp, J.F. Chlebowski, J.E. Coleman, *J. Am. Chem. Soc.* 98 (1976) 5710;  
(c) C.J. Henahan, D.L. Pountney, O. Zerbe, M. Vasak, *Protein Sci.* 2 (1993) 1756;  
(d) H. Li, J.D. Otvos, *Biochemistry* 35 (1996) 13929;  
(e) J.W. Ejniak, A. Muñoz, E. DeRose, C.F. Shaw III, D.H. Petering, *Biochemistry* 42 (2003) 8403;  
(f) A.J. Stewart, C.A. Blindauer, S. Berezhenko, D. Sleep, P.J. Sadler, *Proc. Natl. Acad. Sci. U.S.A.* 100 (2003) 3701;

- (g) A. Muñoz, F. Laib, D.H. Petering, C.F. Shaw III, *J. Biol. Inorg. Chem.* 4 (1999) 495;
- (h) M.J. Daniels, J.S. Turner-Cavet, R. Selkirk, H. Sun, J.A. Parkinson, P.J. Sadler, N.J. Robinson, *J. Biol. Chem.* 273 (1998) 22957;
- (i) G. Meloni, K. Zovo, J. Kazantseva, P. Palumaa, M. Vasak, *J. Biol. Chem.* 281 (2006) 14588;
- (j) M. Matzapetakis, V.L. Pecoraro, *J. Am. Chem. Soc.* 127 (2005) 18229.
- [202] (a) M. Sola, *Inorg. Chem.* 29 (1990) 1113;
- (b) W. Kiang, P.J. Sadler, D.G. Reid, *Magn. Res. Chem.* 31 (1993) S110.
- [203] X. Liang, J.A. Parkinson, S. Parsons, M. Weishäupl, P.J. Sadler, *Inorg. Chem.* 41 (2002) 4539.
- [204] S.D. Siciliano, D.R. Lean, *Environ. Toxicol. Chem.* 21 (2002) 1184.
- [205] M.F. Roberts, D.A. Vidusek, G. Bodenhausen, *FEBS Lett.* 117 (1980) 311.
- [206] J.L. Sudmeier, T.G. Perkins, *J. Am. Chem. Soc.* 99 (1977) 7732.
- [207] D.A. Vidusek, M.F. Roberts, G. Bodenhausen, *J. Am. Chem. Soc.* 104 (1982) 5452.
- [208] (a) L.M. Utschig, J.W. Bryson, T.V. O'Halloran, *Science* 268 (1995) 380;
- (b) D.L. Huffman, L.M. Utschig, T.V. O'Halloran, *Met. Ions Biol. Syst.* 34 (1997) 503.
- [209] S.J. Franklin, *Curr. Opin. Chem. Biol.* 5 (2001) 201.
- [210] H. Kobayashi, S. Kawamoto, T. Saga, N. Sato, T. Ishimori, J. Konishi, K. Ono, K. Togashi, M.W. Brechbiel, *Bioconjug. Chem.* 12 (2001) 587.
- [211] T.J. Wenzel, *NMR Shift Reagents*, CRC Press, Boca Raton, FL, 1987.
- [212] S. Aime, A. Barge, E. Gianolio, S. Geninatti Crich, W. Dastrù, F. Uggeri, in: M. Gielen, E.R.T. Tiekink (Eds.), *Metallotherapeutic Drugs and Metal-Based Diagnostic Agents: The Use of Metals in Medicine*, Wiley-VCH, Weinheim, 2005, p. 541.
- [213] (a) J.A. Petersa, J. Huskensa, D.J. Raber, *Prog. Nucl. Magn. Reson. Spectrosc.* 28 (1996) 283;
- (b) P. Rösch, J. Weizenecker, M.T. Kelemen, J. Ruf, C. Zobel, E. Dormann, *J. Magn. Magn. Mater.* 177–181 (1998) 1071.
- [214] W.W. Cleland, M.M. Kreevoy, *Science* 264 (1994) 1887.
- [215] V. Lemaitre, M.E. Smith, A. Watts, *Solid State Nucl. Magn. Reson.* 26 (2004) 215.
- [216] I.P. Gerothanassis, in: D. Grant, R.K. Harris (Eds.), *Encyclopedia of NMR*, vol. 5, John Wiley and Sons, New York, 1995, p. 3430.
- [217] I.P. Gerothanassis, M. Momenteau, *J. Am. Chem. Soc.* 109 (1987) 6944.
- [218] Y.-J. Shyy, T.-C. Tsai, M.-D. Tsai, *J. Am. Chem. Soc.* 107 (1985) 3478.
- [219] (a) M. Petersheim, V.W. Miner, J.A. Gerlt, J.H. Prestegard, *J. Am. Chem. Soc.* 105 (1983) 6357;
- (b) I.P. Gerothanassis, R.N. Hunston, J. Lauterwein, *Helv. Chim. Acta* 65 (1982) 1774.
- [220] (a) X.-H. Zhu, Y. Zhang, R.X. Tian, H. Lei, N. Zhang, X. Zhang, H. Merkle, K. Ugurbil, W.W. Chen, *Proc. Natl. Acad. Sci. U.S.A.* 99 (2002) 13194;
- (b) X.-H. Zhu, N. Zhang, Y. Zhang, X. Zhang, K. Ugurbil, W. Chen, *NMR Biomed.* 18 (2005) 83.
- [221] D. Kessler, *FEMS Microbiol. Rev.* 30 (2006) 825.
- [222] (a) R.A. Aitken, S. Arumugam, S.T.E. Mesher, F.G. Riddell, *J. Chem. Soc., Perkin Trans. 2* (2002) 225;
- (b) P.S. Belton, I.J. Cox, R.K. Harris, *J. Chem. Soc., Faraday Trans. 2* 81 (1985) 63.
- [223] R. Musio, O. Sciacovelli, *J. Magn. Reson.* 153 (2001) 259.
- [224] L. Johansson, G. Gafvelin, E.S.J. Arnér, *Biochim. Biophys. Acta* 1726 (2005) 1.
- [225] M. Carland, T. Fenner, The use of selenium-based drugs in medicine, in: M. Gielen, E.R.T. Tiekink (Eds.), *Metallotherapeutic Drugs and Metal-Based Diagnostic Agents: The Use of Metals in Medicine*, Wiley-VCH, Weinheim, 2005, p. 313.
- [226] H. Duddeck, *Prog. Nucl. Magn. Reson. Spectrosc.* 27 (1994) 1.
- [227] (a) G. Roy, D. Das, G. Mugesh, *Inorg. Chim. Acta* 360 (2007) 303;
- (b) K.P. Bhabak, G. Mugesh, *Chem. Eur. J.* 13 (2007) 4594;
- (c) C.D. Antoniadis, S.K. Hadjikakou, N. Hadjiliadis, A. Papakyriakou, M. Baril, I.S. Butler, *Chem. Eur. J.* 12 (2006) 6888.
- [228] J.D. Odom, W.H. Dawson, P.D. Ellis, *J. Am. Chem. Soc.* 101 (1979) 5816.
- [229] (a) C.A. Bayse, *Inorg. Chem.* 43 (2004) 1208;
- (b) J.O. Boles, W.H. Tolleson, J.C. Schmidt, R.B. Dunlap, J.D. Odom, *J. Biol. Chem.* 267 (1992) 22217;
- (c) P. Gettins, B.C. Crews, *J. Biol. Chem.* 266 (1991) 4804;
- (d) E. Stocking, J. Schwarz, H. Senn, M. Salzmann, L. Silks, *J. Chem. Soc., Perkin Trans. 1* (1997) 2443.
- [230] R.F. Code, J.E. Harrison, K.G. McNeill, M. Szyjowski, *Magn. Reson. Med.* 13 (1990) 358.
- [231] J. Battiste, R.A. Newmark, *Prog. Nucl. Magn. Reson. Spectrosc.* 48 (2006) 1.
- [232] J.-X. Yu, V.D. Kodibagkar, W. Cui, R.P. Mason, *Curr. Med. Chem.* 12 (2005) 819.
- [233] R. Martino, V. Gilard, F. Desmoulin, M. Malet-Martino, *Chemotherapy* 52 (2006) 215.
- [234] E.B. Lamont, R.L. Schilsky, R.L. Clin, *Cancer Res.* 5 (1999) 2289.
- [235] S.P. Robinson, J.R. Griffiths, *Phil. Trans. R. Soc. Lond. B* 359 (2004) 987.
- [236] B. Lindman, S. Forsen, *Chlorine, Bromine and Iodine NMR. Physico-Chemical and Biological Applications*, Springer-Verlag, Heidelberg, 1976.
- [237] W. Maret, G. Heffron, H.A.O. Hill, D. Djuricic, L.-J. Jiang, B.L. Vallee, *Biochemistry* 41 (2002) 1689.
- [238] A.V. Koulov, J.M. Mahoney, B.D. Smith, *Org. Biomol. Chem.* 1 (2003) 27.
- [239] M. Wolf-Watz, S. Bäckström, T. Grundström, U. Sauer, T. Härd, *FEBS Lett.* 488 (2001) 81.
- [240] P. Gettins, L.W. Cunningham, *Biochemistry* 25 (1986) 5004.
- [241] T.R. Stengle, J.D. Baldeschwieler, *Proc. Natl. Acad. Sci. U.S.A.* 55 (1966) 1020.
- [242] T.R. Collins, Z. Starcuk, A.H. Burr, E.J. Wells, *J. Am. Chem. Soc.* 95 (1973) 1649.
- [243] J.-E. None, S.-G. Hjalmarsson, B. Lindman, M. Zeppezauer, *Biochemistry* 14 (1975) 3401.
- [244] (a) K. Fukuyama, K. Sato, H. Itakura, S. Takahashi, T. Hosoya, *J. Biol. Chem.* 272 (1997) 5752;
- (b) J. Sakurada, S. Takahashi, T. Shimizu, M. Hatano, S. Nakamura, Y. Hosoya, *Biochemistry* 26 (1987) 6478.
- [245] H. Zuccola, PhD thesis, Georgia Institute of Technology, Atlanta, GA, 1982.